Since January 2020 Elsevier has created a COVID-19 resource centre with free information in English and Mandarin on the novel coronavirus COVID-19. The COVID-19 resource centre is hosted on Elsevier Connect, the company's public news and information website.

Coordination Chemistry Reviews 458 (2022) 214417

Contents lists available at ScienceDirect

Coordination Chemistry Reviews

journal homepage: www.elsevier.com/locate/ccr

Review

Nuclease-like metalloscissors: Biomimetic candidates for cancer and bacterial and viral infections therapy

Marzieh Anjomshoa [a,*], Bagher Amirheidari [b,c,*]

[a] Pharmaceutical Sciences and Cosmetic Products Research Center, Kerman University of Medical Sciences, Kerman, Iran
[b] Department of Pharmaceutical Biotechnology, Faculty of Pharmacy, Kerman University of Medical Sciences, Kerman, Iran.
[c] Extremophile and Productive Microorganisms Research Center, Kerman University of Medical Sciences, Kerman, Iran

ARTICLE INFO

Article history:
Received 1 September 2021
Accepted 9 January 2022
Available online 5 February 2022

Keywords:
Artificial metallonucleases
Nuclease-like metalloscissors
Biomimetic
Cancer therapy
Microbial infections therapy

ABSTRACT

Despite the extensive and rapid discovery of modern drugs for treatment of cancer, microbial infections, and viral illnesses; these diseases are still among major global health concerns. To take inspiration from natural nucleases and also the therapeutic potential of metallopeptide antibiotics such as the bleomycin family, artificial metallonucleases with the ability of promoting DNA/RNA cleavage and eventually affecting cellular biological processes can be introduced as a new class of therapeutic candidates. Metal complexes can be considered as one of the main categories of artificial metalloscissors, which can prompt nucleic acid strand scission. Accordingly, biologists, inorganic chemists, and medicinal inorganic chemists worldwide have been designing, synthesizing and evaluating the biological properties of metal complexes as artificial metalloscissors. In this review, we try to highlight the recent studies conducted on the nuclease-like metalloscissors and their potential therapeutic applications. Under the light of the concurrent Covid-19 pandemic, the human need for new therapeutics was highlighted much more than ever before. The nuclease-like metalloscissors with the potential of RNA cleavage of invading viral pathogens hence deserve prime attention.

Contents

* Corresponding authors at: Department of Pharmaceutical Biotechnology, Faculty of Pharmacy, Kerman University of Medical Sciences, Haft-Bagh Highway, Kerman Post Code: 76169-13555, Iran (B. Amirheidari). Pharmaceutical Sciences and Cosmetic Products Research Center, Kerman University of Medical Sciences, Haft-Bagh Highway, Kerman Post Code: 76169-13555, Iran (M. Anjomshoa).

E-mail addresses: anjomshoa_1014@yahoo.com, maranjomshoa@gmail.com (M. Anjomshoa), b_amirheidari@kmu.ac.ir (B. Amirheidari).

https://doi.org/10.1016/j.ccr.2022.214417
0010-8545/

Nomenclature

Abbreviations

ABLM	Activated bleomycin
ac	Acridine
AFM	Atomic force microscopy
AGE	Agarose gel electrophoresis
AIDS	Acquired immunodeficiency syndrome
Ala/A	Alanine
AMNs	Artificial metallonucleases
AMSs	Artificial metalloscissors
ApA	Adenylyl-3′,5′-adenosine
ApU	Adenylyl-3′,5′-uridine
Arg/R	Arginine
Asn/N	Asparagine
Asp/D	Aspartic acid
ATCUN	Amino terminal Cu^{2+}- and Ni^{2+}-binding
BDNPP	Bis-(2,4-dinitrophenyl) phosphate
BLMs	Bleomycins
BNPP	Bis(4-nitrophenyl) phosphate
BODIPY	Boron-dipyrromethene
bpy	2,2′-Bipyridine
bt-tpy	4′-(Benzylthiazolyl)-terpyridine
btp-tpy	4′-(benzothiophene)-terpyridine
Cl-7-IVQ	5-chloro-7-(2-(1,3,3-trimethyl-3H-indol-1-ium-2-yl) vinyl) quinolin-8-olate
COVID-19	Coronavirus disease 2019
CPDT	Cancer photodynamic therapy
CpA	Cytidylyl-3′,5′-adenosine
Cys/C	Cysteine
dach	(1*R*,2*R*)-dichloro(cyclohexane-1,2-diamine)
DFT	Density functional theory
dimethoxybpy	4,4′-dimethoxy-2,2′-bipyridine
dimethylbpy	4,4′-dimethyl-2,2′-bipyridine
dipp	2,6-di*iso*propylphenyl phosphate
DLS	Dynamic light scattering
DMPO	5,5-Dimethyl-1-pyrroline N-oxide
DNA	Deoxyribonucleic acid
DNase	Deoxyribonucleases
dsDNA	Double-stranded deoxyribonucleic acid
dpa	Dipicolylamine
dppn	Benzo[*i*]dipyrido[3,2-*a*:2′,3′-*c*]phenazine
dppz	Dipyrido[3,2-a:2′,3′-c] phenazine
dpq	Dipyridoquinoxaline
dt-dpq	2,3-bis(thiophen-2-yl)pyrazino[2,3–f] [1,10]phenanothroline
EPR	Electron paramagnetic resonance
ESI-MS	Electrospray ionization-mass spectrometry
Fc-tpy	Ferrocenylterpyridine
G^-	Gram-negative
G^+	Gram-positive
G4	G-quadruplex
Gln/Q	Glutamine
Glu/E	Glutamic acid
Gly/G	Glycine
GpA	Guanylyl-3′,5′- adenosine
GpU	Guanylyl-3′,5′-uridine
HC	Hydrolytic cleavage
HCV	Hepatitis C virus
His/H	Histidin
HIV	Human immunodeficiency virus
HPBM	5-methyl-2-(2′-pyridyl) benzimidazole
HPLC	High performance liquid chromatography
HPNPP	2-Hydroxypropyl 4-nitrophenyl phosphate
IRES	Internal ribosome entry site
Iso/I	Isolucine
L	Linear
Leu/L	leucine
LF	Ligand field
LMCT	Ligand-to-metal charge transfer
Lys/K	Lysine
MALDI-TOF MS	Matrix-assisted laser desorption/ionization-time of flight mass spectrometry
Met/M	Methionine
MIC	Minimum inhibitory concentration
MLCT	Metal-to-ligand charge transfer
MPDT	Microbial photodynamic therapy
mRNA	Messenger ribonucleic acid
NAL	Nalidixic acid
Nic	Nicotinamide neutral linker
NMR	Nuclear magnetic resonance
NP	4-Nitrophenolate ion
NPP	4-Nitrophenyl phosphate
NSAIDs	Non-steroidal anti-inflammatory drugs
OC	Open circular
OHPh-tpy	4′-(4-hydroxyphenyl)-2,2′,6′,2″-terpyridine
OxC	Oxidative cleavage
PAGE	Polyacrylamide gel electrophoresis
PC	Photocleavage
PDT	Photodynamic therapy
Phe/F	Phenylalanine
phen	1,10-Phenanthroline
$(php)_2$van	3-Methoxy-4-(hydroxyphenyl) diphenanthropyrromethane
PI	Photocytotoxicity index
Pro/P	Proline
PS	photosensitizer
^{Me2}PyTACN	1,4-dimethyl-7-(2-pyridylmethyl)-1,4,7-triazacyclononane
py-tpy	4′-(4-pyridyl)-2,2′:6 ▫ ,2 ▫ ▫ -terpyridine
RNA	Ribonucleic acid
RNase	Ribonucleases
ROS	Reactive oxygen species
RRE	Rev response element
RRMs	RNA recognition motifs
rRNA	Rib NAL osomal RNA
SARS-CoV-2	Severe acute respiratory syndrome coronavirus 2
SC	Supercoiled circular
Ser/S	Serine
SLIV	Stem-loop IV
SOD	Superoxide dismutase
(*S*,*S*′)-BPBP	(*2S*,*2S*′)-1,1′-bis(pyrid-2-ylmethyl)-2,2′-bipyrrolidine)
tap	1,4,5,8-tetraazaphenanthrene
TBZ	2-(4′-thiazolyl)benzimidazole
TD-DFT	Time-dependent density functional theory
Thr/T	Theronine
tpy	2,2′:6′,2″-Terpyridine
tRNA	Transfer ribonucleic acid
Trp/W	Tryptophan
Tyr/Y	Tyrosine
UpA	Uridylyl-3′,5′-adenosine
UpU	Uridylyl-3′,5′-uridine
5′ UTR	5′-untranslated region
Val/V	Valine
WHO	World Health Organization

1. Introduction

Cancer as well as bacterial and viral infections are among major global diseases which threat human health. While, situations related to these health problems used to be frequently referred to as an "epidemic", the emergence of severe acute respiratory syndrome coronavirus 2 (SARS-CoV-2) pandemic raised the flag higher than ever before. SARS-CoV-2 is a positive-sense single stranded RNA virus responsible for causing the coronavirus disease 2019 (COVID-19) [1]. COVID-19 disease has rapidly spread all over the world and has become one of the most global health concerns in the 20th century with 194 million of confirmed cases and more than 4 million of deaths up to 27 July 2021 [2]. One of the most serious challenges in the treatment of these diseases is no sufficient efficacy of current drugs due to their resistance and mutations. Therefore, the discovery of novel therapeutic agents with different action mechanisms is critically needed.

Inspired by the utility of deoxyribonucleases (DNases) and ribonucleases (RNases) which have been widely used in various therapeutic studies [3–12], the scientific community has made intensive efforts to develop metallonuclease mimics. These biomimetic candidates as remarkable weapons against challenging diseases [13–15] are literally called "artificial metallonucleases" (AMNs) or more illustratively "artificial metalloscissors" (AMSs). DNases are enzymes which are capable to hydrolyze the phosphodiester bonds of DNA. Cleavage of DNA, if left unrepaired, can adversely interfere with replication, transcription, cell proliferation cycle, and ultimately trigger cell death *via* apoptosis [3]. RNases, on the other hand, catalytically cleave the cellular RNA and consequently lead to the perturbation of structural and functional activities of RNA, e.g. selective inhibition of gene expression at mRNA level [6–7].

Over four decades after the nuclease activity of a Cu(II) complex was reported [16], the concept of metal complexes as an extremely promising platform in the construction of AMSs is still enjoying a high level of interest as evidenced by many reviews [13–15,17–26]. Nevertheless, therapeutic potentials of AMSs have not received a substantially deep attention, we therefore try here to highlight the recent progress conducted on the metal complexes employed in mimetic cleavage studies of nucleic acids and shed a light on their potential therapeutic applications. Metal complexes possess rich structural and electronic properties as well as redox-active centers which enable them to cleave nucleic acids through hydrolysis [27–28] and/or by generating reactive oxygen species (ROS) (oxidative cleavage and photocleavage) [29–33]. A rich library of DNA/RNA–cleaving metal complexes have been prepared and submitted to pharma studies as novel therapeutic candidates for the treatment of diseases such as cancer [13–14,34–39], bacterial [13–14,39–45] and viral infections [13–14,46–49], and gene therapy [50–51]. Moreover, metal complexes are considered as suitable photosensitizers for photodynamic therapy (PDT) of cancer and microbial infections due to their efficient *in vitro* DNA photocleavage [52–55]. Meaningful examples will be further discussed in Section 5.

Bioinorganic chemists have applied a series of rational strategies to improve nuclease-like activity of metal complexes. We opted to categorize these creative approaches based on the main reasons and points of views behind the applied methodologies. Of course, the ultimate goal of this diversity lies in the enhancement of the AMSs' biological activity. Accordingly, these actively ongoing techniques are categorized as follow: i) Preparation of multinuclear complexes wherein the metal cores cooperate to provides an efficient active binding site for biomolecules [56–65]. ii) Variation of the first coordination sphere towards synthesis of homoleptic and hetroleptic complexes [66–71]. iii) Modification of the second coordination sphere *via* addition of the functional groups or by using the supramolecular hosts such as cyclodextrins (CDs) [56–57,72–83]. iv) Development of supramolecular systems by the self-assembly of metal complexes and organic building units [84–88]. v) Construction of metallomicell catalysts from the self-assembly of amphiphilic metal complexes [89–91]. vi) Conjugation of metal complexes with bioactive molecules such as peptides, nucleotides, and vitamins as well as DNA binders to recognize specific targets and promote highly efficient catalytic reaction [92–99]. vii) Nanoformulation of metal complexes with nanoparticles (nano-nucleases) to obtain cooperative systems with enhanced nuclease-like activity [41,90,100–107].

In continuation of our investigations to provide further insights into the therapeutic properties of metal-based compounds [108–118], we herein highlight the recent progress conducted on the potential therapeutic applications of AMSs. This review begins with mechanistic concepts of AMS-catalyzed nucleic acids cleavage (Section 2), followed by model substrates and instrumentations employed in cleavage studies (Section 3). The fourth section summarizes the application of AMSs as DNA/RNA–targeting therapeutics. The recent outstanding reports on designing and development

of novel AMSs as well as their pharma studies are elaborated in Section 5. The review ends by conclusion and future perspectives section (Section 6). Authors are well aware of the fact that the subject of artificial metalloscissors is a fast-expanding field; Authors hope that a universal and comprehensive review of this subject at the moment would motivate scientists with novel subtopics and visions to improve new research opportunities. This fact should not be ignored that any review is prone to be considered a snapshot in a longer time frame. Bearing in mind the numerous and fast growing AMS-related publications, it is very likely that some possibly important research groups have been unawares overseen, and apologies are therefore offered in advance to the authors of the probable missing citations.

2. Mechanism of nucleic acids cleavage

Generally, AMSs can promote cleavage reactions by targeting various parts of nucleic acids: the phosphodiester bond, sugar moiety, and nucleobases [119]. Mechanistically, two major types of DNA cleavage can be distinguished, namely i) hydrolytic and ii) ROS-induced cleavage. The latter itself can be categorized into oxidative cleavage and photocleavage [120]. In the hydrolytic pathway, DNA is degraded by hydrolysis of its phosphodiester bond *via* a reversible reaction, while in the oxidative pathway; DNA is cleaved by oxidation of the sugar and/or base moieties through generation of DNA damaging ROS, an irreversible reaction [68,120].

2.1. Hydrolytic cleavage

Hydrolysis of nucleic acids can be defined as a method that in the presence of water, phosphodiester bonds are cleaved to generate nucleic acid fragments and is a vigorous process in all living systems. According to its generally accepted mechanism of DNA hydrolysis as represented in Fig. 1 (A), first a water-derived nucleophile (OH^-) attacks to the phosphorus atom of the phosphate group to form a five–coordinated transition state. Finally, by protonation of the leaving group, P–O bond is cleaved *via* either the 3′ P–O (most frequent in enzymatic systems) or the 5′ P–O and results in a strand scission occurs and scission unites are separated [26,121–122].

As seen in Fig. 1 (B), in the RNA hydrolysis initially an intramolecular transesterification takes place which is followed by the cleavage of the strained cyclic phosphate intermediate. The hydrolysis rate of RNA is greater than of DNA due to the presence of a 2′-OH group that acts as an intramolecular nucleophile, deprotonation of which is facilitated by the metal ions in enzymes [122].

Metallonucleases are able to powerfully catalyze the hydrolysis of P–O bonds in the nucleic acids backbone *in vivo*. Therefore in the presence of such metal catalysts, hydrolysis of the phosphate backbone is accelerated at least to 17 orders of magnitude [26]. Interestingly, crystallographic studies indicate that one to three metal ions sit in the natural nuclease active sites; this can promote research to increase the efficiency and effectiveness of artificial multinuclear complexes [23]. Accordingly, AMSs provide a metal center with Lewis acidity that can hydrolytically cleave nucleic acids [27–28,123].

2.2. ROS-induced cleavage

In ROS- induced cleavage, the AMSs' metal core is involved as a redox-active center or photosensitizer that can generate DNA damaging ROS (Fig. 2 (A) and (B)). The generated ROS include free radicals as well as nonradical molecules that can damage the nucleobases or the sugar moiety (Fig. 2 (C)). To generate ROS in situ, this pathway is usually initiated by the addition of oxidizing or reducing reagents (oxidative cleavage) or light exposure (photocleavage) [124]. Although many metal complexes require the addition of external agents to produce ROS, some metal complexes oxidatively cleave DNA without any type of activator, hence called "self-activating" systems [29,125–126].

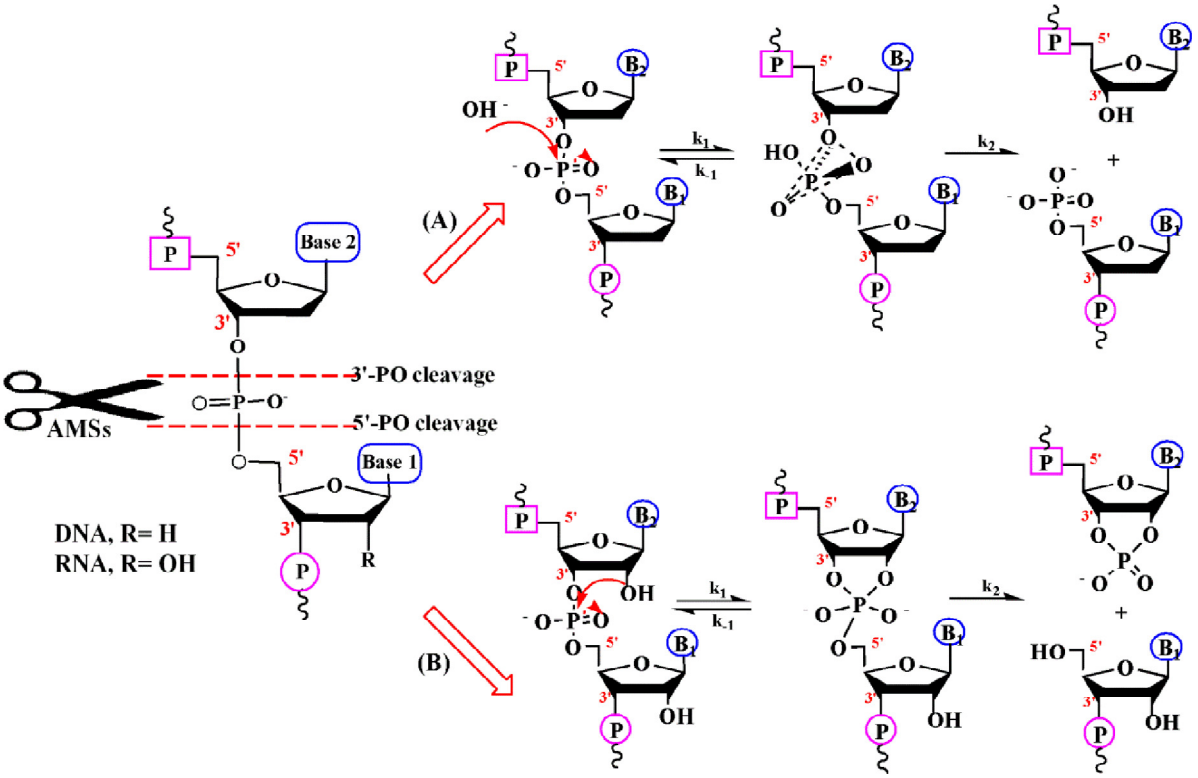

Fig. 1. Mechanism of hydrolytic cleavage of (A) DNA *via* the 3′-PO scission and (B) RNA *via* intramolecular transesterification [26,121–122].

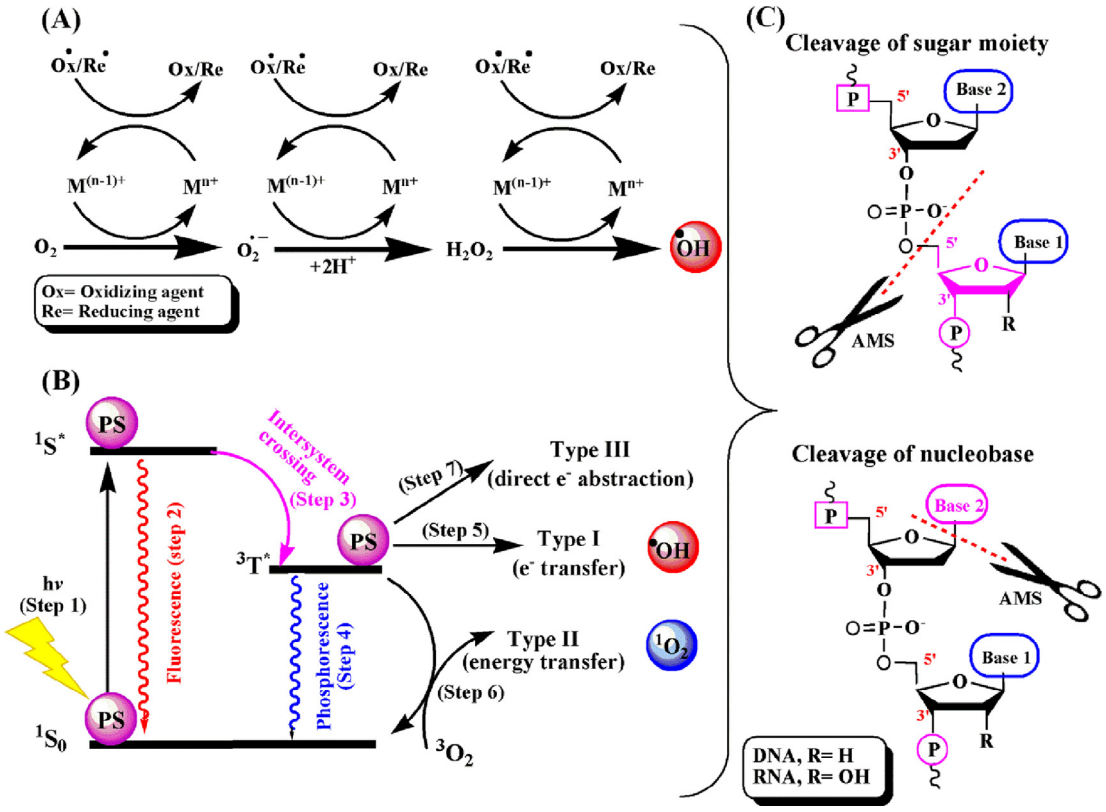

Fig. 2. (A) The AMSs' metal core in the presence of oxidizing or reducing reagents as a redox-active center in generation of ROS to cause oxidative cleavage. (B) The AMSs as a photosensitizer in generation of ROS (a simplified Jablonski diagram) involved in DNA photocleavage. (C) ROS-induced cleavage of the sugar and/or base moieties.

2.2.1. Oxidative cleavage

In this pathway, the stepwise reduction of O_2 molecules by electron-transfer reactions causes production of damaging ROSs (Fig. 2 (A)). In this case, metal ions play a pivotal role in the redox cycle by donating their electrons [72,124]. Oxidative cleavage is in-turn divided into two sub-categories:

i) Oxidation at the pentose sugar ring (C–O cleavage): abstraction of one hydrogen atom of the ring resulting in the formation of radical species can trigger the process. Generally, this process involves three steps: Step 1) One H atom of the ring is abstracted *via* a radical process and leaving a sugar radical; Step 2) An $^{\bullet}OH$ or $^{\bullet}O_2^-$ attacks to the sugar radical; and Step 3) Strand scission takes place, followed by a series of elimination reactions which ultimately result in the formation of a variety of characteristic small molecule byproducts and DNA fragments. In each type of H—C abstraction, one or two particular products are produced. Therefore, specific products can be utilized as indicators to investigate the action mechanism of synthetic complexes [121,124,127].

ii) Oxidation at the nucleobase ring: both purine and pyrimidine nitrogenous bases of nucleic acids are electron-rich heterocycles and can react with electrophiles ultimately ending with strand scission. Although ROS species can oxidatively damage all four DNA nucleobases, guanine is the prime target of oxidative damage owing its lowest oxidation potential among the DNA nucleobases [121,124]. Various types of base lesions have been identified as products of oxidative damage of nucleobases including base fragments, ring-opened forms, and oxidized aromatic derivatives [128].

2.2.2. Photocleavage

DNA photocleavage involves production of ROS through activation of a photosensitizer (PS) by visible or near-infrared light [52–53]. Fig. 2 (B) depicts the photophysical processes involved in DNA photocleavage. When irradiated at a precise wavelength, the PS from its singlet ground state ($^1S_0$) is excited electronically to a first singlet excited state ($^1S^*$) (Step 1). The $^1S^*$ state is relatively unstable and can undergo two different processes: emit the absorbed energy and return to the $^1S_0$ state (step 2) in a process called fluorescence or alternatively, turn into the more stable excited triplet state *via* intersystem crossing ($^3T^*$) (Step 3). At $^3T^*$ stage, the compound can emit its energy as phosphorescence and return to the $^1S_0$ state (step 4) or can take part in different types of photosensitized reactions. Here, PS-mediated reactions generally fall into three categories: Type I and Type II photoprocesses which absolutely depend on molecular oxygen and type III, independent of O_2. The Type I involves electron transfer to O_2 in solution which eventually leads to the formation of oxygen-containing radicals like superoxide anion ($^{\bullet}O_2^-$), hydroxyl ($^{\bullet}OH$) (step 5). In the Type II, energy transfer occurs from $^3T^*$ state of the PS to the triplet ground state of O_2 and results in generation of the highly reactive singlet oxygen ($^1O_2$) (step 6) [129–131]. Both photochemical pathways (Type I and Type II) can take place simultaneously, but it is the chemical properties of PS (especially its redox characteristics) and the concentration of O_2 that determine the balance between them [132]. A less common photoreaction that PS can undertake is the Type III involving photocleavage DNA through direct electron abstraction from DNA bases (step 7) [131].

3. Models substrates and instrumentations employed

3.1. Substrates models

Before reviewing DNA/RNA-cleaving metal complexes in section 5, it is useful to first elaborate on the typical nucleic acids models used in various *in vitro* cleavage experiments. Inevitably, to smoothly realize mechanistic or applicative features, these experimental substrates have to be easy to study - easy to obtain DNA/RNA models. There are two main points of bisection in the backbone of nucleic acids, the phosphate and the sugar moieties, the latter being either ribose or deoxyribose. Consequently, the types of substrates can be addressed in three main classes as follows:

3.1.1. Activated phosphoester models

To probe the phosphoesterase-like activity of the AMSs, synthetic phosphate ester models are employed as the substrate. Fig. 3 (A) depicts the most commonly used phosphoester models. The representative phosphomonoester mimic 4-nitrophenyl phosphate (NPP) [67,84–85] and phosphodiester mimics bis(4-nitrophenyl) phosphate (BNPP) [60,69,74,79] and bis-(2,4-dinitrophenyl) phosphate (BDNPP) [57,75–76,78] are used for mimicking the nature of various phosphoester bonds. While all

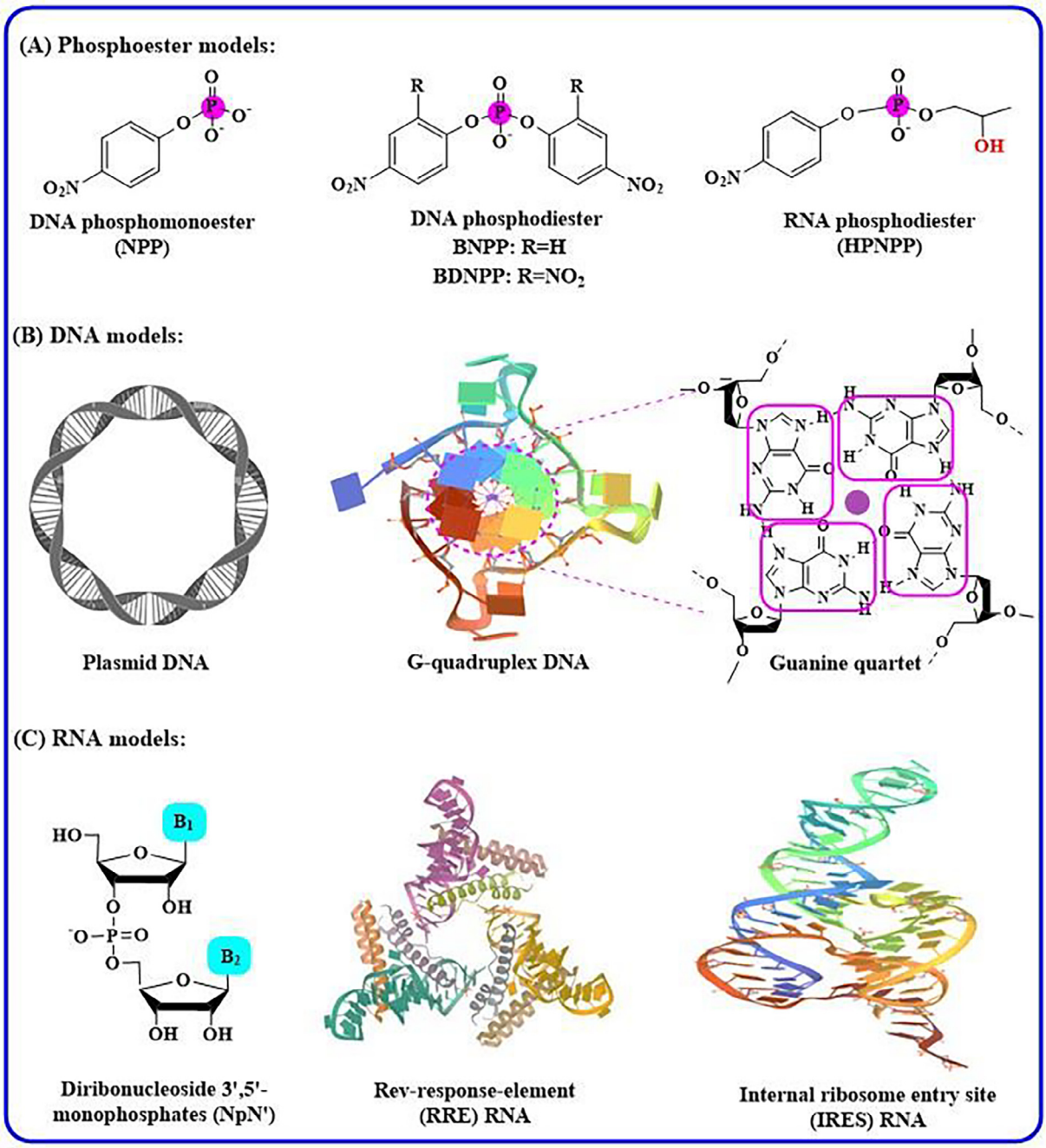

Fig. 3. (A) Typical activated phosphoester models: NPP, BNPP, BDNPP, and HPNPP. (B) DNA models: Plasmid DNA and the human telomeric G-quadruplex DNA (the crystal structure of G4 (PDB: 1KF1) and structure of guanine quartet). (C) RNA models: The structure of diribonucleoside 3′,5′-monophosphates as well as the crystal structures of RRE RNA complex (PDB ID: 4PMI) and HCV IRES pseudoknot domain (PDB ID: 3T4B).

the above play a typical deoxynucleotide role, 2-hydroxypropyl 4-nitrophenyl phosphate (HPNPP) has a hydroxyl group on the side chain displaying an RNA analogue. This internal nucleophile is employed to play the role of RNA's 2′-OH which is involved in a transesterification reaction in hydrolytic cleavage [63,74,83].

3.1.2. DNA models

3.1.2.1. Plasmid DNA. Plasmids are extrachromosomal, circular, and double-stranded DNA (so called supercoiled form) which frequently used in DNA cleavage studies (Fig. 3 (B)). These inheritable small DNA molecules are routinely found in prokaryotes and typically carry genes of secondary metabolism. Plasmids have a wide range of lengths, roughly from 1 to 100 kbp [96,99,108,115].

3.1.2.2. G-quadruplex DNA. Arms of the human chromosomes end with telomeres, which contain multiple repeats of the unique sequence d(TTAGGG). Telomeres have a vital role in cell prolifferation and the protection of the chromosomes from damage. Human telomeric DNA has the tendency to form intramolecular G-quadruplex (G4) structures that is a four-stranded DNA secondary structure usually formed in guanine-rich regions [133–134]. Fig. 3 (B) represents the top view of crystal structure of the human telomeric quadruplex (PDB ID: 1KF1) [134] as well as a G-quartets structure which involves a very stable planar orientation of the four guanine bases that are tied by Hoogsteen hydrogen bonds and further stabilized by monovalent metal cations (commonly K^+) [133–134].

One of the most important hallmarks of cancer cells is harboring a mutation resulting in the overexpression of telomerase, the enzyme responsible for the production of telomeric sequences. This allows the cancerous cells to circumvent natural telomere shortening and divide endlessly or "live forever". Today, telomeric sequences are targets for anticancer therapeutics [36–38]. In the literature G4 oligonucleotides of human telomeric DNA is used as a substrate model for G4 DNA–binding and –cleavage studies [36–38,135–138].

3.1.3. RNA models

3.1.3.1. Oligoribonucleotides. In some studies diribonucleoside 3′,5′-monophosphates viz. guanylyl-3′,5′-uridine (GpU), uridylyl-3′,5′-uridine (UpU), adenylyl-3′,5′-uridine (ApU), uridylyl-3′,5′-adenosine (UpA), adenylyl-3′,5′-adenosine (ApA), cytidylyl-3′,5′-adenosine (CpA), and guanylyl-3′,5′- adenosine (GpA) have been used as RNA models for cleavage activity studies (Fig. 3 (C)) [81–82].

3.1.3.2. Viral RNAs. Human immunodeficiency virus (HIV) and hepatitis C virus (HCV) have also been subjected to AMS-induced RNA cleavage studies. The Rev response element (RRE) of HIV RNA and internal ribosome entry site (IRES) of HCV RNA have been employed as a model for RNA cleavage studies [46–49]. Fig. 3 (C) depict the crystal structures of HIV RRE (PDB ID: 1CSL) and HCV IRES (PDB ID: 3T4B).

RRE has been exploited in numerous studies involving AMSs due to its critical role in viral mRNA export and HIV replication. RRE is an approximately 350 nucleotide stretch of the viral RNA, a highly conserved and structured region and a *cis*-acting RNA element which located in the *env* gene. RRE folds into a secondary RNA structure characterized by five distinct stem-loops (I–V) [139–142]. The Rev is a virally-encoded and conserved protein that has 116-amino acids and can penetrate the cell nucleus and recognize the RRE. Indeed, this small regulatory protein is essential for virus viability [142].

IRES of HCV RNA is a highly structured 5′-untranslated region (5′ UTR), consists of 341 nucleotides. IRES folds into a secondary structure that consisting of four distinct stem-loops (I– IV). HCV translation is started by a cap-independent mechanism from IRES which contains the sequence and structural elements responsible for this process [143–145].

3.2. Instrumentations

Efficient investigation of nuclease activity of a compound would definitely depend on techniques applicable to the determination of active intermediates, scission products, the reaction mechanism and kinetics. In this section, the methodologies utilized in the field of cleavage activity are discussed.

3.2.1. UV–Visible spectroscopy

The catalytic scission of phosphate ester models by the AMSs at particular pH can be monitored spectrophotometrically by tracking the changes in absorbance at 400 nm. As seen in Fig. S1 (A) (in supplementary file), when the DNA phosphate ester models undergo hydrolysis, the scission product 4-nitrophenolate ion (NP) is produced. The chromophore NP has a characteristic band around 400 nm in UV–Vis spectra, whilst the absorbance of the intact ester substrate at 400 nm is negligible [69,75–76]. Thus, the hydrolysis rate can be measured by UV–Vis spectrophotometry probing the formation of NP, usually measured at regular intervals. As shown in Fig. S1 (B) (in supplementary file), also HPNPP (RNA model) undergoes intramolecular transesterification and finally releases the NP ion [83] making the progress suitable for UV–Vis monitoring.

3.2.2. Gel electrophoresis

Agarose gel electrophoresis (AGE) is the most commonly used method for the investigation of the cleavage activity of AMSs. AGE provides a straightforward, low-cost, and relatively accurate tool to separate plasmid conformations for quantification assay. All isoforms of a typical plasmid DNA have the same size and charge but they conform to different shapes. Plasmid DNA is naturally found in a compact supercoiled (SC, or form I), so its hydrodynamic size is much smaller and its electrophoretic mobility is greater than the other two isoforms. When a nick occurs within one of the strands of the supercoiled plasmid and this phenomenon converts SC to a semi-relaxed form, open circular form (OC, or form II). The electrophoretic mobility of this isoform is smaller than other forms and can be readily separated from the supercoiled species which is more compact. When the second scission happens in close proximity (12 bp distance) to the first, linear form (L, or form III) of the plasmid is produced that has an intermediate mobility between the SC and OC forms [23]. These phenomena are clearly presented in the electrophoretic image shown in Fig. 4. Thus, the cleavage activity of artificial nucleases is their practical ability to convert the SC form into OC and/or L forms [23,127]. In order to gain further insight and identify possible ROS into the cleavage mechanism, reactions performed with ROS-specific scavengers/quenchers for example potassium iodide (KI) as a H_2O_2 scavenger, DMSO and EtOH as hydroxyl radical scavengers, sodium azide (NaN_3) as a singlet oxygen quencher, superoxide dismutase (SOD) as the superoxide anion radical scavenger, and pyruvate as a hydrogen peroxide scavenger [27–31].

While agarose gel is routinely used to separate different conformations of plasmid DNA, polyacrylamide gel electrophoresis (PAGE) is applied to separate shorter nucleic acid oligos such as G4 DNA [36–37,135–138].

3.2.3. Nuclear magnetic resonance (NMR)

The hydrolysis reaction of phosphate ester models catalyzed by AMSs can also be monitored by ^{1}H NMR and ^{31}P NMR spectroscopy [63,146–148]. For example, when ^{1}H NMR of NPP hydrolysis reaction is recorded at certain time intervals, it initially indicates two doublets which gradually disappear as the reaction proceeds.

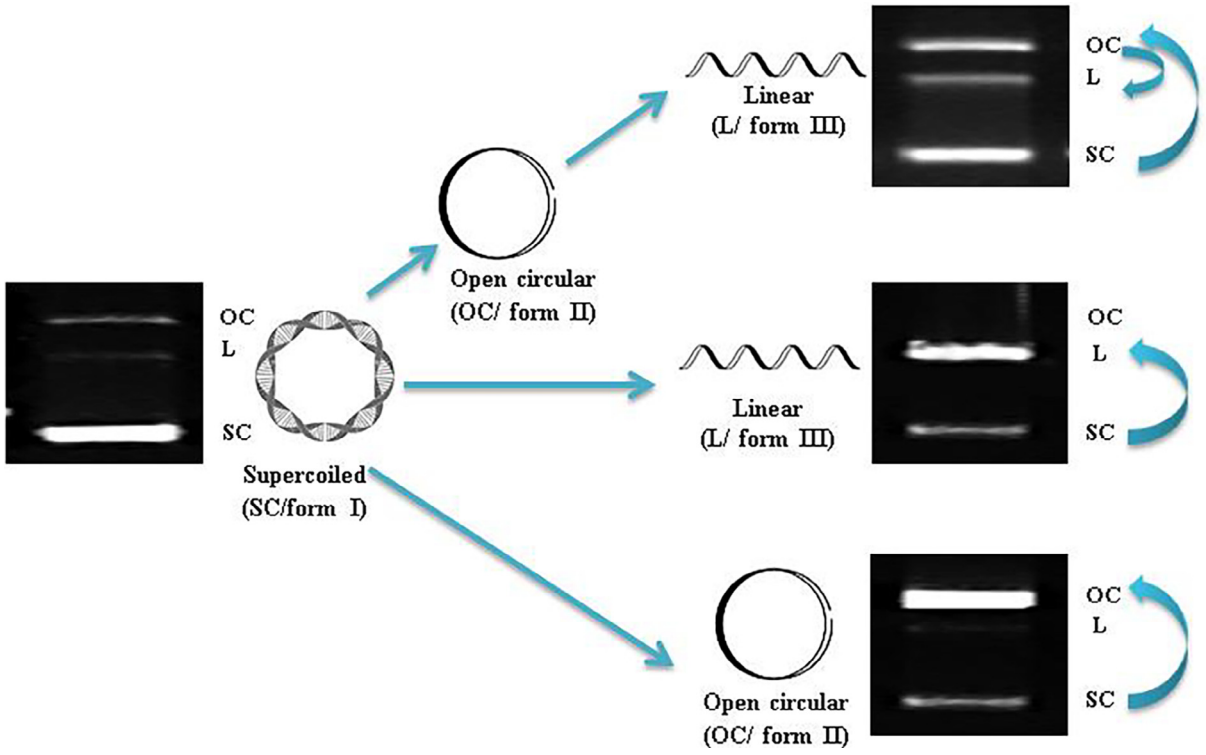

Fig. 4. The cleavage process of the supercoiled plasmid DNA into open circular and/or linear forms and corresponding gel electrophoresis images [23,127].

Instead, two new doublets assignable to the newly formed hydrolysis product NP appear. Moreover, upfield shifts of the NP resonances to higher energy zone (right side) of the NMR spectrum is observed which can be assigned to the presence of the hydroxyl group rather than the phosphate group in NPP [146].

3.2.4. Electron paramagnetic resonance (EPR)

EPR spectroscopy is an analytical technique relying on singlet electrons of free radicals for the detection of paramagnetic species through spin trapping. This provides a powerful procedure to identify the nature of ROS species in the nucleic acid cleavage process [149–150]. Since transient ROS generated in cleavage reactions are at too low quantity and also too short-lived to be directly detected, spin trapping compounds are employed to react with them and produce more stable and long-lived radical adducts enabling easy detection by EPR. One of the most commonly utilized spin traps is 5,5-dimethyl-1-pyrroline N-oxide (DMPO). Interestingly, DMPO is diamagnetic and does not signal in EPR, while after addition of free radical to its C = N bond and formation DMPO-adduct shows a characteristic EPR signal. An advantage of employing spin trapping is that not only quantifies the amount of radicals produced but also identify nature various radicals formed by profiling their spin adduct spectra (e.g., number of characteristic signals, intensities, and/or hyperfine splitting constants) [151–153].

3.2.5. Electrospray ionization-mass spectrometry (ESI-MS)

The hydrolysis reaction of phosphate ester models catalyzed by AMSs can also be monitored by ESI-MS [63,136,154]. Matrix-assisted laser desorption/ionization-time of flight mass spectrometry (MALDI-TOF MS) is an efficient technique for the elucidation of the NA-cleavage sites and products. Cowan and co-workers studied RNA cleavage by matrix-assisted laser desorption/ionization-time of flight mass spectrometry (MALDI-TOF MS) to determine products of RNA cleavage and the kinetics of the reaction [155].

3.2.6. Other techniques applied

In addition to the methodologies enlisted above, many other techniques have been utilized to evidence the process of nucleic acid cleavage promoted by various metal complexes. These include High performance liquid chromatography (HPLC) [69,156], fluorescence assay [157–158], atomic force microscopy (AFM) [159–160], dynamic light scattering (DLS) [161], linear dichroism [162], and electrochemical methods [163].

3.2.7. Theoretical methods

Despite extensive experimental studies concerning the NA-cleavage catalyzed by AMS's, theoretical methods have also been developed to systematically investigate these processes. Such theoretical methods on DNA cleavage activity of metal complexes have been performed using quantum mechanics calculations, density functional theory (DFT), molecular docking, and dynamic simulation methods. These methodologies are able to probe the mechanism of cleavage reaction through analysis of all the involved intermediates and transition states throughout the catalytic process. These methods are able to predict the effective factors on the nuclease activity of AMSs [164–174]. Moreover, the photophysical properties of metal complexes suitable for the use in PDT have been investigated by DFT and time-dependent DFT (TD-DFT) approaches [175].

4. Therapeutic applications of metalloscissors

This section addresses the applications of AMSs as DNA– and RNA–targeting therapeutics that have been proposed for the cure of some human diseases and/or are currently under *in vivo* investigation by the research community.

4.1. Cancer therapy

One the most typical examples of catalytic metallodrugs is the anticancer bleomycins (BLMs) family; a group of glycopeptide-derived "antitumor antibiotics" produced by several *Streptomyces* species. BLM displays significant intrinsic anticancer activity, and is in clinical use for the treatment of various cancers. In bleomycin structure, metal ions tightly coordinate to donor atoms and form the complex, hence the name metalloantibiotics. BLMs rely on metal ions to properly interact with biomolecules and perform their biological activities so that removal of metal ions causes BLM deactivation and/or structure changes [176]. The bleomycin family congeners share a core structure but differ in their sugars and positively charged region on bithiazole tails. As seen in Fig. 5 (A), the general structure of BLM contains four functional domains: (i) A metal-binding domain which contains nitrogen atoms that can be coordinated to metal ions. (ii) A DNA-binding domain consisting of peptidyl bithiazole tail and C-terminal amine tail. (iii) A linker peptide domain connecting the metal-binding and DNA-binding domains. (iv) A disaccharide domain consisting of glucose and mannose sugars [176–177]. However, similarly to many other natural products, BLMs exist as a mixture of several congeners. For

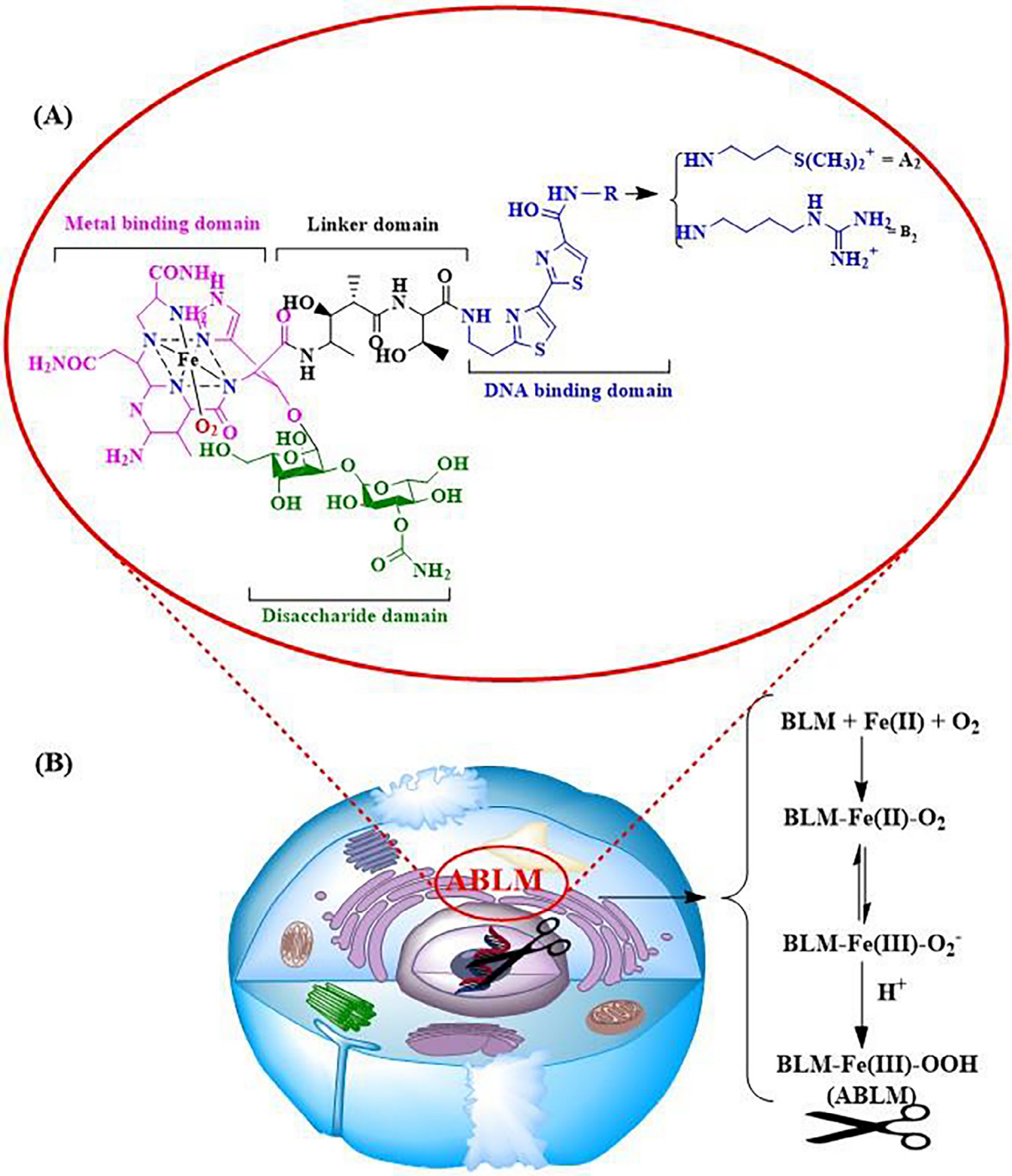

Fig. 5. (A) Structure of activated bleomycin and its functional domains: The metal-binding domain (pink), the linker domain (black), the DNA binding domain (blue), and the disaccharide domain (green). (B) Formation of activated bleomycin (ABLM) and cleavage of interacellular DNA [176].

instance, Blenoxane® which is the commercial form of BLM consists mainly of bleomycins A2 and B2, differing solely in the structure of the C-terminal tail [177].

Functionally, oxygen activation and site-specific DNA cleavage is assigned to the BLM's metal binding domain. According to BLM crystal structures, this domain acts as a five-coordinated ligand with affinity to bind metal ions (Fig. 5 (A)). The metal-BLM coordination involves four equatorial N atoms; these include an imidazole nitrogen, a deprotonated amide, a pyrimidine nitrogen, and the secondary amine of the β-aminoalanine. The fifth, an axial ligand, also comes from the primary amine of the β-aminoalanine [176–177]. BLM can coordinate to a variety of metal ions such as copper, manganese, vanadium, iron and cobalt to form metal-BLM complex, but *in vivo* the Fe(II)•BLM complex is reportedly the most dominant [178]. In addition, BLM's interaction with DNA *via* intercalation or fitting into the minor groove has been assigned to the DNA binding domain, where the presence of the positive charge on the bithiazole tail enhances the electrostatic binding between bleomycin and DNA. Finally, the sugar domain plays the key role for selective uptake of BLM by tumour cells [176].

The mechanism of BLM activation cycle by Fe(II) and O_2 and oxidative DNA cleavage have been extensively reported [176–178]. To execute DNA cleavage, BLM requires being activated by a redox-active metal ion such as Fe(II) in presence of a molecular oxygen, both functioning as cofactors in DNA cleavage. Fig. 5 (B) depicts a detailed BLM activation cycle by Fe(II) ion and O_2 molecule. Accordingly, BLM-Fe(II)–O_2 is first formed from the reaction of BLM-Fe(II) with O_2. Then, the "activated bleomycin" (ABLM), BLM-Fe(III)–OOH, is generated *via* an electron transfer from Fe(II) to oxygen followed by addition of a H^+. The ABLM is the DNA cleaving/binding species. The ABLM causes oxidative cleavage of both single-stranded and double-stranded DNA. Strand scission by the ABLM is initiated through H atom abstraction from C4′ of the deoxyribose moiety to form intermediate sugar radical. Depending on oxygen availability, the intermediate cleavage reaction can proceed *via* two separate pathways and different scission products are generated [177–178].

Inspired by the vast therapeutic application of antibiotics such as antibacterial, antifungal, antiviral, and anticancer, which has made them very powerful and promising medical tools, enormous effort has been put in the preparation of AMSs as remarkable weapons against cancer and other challenging health issues, to be discussed in section 5.

AMSs as metal complexes are considered as ideal PS in PDT due to their *in vitro* effective DNA photocleavage [52–53]. The most important reason is that despite of organic PSs that just the $\pi\pi^*$ transitions lead to PDT effects, in the electronic spectrum of metal complexes four types of transitions may be observed which depend on the type of metal and ligands. These transitions include: (i) a single metal-centered (d – d transitions or ligand field (LF) states). (ii) a single ligand-centered (intraligand $\pi\pi^*$ transitions). (iii) Both the metal and the ligand(s) in charge-transfer states. The latter involves either metal-to-ligand charge transfer (MLCT) or ligand-to-metal charge transfer (LMCT) [130].

PDT non-invasively and selectively acts over the target tumor and consequently reduces systemic toxicity and the undesired side-effects of conventional therapeutic drugs [129–132,179]. Cancer photodynamic therapy (CPDT) is a promising, emerging, and successful alternative treatment for many cancers. Mechanistically, CPDT is a light-assisted chemotherapeutic treatment that actually comprises a synergic action of three individually less- or nontoxic components: light, oxygen and PS and eventually production of highly toxic species. The clinical process for CPDT initiates with an intravenous injection of an appropriate PS. The tumor is later irradiated with light at a specific wavelength window (600–900 nm). Through this, PS is excited and photoactivated [129–132]. The fate of this activated species and how it exerts its biological activity has already been discussed in the section **2.2.2.** Therefore, metal complexes possess many ideal features as PS and have received considerable attention. Promising examples of application of metal complexes as ideal PS agents for CPDT is going to be discussed in section 5.

4.2. Bacterial infections therapy

Infectious diseases are a significant cause of illness and mortality all over the world. Antibacterial drugs either belong to natural antibiotics (penicillins, cephalosporins, aminoglycosides, tetracyclines, and glyco- or lipo-peptides) or synthetic drugs (sulfonamides and quinolones). Antibacterial drugs exert their activity either by killing (bactericidal) or inhibition of the growth of bacteria (bacteriostatic) [180]. The most common mechanisms of action of antibacterial drugs embrace inhibition of cell-wall, protein, and essential metabolites biosynthesis as well as nucleic acid replication and transcription [180–182]. Antimicrobial agents, especially peptide antibiotics, have potent activity against many pathogens, including bacteria, fungi, parasites, and enveloped viruses [181]. Generally, bacteria are classified in two main types, Gram-positive (G^+) and Gram-negative (G^-), which mainly differ in membrane permeability. G^- bacteria have a cell-wall constructed from an inner plasma membrane, a thin layer of peptidoglycan, and an outer membrane, while a typical G^+ bacterial cell possesses a thick cell wall with many peptidoglycan layers. Consequently, it is this structural diversity that is mostly responsible for the different antimicrobial activity seen for medicines on these two G^+ and G^- bacteria [183].

However, the use of antibacterial drugs for treatment of patients is limited because the bacterial resistance [180,182] which is developed and spread more quickly than the antibacterial drug development. Many antibiotics like members of tetracyclines have already been exhausted to a high extent. Consequently, it is vital to focus on discovery of new antibacterial drugs that destroy pathogens through novel modes of action with minimal damage to the host. AMSs have been investigated as promising new drug leads against bacterial infections through DNA cleavage [39–45,184–185].

Currently, PDT is attracting special attention as a promising and novel strategy to treat cancers or inactivate pathogenic microorganisms (bacteria, viruses, fungi, and parasites), where it earns another name, microbial infections photodynamic therapy (MPDT). According to increasing number of pathogens resistant towards commonly used antibiotics, MPDT seems to be a very hopeful substitute to conventional antibiotics [186–189]. Metal complexes due to their effective DNA photocleavage ability are suitable candidates as PS in MPDT. This indeed envisions the presence of AMSs as antibacterial agents on the market in near future. Other examples of AMSs will be discussed in section 5.

4.3. Viral infections therapy

HIV and HCV are human pathogens that belong to retroviruses and carry their genetic material as RNA instead of DNA. HIV causes acquired immunodeficiency syndrome (AIDS) in humans, a disease that destroys the immune system and can eventually lead to death of the infected persons [140]. HCV, in turn, is a major causative agent of chronic liver disease, a condition which can eventually lead to hepatocellular carcinoma or outright liver failure if left untreated [144]. Although these viral diseases are managed with current antiretroviral therapies, but their retrovirus nature and also high rate of replication and mutation have placed them in the forefront worldwide epidemic diseases and make their treatment even more challenging. Therefore, new drugs with different

modes of action are needed. A novel therapeutic strategy involves development of RNA-targeting catalytic metallodrugs that could promote cleavage of RNA and consequently inhibit its replication [46–49]. More examples of application of metal complexes as antiviral agents is going to be discussed in section 5.

With the growing number of viruses resistant towards commonly used antiviral drugs, similar to antibiotic resistance, is also a present cause of concern. Therefore, the PDT of viruses can be considered as an alternative and promising tool in antiviral treatments [190].

5. AMSs in pharma studies

Inspired by natural metallonucleases, a great deal of metal complexes have been designed and submitted to vigorous studies as AMSs aimed to scissor cellular nucleic acids. Chemically the ligands employed for this purpose contain multidentate N–donor and/or O–donor atoms and have shown potential efficacies for preparation of artificial metalloscissors with medical application outlook. This section of our review is divided into three subsections based on the nature of ligands frequently exploited. These include polypyridyl ligands, peptide ligands, and ligands derived from known antibacterial and non-steroidal anti-inflammatory drugs.

5.1. Polypyridyl ligands

Ligands containing polypyridyl moieties are heterocyclic uncharged species with N–donor atoms resembling pyridine and able to coordinate transition metals. Examples of simple polypyridyl ligands extensively used as metal chelating ligands include 2,2′-bipyridine (bpy), 1,10-phenanthroline (phen), and 2,2′:6′,2″-terpyridine (tpy) (Fig. 6). A notable illustration is phen-copper(I)

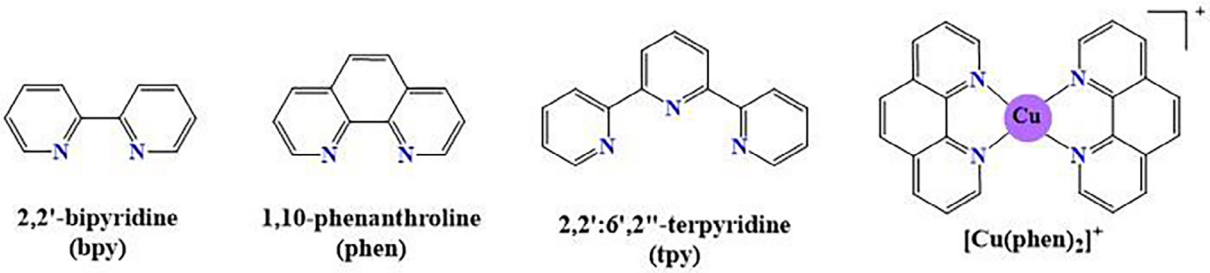

Fig. 6. The molecular structures of polypyridyl ligands (bpy, phen, and tpy); and $[Cu(phen)_2]^+$ [19].

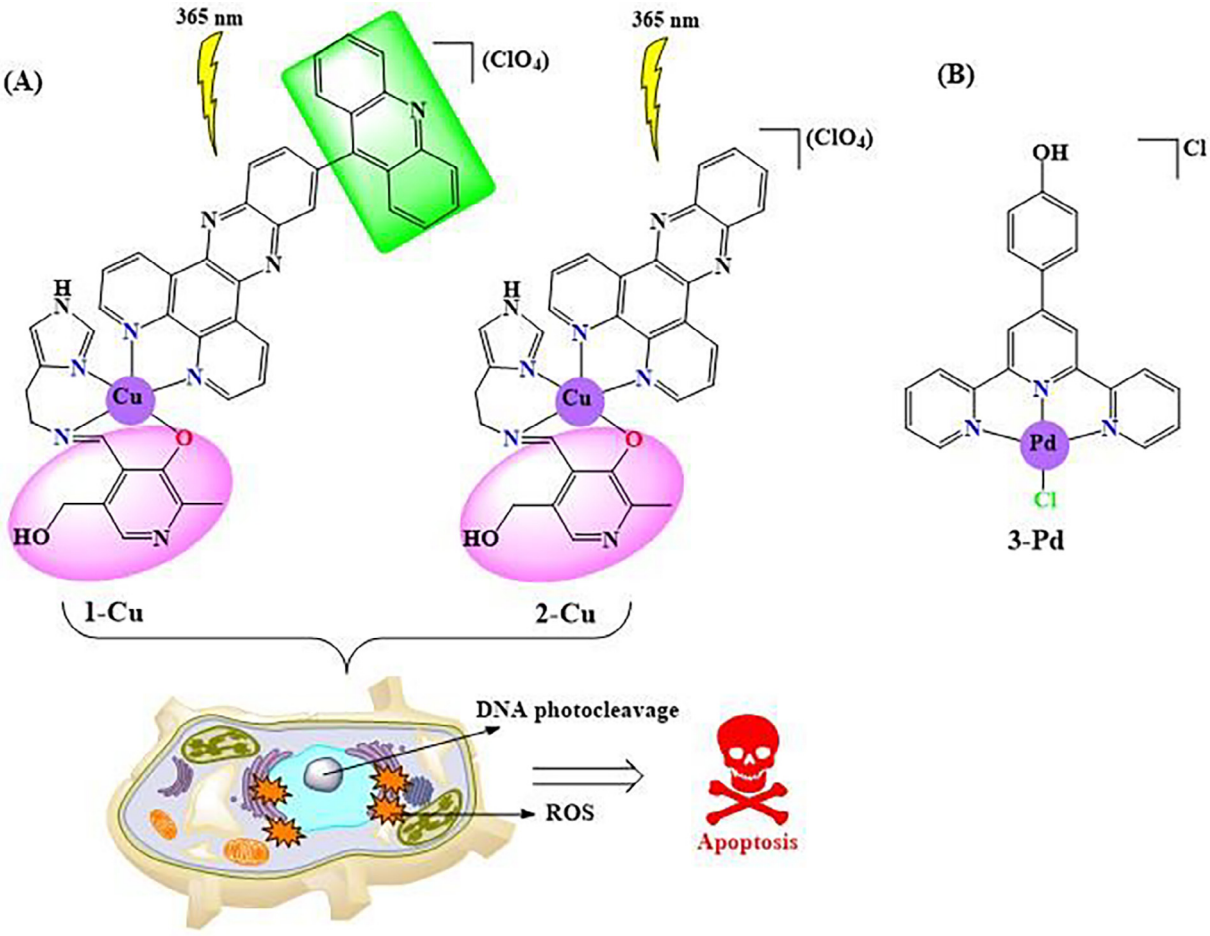

Fig. 7. (A) The molecular structures and proposed mechanism of anticancer activity of $[Cu(L1)(acdppz)]^+$ (**1-Cu**) and $[Cu(L1)(dppz)]^+$ (**2-Cu**) [191]. (B) The molecular structure of $[Pd(OHPh\text{-}tpy)Cl]^+$ (**3-Pd**) [192].

complex, $[Cu(phen)_2]^+$ (Fig. 6), which is the first AMS with ability of DNA cleavage through oxidation of deoxyribose ring [19].

5.1.1. Mononuclear polypyridyl complexes

In 2016, the biological properties of Cu(II) complexes containing photoactive acridine-dppz (ac-dppz) moiety were investigated by Nandi and Chakravarty et al. [191]. They prepared Cu(II) complexes coordinated to the dppz-based ligands and a vitamin B6-derived Schiff base (L1), $[Cu(L1)(ac\text{-}dppz)]^+$ (**1-Cu**) and $[Cu(L1)(dppz)]^+$ (**2-Cu**), where dppz is dipyrido[3,2-a:2′,3′-c] phenazine, Fig. 7 (A). Their compounds were efficient photo-cleavers of pUC19 DNA in UV-A light (365 nm). Significant photocytotoxicity imposed to the human cervical (HeLa) and breast (MCF-7) cancer cells by **1-Cu** and **2-Cu** upon visible light exposure with IC_{50} values ranging from 0.36 to 5.3 μM, while being relatively less toxic in the dark. Nonetheless, both complexes performed less cytotoxic in non-transformed human epithelial lung cells (HPL1D). In terms of mechanisms, their results indicated that **1-Cu** generates intracellular ROS in HeLa cells and promotes cell death mainly through apoptotic pathway upon irradiation. Finally, **1-Cu** was found to be a better PDT agent than **2-Cu** with PI values, [photocytotoxicity index (PI) = IC_{50} (dark) / IC_{50} (light)] of 39 and 14 in HeLa and MCF-7 cells, respectively. In addition, the complexes illustrated more selectivity towards cancer cells putatively owing having vitamin-B6 moiety.

In the same year, Hadadzadeh and co-workers [192] investigated a water-soluble Pd(II) complex coordinated to a terpyridine derivative, [Pd(OHPh-tpy)Cl]Cl **(3-Pd)**, where OHPh-tpy is 4′-(4-hydroxyphenyl)-2,2′,6′,2″-terpyridine, Fig. 7 (B). Their results indicated that the complex has potential to effectively scissor pUC57 DNA through a hydrolytic mechanism. Also, **3-Pd** exhibited significant *in vitro* cytotoxicity against MCF-7, lung (A549), colorectal (HT-29), erythroleukemic (K-562), and hepatocellular (HepG2) cancer cells with IC_{50} values less than 9.5 μM. They suggested that this Pd(II) complex can be introduced as a new anticancer agent.

In 2017, in order to introduce an ideal PS with a strong absorption capability in the phototherapeutic window, Zhou and Wang et al. [193] prepared a ruthenium(II) complex, $[Ru(bpy)_2(Cl\text{-}7\text{-}IVQ)]^{2+}$ (**4-Ru**), in which Cl-7-IVQ is 5-chloro-7-(2-(1,3,3-trimethyl-3H-indol-1-ium-2-yl)vinyl)quinolin-8-olate, Fig. 8. The complex exhibited an efficient $^{\bullet}OH$-mediated DNA scission when exposure to light above 600 nm, and no cleavage in the dark. Interestingly, whilst **4-Ru** selectively and efficiently showed photoinactivation toward *E. coli*, it did not affect HeLa cells, projecting a selective photo-induced antimicrobial activity required for potential application as MPDT agents.

In the same year, new PDT agents with high target selectivity and ROS photogeneration capabilities were prepared by Silva Sousa's group [55]. They synthesized two Ru(II) complexes coordinated to dppz as an efficient DNA binding motif along with naphthyl- and anthracenyl-modified bipyridines as strong ROS generators, $[Ru(bpy)(dppz)(naphthyl\text{-}modified\ bpy)](PF_6)_2$ (**5-Ru**) and $[Ru(bpy)(dppz)(anthracenyl\text{-}modified\ bpy)](PF_6)_2$ (**6-Ru**), Fig. 8. These complexes demonstrated moderate selectivity toward G4 DNA but rather higher binding affinity to the DNA minor groove. The pendants of naphthalene and anthracene strongly influenced on the $^1O_2$ generation with high quantum yield result in the complexes exhibited DNA photocleavage activity even under yellow LED irradiation that supports their favorable use as PS agents in PDT. Moreover, the complexes exhibited strong antibacterial activity against G^+ bacteria (*S. aureus* and *S. epidermidis*) with MIC values (Minimum inhibitory concentration) in the range of 6.4 to 25.6 $\mu g\ mL^{-1}$, when coupled with a blue LED irradiation, supporting the introduction of these complexes as MPDT agents.

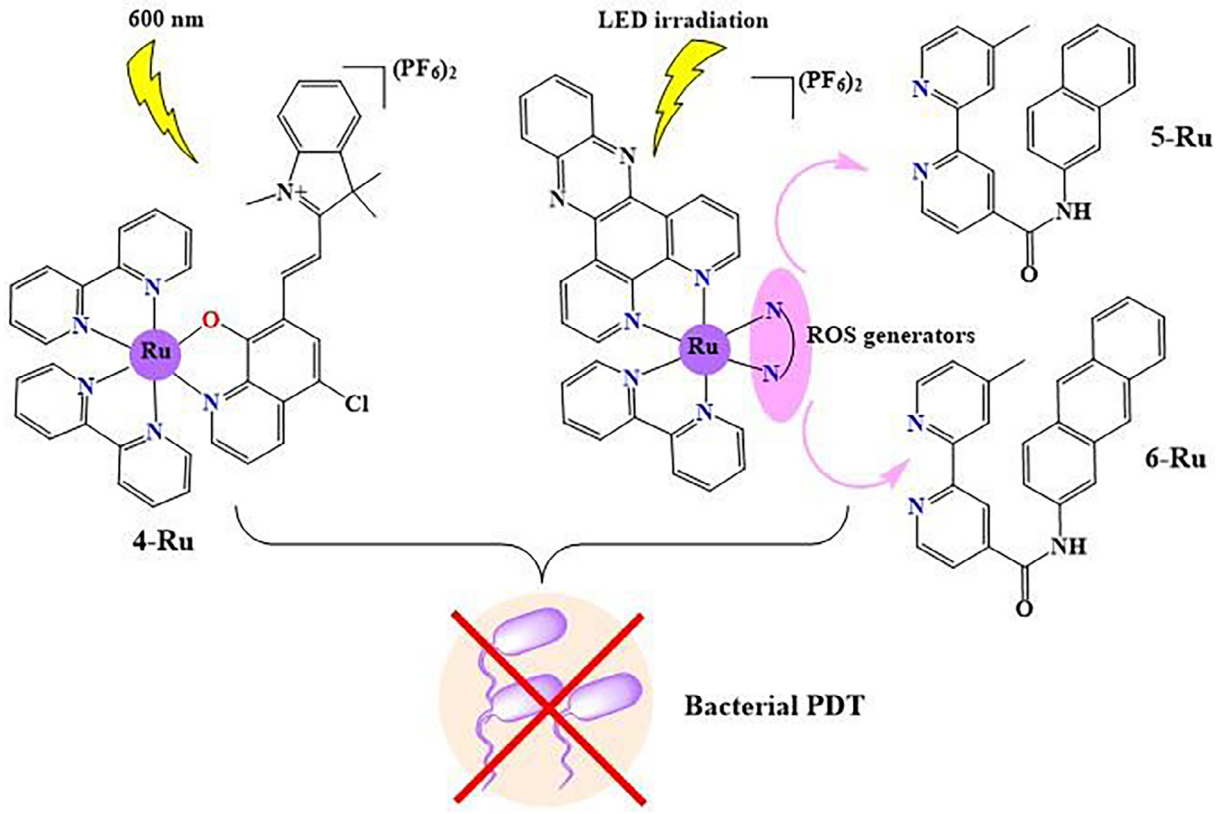

Fig. 8. The molecular structures and proposed mechanism of antibacterial activity of $[Ru(bpy)_2(Cl\text{-}7\text{-}IVQ)]^{2+}$ (**4-Ru**) [193] and $[Ru(bpy)(dppz)(naphthyl\text{-}modified\ bpy)]^{2+}$ (**5-Ru**) and $[Ru(bpy)(dppz)(anthracenyl\text{-}modified\ bpy)]^{2+}$ (**6-Ru**) [55].

In the same year, two Cu(II) complexes with terpyridine derivatives were studied by Manikandamathavan et al. [194]. They prepared [Cu(btp-tpy)(ClO_4](ClO_4) (**7-Cu**) and [Cu(bt-tpy)(ClO_4)] (ClO_4) (**8-Cu**), where btp-tpy is 4′-(benzothiophene)-terpyridine and bt-tpy is 4′-(Benzylthiazolyl)-terpyridine, Fig. 9 (A). The complexes **7-Cu** and **8-Cu** cleaved DNA differently *via* oxidative and hydrolytic pathway, respectively. According to them, both complexes exhibited significant cytotoxicity against triple negative human breast (CAL-51) and HepG2 cancer cells, while they were non–toxic towards normal liver cells. The complexes induced ROS generation and oxidative stress in cancer cells but not in normal cells. Furthermore, cell cycle analyses exhibited that the two complexes induce apoptosis by growth phase cell cycle arrest.

Functionalization of ligands with reactive substitutions bioconjugate with active protein-vectors is a novel strategy for the targeted drug delivery to carcinoma cells. These protein-vectors can recognize specific receptors on the surface of cancer cells. This strategy was published in 2017 by Martinez and co–workers [159], who investigated the effect of carboxyl group on the tpy and bpy ligands in Pt(II) and Ru(II) complexes, [Pt (carboxyphenyl-tpy)Cl]Cl (**9-Pt**), [Ru($bpy)_2$(carboxyl-methyl-bpy)] ($PF_6)_2$ (**10-Ru**) and [Ru(tpy)(carboxyphenyl-tpy)]($PF_6)_2$ (**11-Ru**),

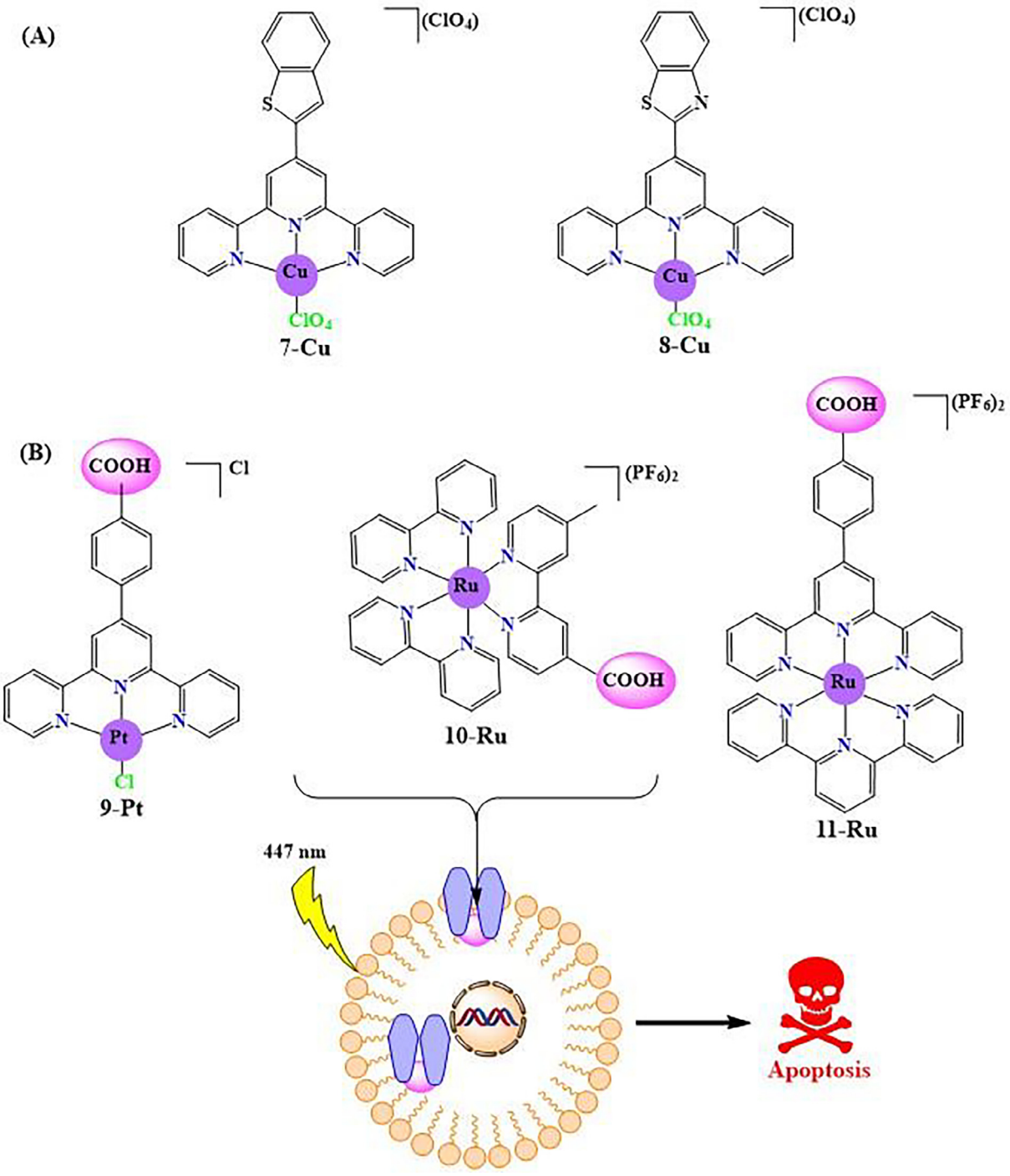

Fig. 9. (A) The molecular structures of [Cu(btp-tpy)(ClO_4)]$^+$ (**7-Cu**) and [Cu(bt-tpy)(ClO_4)]$^+$ (**8-Cu**) [194]. (B) The molecular structures and proposed mechanism of anticancer activity of [Pt(carboxyphenyl-tpy)Cl]$^+$ (**9-Pt**), [Ru($bpy)_2$(carboxyl-methyl-bpy)]$^{2+}$ (**10-Ru**), and [Ru(tpy)(carboxyphenyl-tpy)]$^{2+}$ (**11-Ru**) [159].

for conjugation to a carrier peptide, see Fig. 9 (B). The complexes **9-Pt** and **11-Ru** interacted with DNA *via* intercalation possibly due to the presence of the π-extended ligand carboxyphenyl-tpy, but complex **10-Ru** did not show any interaction. The results of AGE and AFM experiments indicated that the complexes are able to efficiently photocleave pUC18 DNA when irradiated at λ = 447 nm. Strikingly, the complex **9-Pt** caused significant dark cytotoxicity in MCF-7, pancreatic cancer (CAPAN-1), prostate cancer (PC-3), and colon adenocarcinoma (CACO-2) cells, but photocytotoxicity was not observed when irradiated. Also, the complex **9-Pt** induced apoptosis in PC-3 cells. Remarkable DNA photocleavage along with a noticeable increase in photocytotoxic activity was observed only for **10-Ru**, which supports its potential use as a PDT agent.

In 2019, our group [115] investigated structure–activity relationships of two Ni(II) complexes with substituted bipyridine ligand, $[Ni(dimethylbpy)_3](ClO_4)_2$ (**12-Ni**) and $[Ni(dimethoxybpy)_3](ClO_4)_2$ (**13-Ni**), where dimethylbpy is 4,4′-dimethyl-2,2′-bipyridine and dimethoxybpy is 4,4′-dimethoxy-2,2′-bipyridine, Fig. 10 (A). The complexes **12-Ni** and **13-Ni** indicated different biological activities, probably due to the different functional groups on their ligand being either a CH_3– or a CH_3O– group. The complexes oxidatively cleaved pET28a DNA in the presence of H_2O_2. The complex **12-Ni** exhibited more efficient DNA scission than **13-Ni** and hence represented a stronger chemical nuclease. The complexes **12-Ni** and **13-Ni** indicated cytotoxicity activity against MCF-7, HT-29, and glioblastoma (U-87) cells. The findings displayed a strong correlation between their cytotoxicity activity and DNA-binding affinity.

In the same year, Wang and co-workers investigated the role of the thiophenyl group in CPDT Figs. 1–28 [195]. They prepared a dithiophenyl-containing dpq-based mixed-ligand complex of Ru(II), $[Ru(bpy)_2(dt\text{-}dpq)](ClO_4)_2$ (**14-Ru**), where dt-dpq is 2,3-bis(thiophen-2-yl)pyrazino[2,3–f] [1,10]phenanothroline, Fig. 10 (B). This complex was able to scissor DNA by a photoinduced process through $^1O_2$ and $^{\bullet}O_2^-$ radical mediated pathway. **14-Ru** demonstrated $^1O_2$ generation in aqueous solution under irradiation with high quantum yields. It also showed high cellular uptake and quickly and selectively targeted mitochondria. Consequently, **14-Ru** indicated significant phototoxic effect against HeLa, MCF-7, and A549 cells upon irradiation with visible light, while was noncytotoxic in the dark. Their findings indicated that high phototoxic effect of **14-Ru** can be due to its ability in efficient generation of $^1O_2$ that cause induction of apoptosis in cells.

In 2020, Kondaiah and Chakravarty's group investigated tumor targeting of the biotin-conjugated complexes as photosensitizers for PDT applications [196]. Biotin belongs to the B vitamins (B7) and is known to be more efficiently uptaken by certain cancer cells. The group prepared two mixed-ligand ruthenium(II) complexes (**15-Ru** and **16-Ru**) containing a dipicolylamine (dpa) having PEGylated-BODIPY (boron-dipyrromethene) moiety and a phenanthroline derivative appended to the biotin unit, Fig. 11. The complex **16-Ru** showed significant pUC19 DNA cleavage under red light (660 nm) *via* $^1O_2$ generation as ROS, while no detectable cleavage in the dark. Even though the toxicity caused by these complexes in A549 was very low in the dark, while PI values of 2500 and 5000 were observed for **15-Ru** and **16-Ru**, respectively upon light exposure. The significant photocytotoxicity of these complexes may be due to high cellular uptake which in turn can be attributed to the PEGylated-BODIPY and biotin units. Thus, the complex **16-Ru** has all the essential properties of a PS agent and is therefore suitable for further studies aimed toward potential therapeutic applications.

In the same year, a reasonable strategy for design of a tris-heteroleptic Ru(II) complex containing polypyridyl ligands as promising PS for CPDT was investigated by Zhao and Gou' group [197]. They prepared a Ru(II) complex with dppn ligand **(17-Ru),** to achieve the strong absorption into the PDT window (600–850 nm), where dppn is benzo[*i*]dipyrido[3,2-*a*:2′,3′-*c*]phenazine, Fig. 12 (A). They investigated DNA photocleavage ability of **17-Ru** in comparison with its parent complex (**18-Ru**) under blue-(465 nm) and red-light (650 nm) irradiation. Their results indicated that **18-Ru** did not display any noticeable DNA photocleav-

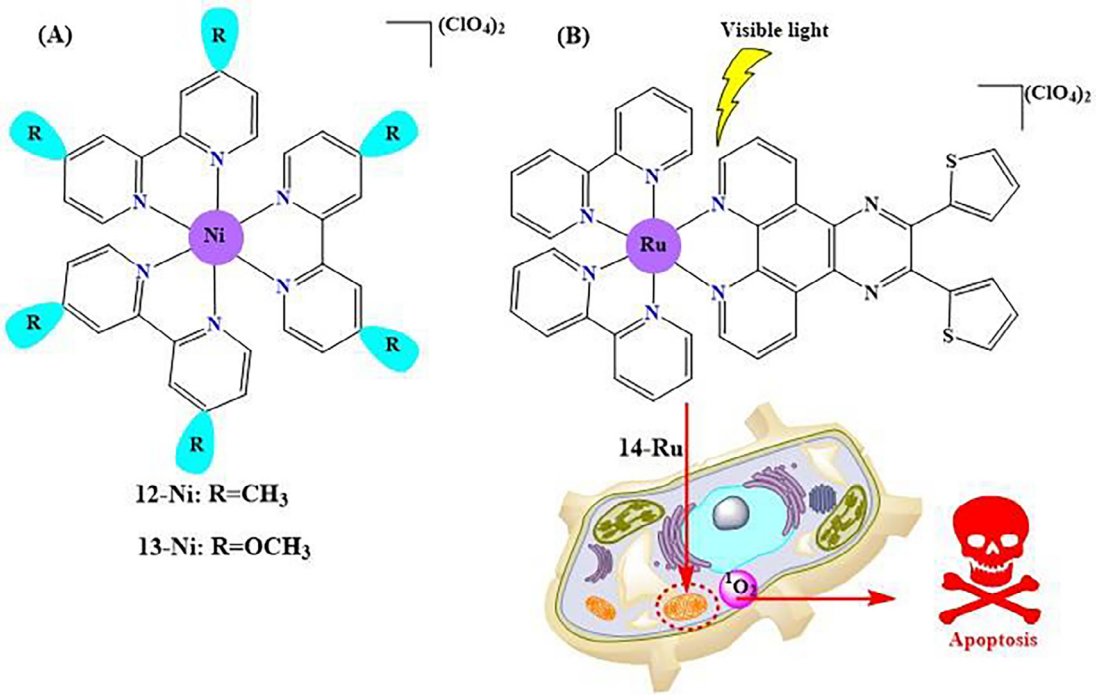

Fig. 10. (A) The molecular structures of $[Ni(dimethylbpy)_3]^{2+}$ (**12-Ni**) and $[Ni(dimethoxybpy)_3]^{2+}$ (**13-Ni**) [115]. (B) The molecular structure and proposed mechanism of anticancer activity of $[Ru(bpy)_2(dt\text{-}dpq)]^{2+}$ (**14-Ru**) [195].

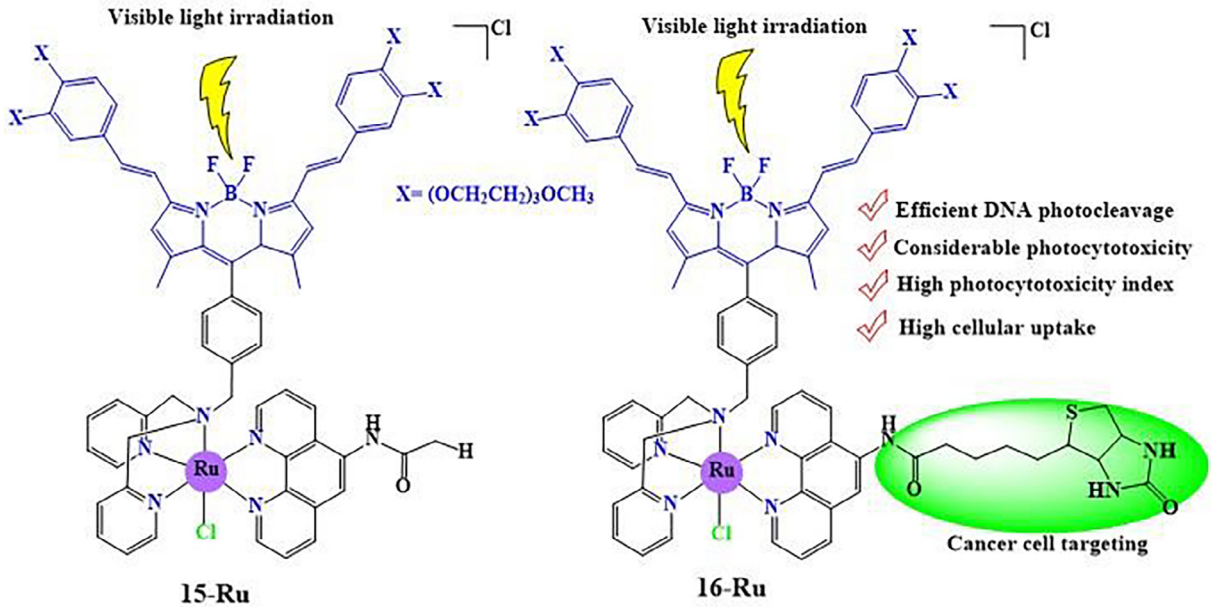

Fig. 11. The molecular structures of **15-Ru** and **16-Ru** [196].

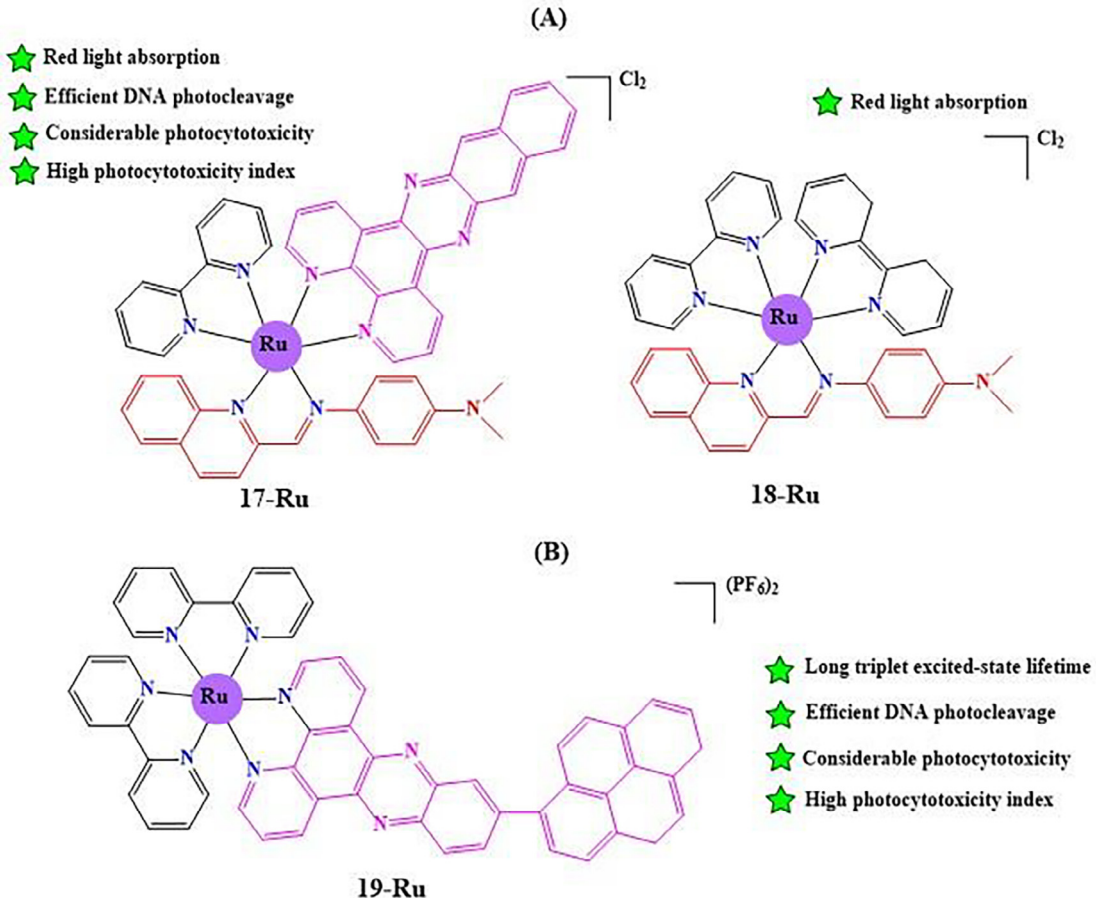

Fig. 12. The molecular structures of (A) **17-Ru** and **18-Ru** [197] and (B) **19-Ru** [198].

age, while **17-Ru** demonstrated significant DNA photocleavage activity when exposed to blue- and red-light irradiation. They deduced that the remarkable photocleavage activity of **17-Ru** may be due to its strong DNA binding affinity and generation of $^1O_2$. The complex **17-Ru** indicated considerable photocytotoxic effect against A549 and HepG2 cancer cells under both light irradiation, while photocytotoxicity of **18-Ru** was modest in blue-light irradiation. Results showed both complexes can induce apoptosis in A549 under blue- and red-light irradiation. In another report [198], they prepared a DNA targeting Ru(II)-polypyridyl complex

(**19-Ru**) by modification through linking of pyrenyl group on the dppz ligand, Fig. 12 (B). The complex exhibited considerable pBR322 DNA cleavage when exposed to light (460 nm). Their results demonstrated that **19-Ru** has a significant photocytotoxic effect in A549 and MCF-7 cells with IC_{50} values of 10 and 4 nM as well as large PI values of 1030 and 3004, respectively. Cellular ROS measurements demonstrated that **19-Ru** has the ability to induce ROS in MCF-7 cells upon light exposure. Their flow cytometry results also indicated that **19-Ru** induces apoptosis in MCF-7 cells when exposed to light.

5.1.2. Multinuclear polypyridyl complexes

In 2016, Wang's group investigated dinuclear Ru(II) complexes with varying lengths of bridging alkyl linkers [199]. They prepared Ru(II) complexes comprising the general formula of $[(bpy)_2Ru(L1)Ru(bpy)_2]^{4+}$, where L1 is 1,6-bis(3-(1*H*-imidazo[4,5–f] [1,10]phenanthrolin-2-yl)-9H-carbazol-9-yl)alkyl, structures **20-Ru$_2$**, **21-Ru$_2$**, and **22-Ru$_2$**, Fig. 13. The complexes effectively cleaved pUC18 DNA upon irradiation at 360 nm with efficiency order of **21-Ru$_2$** > **20-Ru$_2$** ≈ **22-Ru$_2$**. Interestingly, the cytotoxicity results indicated that **20-Ru$_2$** is more effective against the cancer cells than **21-Ru$_2$** and **22-Ru$_2$** under the same conditions. All of the complexes exhibited high cellular uptake and accumulated into the lysosomes. The cell cycle analyses revealed that these complexes induce the antiproliferative effect in HeLa cells through G0/G1 phase and in S phase arrest. Also, their findings indicated that **20-Ru$_2$** and **22-Ru$_2$** effectively induce apoptosis in HeLa cells.

In the same year, Smythe and Thomas' group [200] studied first water-soluble metallomacrocycles including Ru(II)– and Re(I)–polypyridyl units (**23-Ru$_2$Re$_2$**) as an intracellular $^1O_2$ photosensitizer, Fig. 14. The complex indicated significant cleavage of pBR322 DNA under illuminated condition (476 nm, 100 mW,

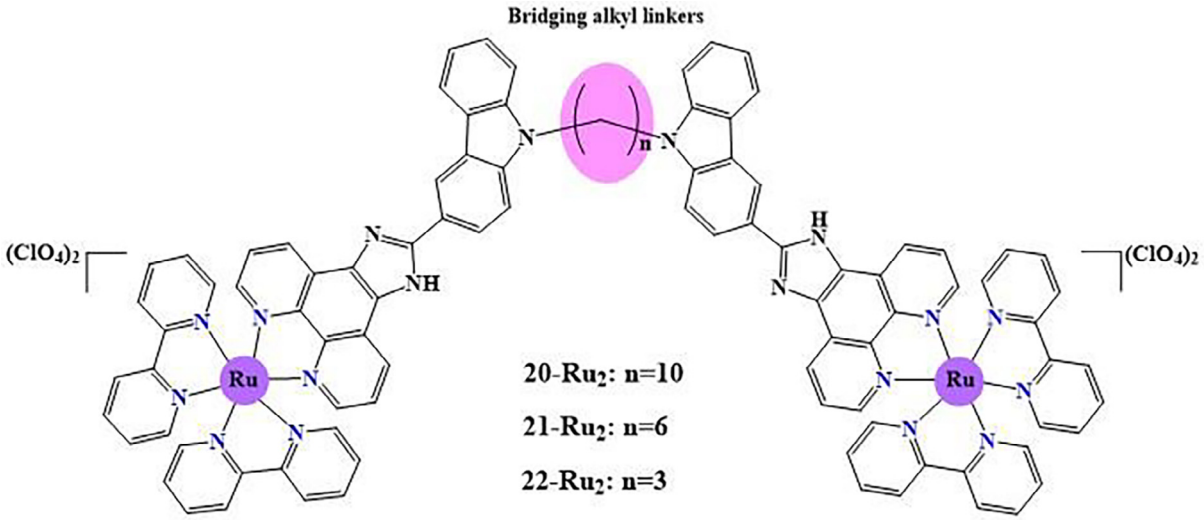

Fig. 13. The molecular structures of $[(bpy)_2Ru(L1)Ru(bpy)_2]^{4+}$ (**20-Ru$_2$**, **21-Ru$_2$**, and **22-Ru$_2$**) [199].

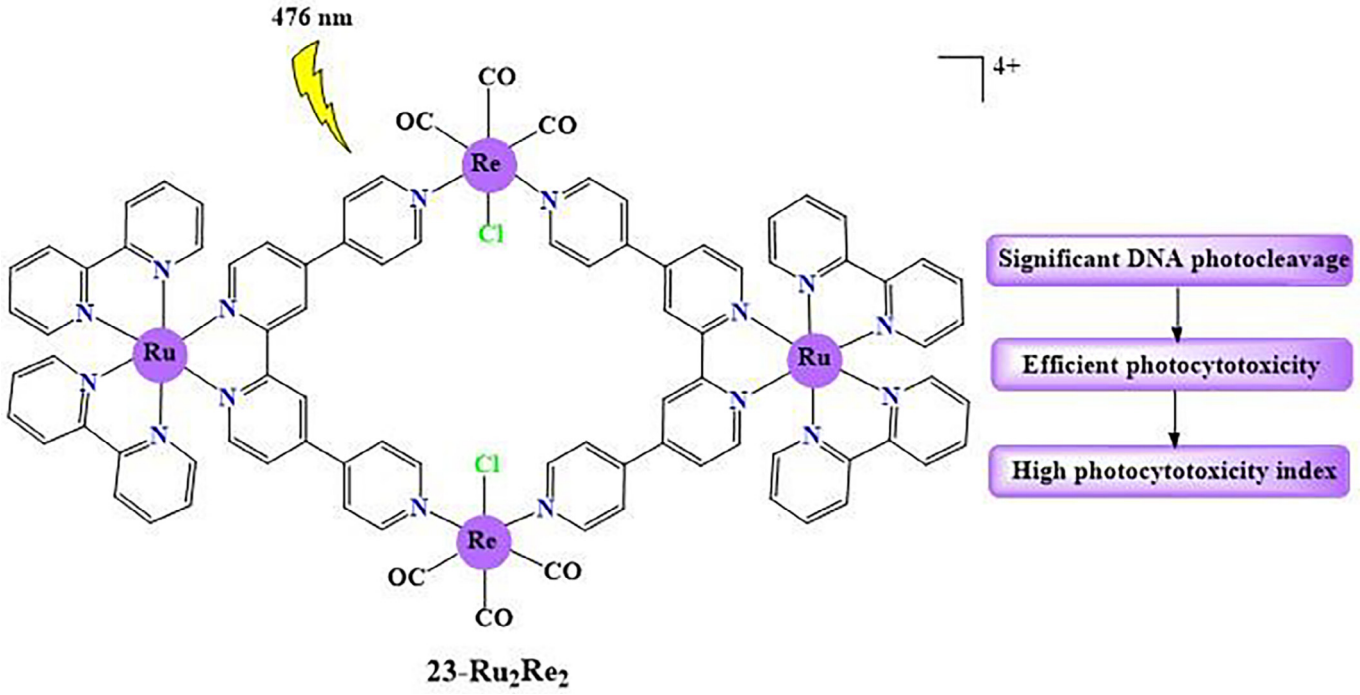

Fig. 14. The molecular structure of **23-Ru$_2$Re$_2$** [200].

10 min exposure), while in the dark no significant cleavage was observed, confirming necessity of light for nuclease activity. The *in vitro* cytotoxicity data showed that the complex **23-Ru$_2$Re$_2$** has lower cytotoxicity towards the cisplatin-resistant ovarian cancer cells (A2780cis) in the dark with IC_{50} value of 61.7 μM as compared to the dramatic photocytotoxicity with IC_{50} value of 0.3 μM when exposed to the higher light dose of 48 Jcm^{-2}. Therefore, PI value for **23-Ru$_2$Re$_2$** was 206. These findings support the potential of complex as a PS for CPDT.

Kondaiah and Chakravarty's group in 2016 investigated tumor targeting of the biotin-conjugated complexes [54]. They prepared biotinylated platinum(II) complexes with ferrocenylterpyridine (Fc-tpy), [Pt(Fc-tpy)(R)]Cl (**24-PtFe**) and [Pt(Fc-tpy)(R)]Cl (**25-PtFe**), and [Pt(Fc-tpy)(R)]Cl (**26-PtFe**), where R is biotinylated acetylide ligands or N-(prop-2-yn-1-yl)acetamide, Fig. 15. The complexes indicated photocleavage ability of pUC19 DNA upon irradiation at red light (647 nm) *via* the formation of hydroxyl radicals. The complexes could not cleave pUC19 DNA in the dark. Moreover, the complex **24-PtFe** exhibited higher photocytotoxicity in human breast carcinoma cancer cells (BT474) with IC_{50} of 7 μM than in the normal breast cells (HBL-100), while being essentially nontoxic in the dark (IC_{50} > 50 μM). The complexes **25-PtFe** and **26-PtFe** showed less photocytotoxicity with IC_{50} values of 16 μM. The authors concluded that better cellular uptake of **24-PtFe** due to the presence of a spacer moiety can be correlated with its improved cellular toxicity. All of the complexes showed ROS generation in BT474 cells only upon light exposure but not in the dark. The results indicated the key role of light irradiation in observed apoptotic cell death (65, 50, and 46% of early apoptosis for the complexes, respectively).

In 2017, Fernandes and Fernandez' s group [201] investigated dinuclear Ru(II) complexes with formula of $[\{Ru(bipy)_2\}_2(\mu\text{-}C_{12}H_8N_6)][CF_3SO_3]_4$ (**27-Ru$_2$**), $[\{Ru(bipy)_2Cl\}_2\{\mu\text{-}Ph_2P(CH_2)_2AsPh_2\}][CF_3SO_3]_2$ (**28-Ru$_2$**), $[\{Ru(bipy)_2Cl\}_2\{\mu\text{-}Ph_2P(CH_2)_4PPh_2\}][CF_3SO_3]_2$ (**29-Ru$_2$**), and $[\{Ru(bipy)_2Cl\}_2\{\mu\text{-}Fe(\eta^5\text{-}C_5H_4PPh_2)_2\}][CF_3SO_3]_2$ (**30-Ru$_2$Fe**), Fig. 16. The complexes interacted with CT-DNA through an intercalative mode, in particular, **28-Ru$_2$**, **29-Ru$_2$**, and **30-Ru$_2$Fe** and also induced some extent of pUC18 DNA degradation. The *in vitro* data indicated that the complexes have high cytotoxicity in human ovarian carcinoma (A2780) and MCF-7 cells. Their findings proved that the complexes have more selective and effective cytotoxic effect than cisplatin. Additionally, all the Ru(II) complexes could induce apoptotic cell death in A2780 cells. Cellular ROS measurements demonstrated that **28-Ru$_2$**, **29-Ru$_2$**, and **30-Ru$_2$Fe** have the capability to induce ROS in A2780 cells. Finally, *in vivo* toxicity assessments on zebrafish embryos indicated **27-Ru$_2$** seems to be the safest compound (see Fig. 16.

In 2017, Murugavel's group [202] synthesized a novel class of bimetallic copper(II) phosphate complexes, $[Cu(X\text{-}dipp)(py\text{-}tpy)]_2$ [X = H (**31-Cu$_2$**) and Br (**32-Cu$_2$**)] where X-dipp is 2,6-di*iso*propylphenyl phosphate and py-tpy is 4′-(4-pyridyl)-2,2′:6′,2″-terpyridine. These complexes can themselves act as metalloligands *via* the free pyridinic moieties present in their ligands (Fig. 17 (A)). Their DNA cleavage studies revealed that both complexes are effective in scission of DNA, but the activity of **31-Cu$_2$** was more significant than **32-Cu$_2$**, as it converted ~ 90% of SC form into L form. Also, both complexes indicated cytotoxicity against human colon cancer (HCT-116) and MCF-7 cells and induce apoptosis in HCT-116 cells but again the activity of **31-Cu$_2$** as an antitumor agent was superior to **32-Cu$_2$**.

In 2019, Conti and Giorgi et al. [203] reported two novel Ru(II) and Ru(II)/Cu(II) polypyridyl complexes containing a polyaaza-macrocyclic unit, $[Ru(phen)_2L]^{2+}$ (**33-Ru**) and $[Ru(phen)_2LCu]^{4+}$ (**34-RuCu**), where L is 4,4′-(2,5,8,11,14-pentaaza[15]-2,2′-bipyridi lophane, Fig. 17 (B). These complexes are highly water soluble because of the presence of 5 nitrogen atoms in L, which can readily undergo protonation in water. The complexes indicated high photocleavage activity with different mechanisms of action. The complex **33-Ru** exhibited single-strand nicks on the pUC19 plasmid DNA by generation of singlet oxygen, while **34-RuCu** caused double strand breaks *via* formation of ROS in a Fenton-like reaction involving the copper ion. No DNA cleavage occurred with **33-Ru** in the dark. In the dark, neither of the complexes showed cytotoxic effect but both displayed great photocytotoxicity when exposed to

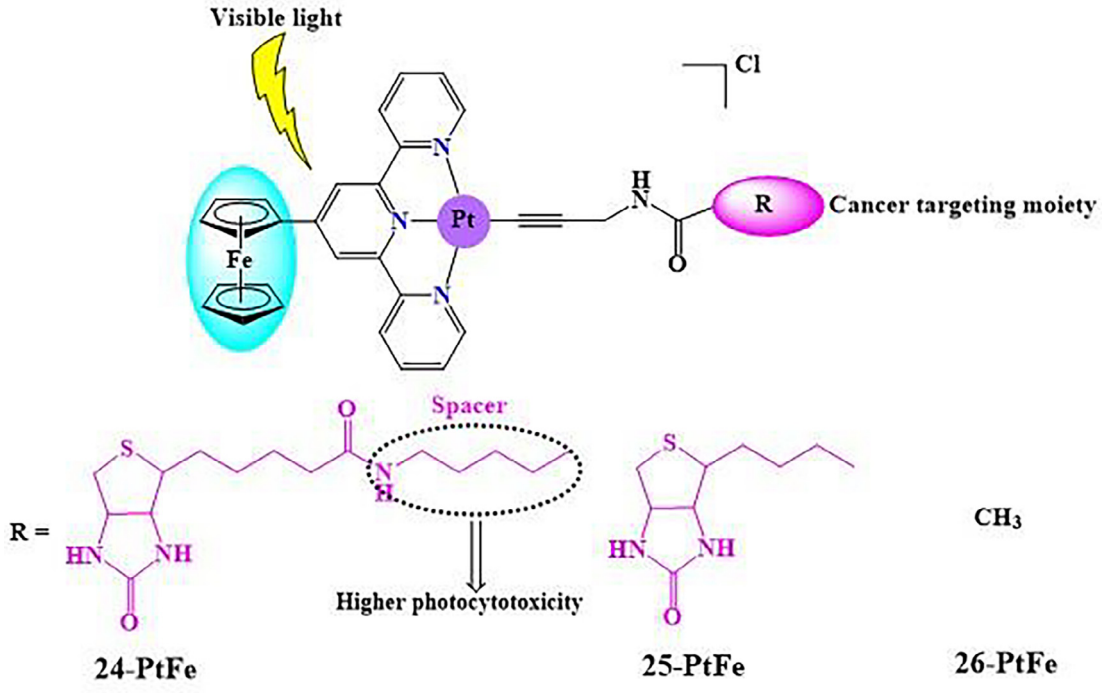

Fig. 15. The molecular structures of $[Pt(Fc\text{-}tpy)(L1)]^+$ (**24-PtFe**), $[Pt(Fc\text{-}tpy)(L2)]^+$ (**25-PtFe**), and $[Pt(Fc\text{-}tpy)(L3)]^+$ (**26-PtFe**) [54].

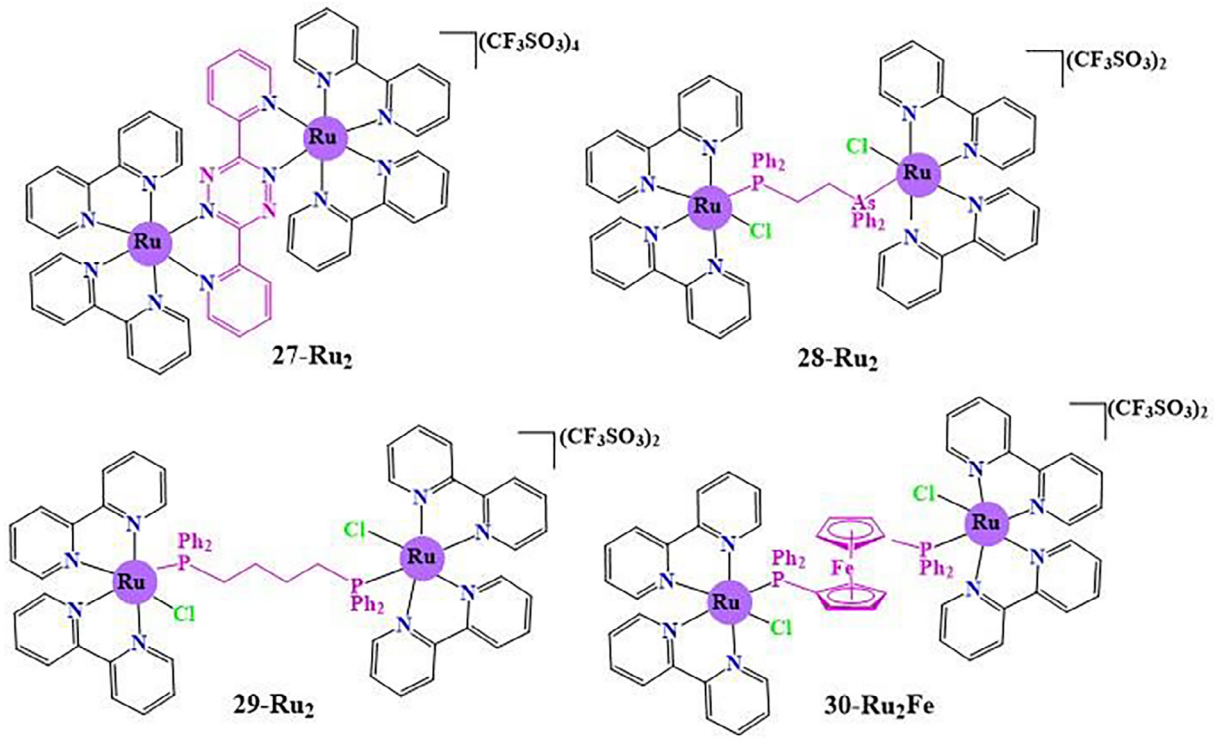

Compound	IC_{50} (*10^{-6} M) A2780	MCF-7	LC_{50} (mg/L) (Zebrafish embryos)
27-Ru_2	7.6	30.1	39.4
28-Ru_2	2.2	8.5	15.3
29-Ru_2	15.3	22.7	7.0
30-Ru_2Fe	1.6	4.1	5.4

Fig. 16. The molecular structures as well as *in vitro* and *in vivo* toxicity results of **27-Ru_2**, **28-Ru_2**, **29-Ru_2**, and **30-Ru_2Fe** [201].

light. Moreover, **34-RuCu** exhibited higher photo-induced cytotoxicity than **33-Ru** in human melanoma cells (A375), supporting the fundamental role of the Cu(II) ion in biological activity of such compounds. Their findings supported a promising strategy for preparation of efficient PS agents in PDT. In 2021, they investigated antimicrobial activity of **33-Ru** and **34-RuCu** as well as **35-Ru** and **36-$RuCu_2$** (Fig. 17 (B)) against G^+ bacteria (B. *subtilis*) in the dark and under light-iiradiation [204]. In the dark condition, the mixed Ru^{2+}/Cu^{2+} complex (**34-RuCu)** showed higher antibacterial ability than **33-Ru** at 3.12 μM while at higher concentrations both of them exhibited a similar antibacterial effect. Significant difference in their activity were not observed upon irradiation with LED light. Moreover, their antibacterial efficacy did not improve upon irradiation relative to measurements achieved under dark.

Nonetheless, one can find an array of more AMSs comprising of polypyridyl ligands in the literature. A few further instances of such complexes are summarized in the Table 1.

5.2. Amino acid and peptide ligands

Amino acids- and peptides-based AMSs have revealed a new strategy for DNA- and RNA-targeted metallodrugs. Such metal–peptide conjugates have potency to perform sequence-specific DNA-binding and -cleavage in a manner similar to transcription and recognition processes carried out by enzymes [216].

5.2.1. Amino acids and peptides

For design of amino acids-based AMS, they can usually act as bidentate ligands through their amine and carboxyl groups. Amino acids include Alanine (Ala/A), Arginine (Arg/R), Asparagine (Asn/N), Aspartic acid (Asp/D), Cysteine (Cys/C), Glutamic acid (Glu/E), Glutamine (Gln/Q), Glycine (Gly/G), Histidin (His/H), Isolucine (Iso/I), Lysine (Lys/K), leucine (Leu/L), Methionine (Met/M), Phenylalanine (Phe/F), Proline (Pro/P), Serine (Ser/S), Theronine (Thr/T), Tryptophan (Trp/W), Tyrosine (Tyr/Y), and Valine (Val/V).

In 2016, Iranzo and co-workers [217] studied two Cu(II) complexes, [Cu(L1)Cl] (**50-Cu**) and [Cu(L2)Cl] (**51-Cu**), where L1 and L2 are 2-carboxy-phen unit that covalently attached to the amino group of histidine (His) and its derivative, respectively, Fig. 18 (A). These ligands only are different in their C-terminal groups; L1 and L2 have an amide C-terminal and a carboxylic C-terminal group, respectively. Their studies revealed that in the presence of activator agents both complexes cleaved ϕX174 phage DNA with the formation of ROS. The complexes presented low to moderate cytotoxicity against MCF-7, A2780 and its cisplatin-resistant variant (A2780cisR) in comparison to cisplatin. Interestingly, **51-Cu** showed higher cleavage and cytotoxicity activity than **50-Cu**. Their

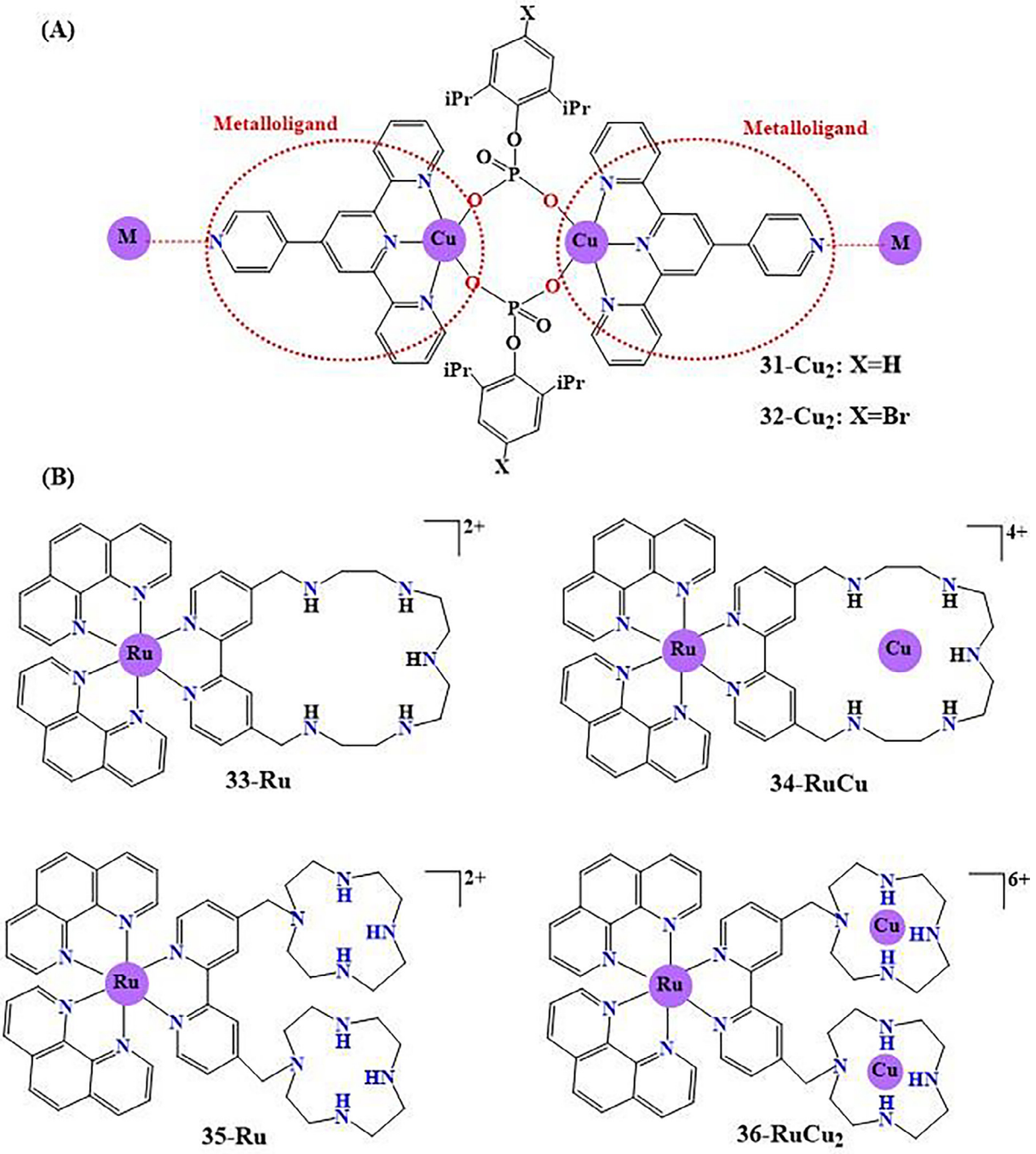

Fig. 17. The molecular structures of (A) **31-Cu$_2$** and **32-Cu$_2$** [202] and (B) **33-Ru, 34-RuCu, 35-Ru**, and **36-RuCu$_2$** [203–204].

findings indicated that **51-Cu** is the weaker oxidant but has higher biological activity.

In 2019, Aydın et al. [218] investigated the biological activity of water soluble palladium(II) complexes containing amino acid and polypyridyl ligands, [Pd(phen)(L-Tyr)](NO_3) (**52- Pd**), [Pd(5-methylphen)(L-Tyr)](NO_3) (**53- Pd**), and [Pd(phen)(Gly)](NO_3) (**54- Pd**), Fig. 18 (A). The results indicated that the complexes cleaved pUC19 without any type of activator, probably *via* the hydrolytic mechanism. It was found that the Pd(II) complexes did not display oxidative DNA cleavage activity because Pd(II) ion is not redox active. The *in vitro* cytotoxic properties of the complexes were assessed on colon cancer (Caco-2), A549, MCF-7 and normal respiratory epithelial cells (BEAS-2B). The complexes exhibited much less cytotoxicity activity against all the tested cells than cisplatin.

In 2015 and 2018, the biological properties of Cu(II) complexes coordinated to dipeptide ligands were investigated by Le and co-workers [219–220]. First, they synthesized two Cu(II)–dipeptide complexes, [Cu(Gly-Gly)(TBZ)(Cl)] (**55-Cu**) and [Cu(Gly-L-Leu)(TBZ)(Cl)] (**56-Cu**), where TBZ is 2-(4′-thiazolyl)benzimidazole, Fig. 18 (B). Both complexes efficiently cleaved pBR322 plasmid through an oxidative mechanism mediated by hydroxyl radicals. *In vitro* cytotoxicity results against HeLa, A549, and HepG2 cells exhibited that the complexes have lower cytotoxic effect than cisplatin with IC_{50} values varying from 33.17 to 100 μM, but despite of cisplatin have selective cytotoxicity toward HeLa cell lines [219].

Table 1
Further instances of AMSs containing polypyridyl ligands.

AMS	Substrate, Method, Mechanism	Toxicity studies	Molecular structure	Ref.
37-Ru	pUC18, [a]AGE, [b]PC	*Cytotoxicity activity: MTT assay.	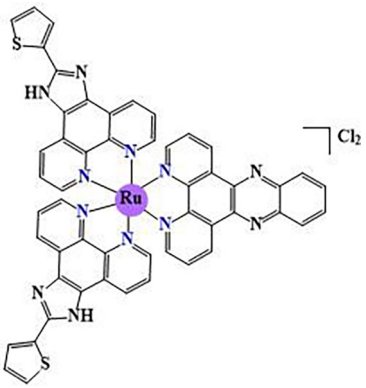	[205]
38-Cu	pUC19, AGE, [c]HC	*Cytotoxicity activity: MTT assay. Apoptosis induction studies.	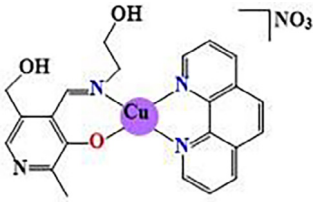	[206]
39-Ru	pUC19, AGE, PC	*Photocytotoxicity activity: MTT assay. Apoptosis induction studies.	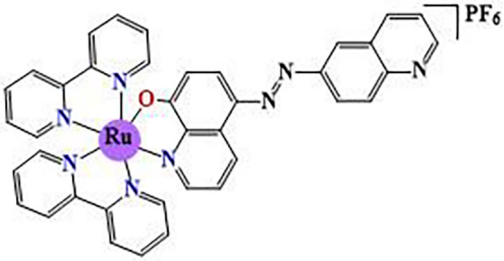	[32]
40-Cu	pUC18, AGE, HC	*Cytotoxicity activity: MTT assay	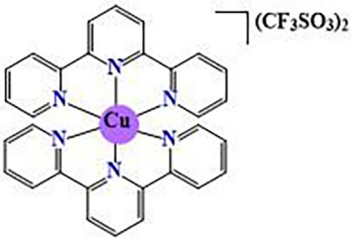	[207]
41-Cu	pBR322, AGE, HC	*Cytotoxicity activity: MTT assay	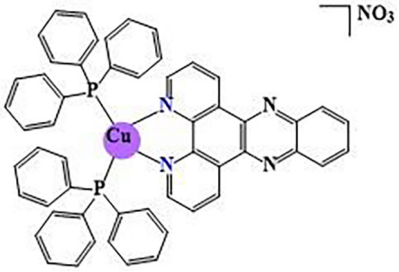	[208]
42-Pt	pBR322, AGE,	*Cytotoxicity activity: MTT assay *Antibacterial activity.	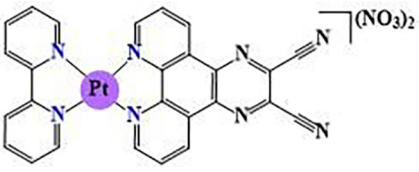	[209]

Table 1 (*continued*)

AMS	Substrate, Method, Mechanism	Toxicity studies	Molecular structure	Ref.
43-Co	pBR322, AGE, HC	***Cytotoxicity activity:** MTT assay ***In vivo* genotoxicity assay.**	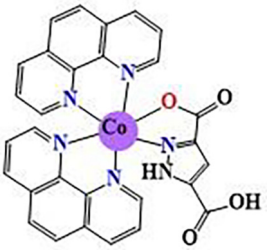	[210]
44-Fe	pEGFP-Actin, AGE, HC	***Anti-Mycobacterium Tuberculosis activity.** ***Cytotoxicity activity:** TUNEL assay. Apoptosis induction studies. Cellular ROS generation. Caspase 3/7 activity assay. COMET assay.	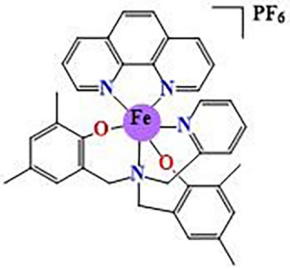	[211]
45-Cu	pUC19, AGE,	***Cytotoxicity activity:** MTT assay. Cell cycle assay. Apoptosis induction studies. Cellular ROS generation. Western blot assay.	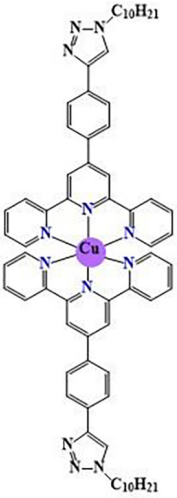	[212]
46-Cu	pBSK II/ oligonucleotide, AGE, [d]PAGE PC	***Cytotoxicity activity:** MTT assay ***Clonogenic assay.**	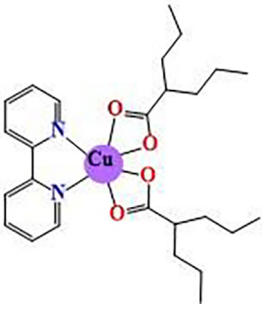	[213]
47-Ru	pBR322, AGE, PC	***Antibacterial activity.**	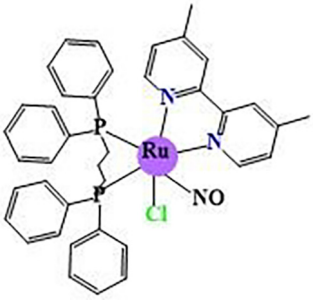	[214]

(*continued on next page*)

Table 1 (*continued*)

AMS	Substrate, Method, Mechanism	Toxicity studies	Molecular structure	Ref.
48-Cu	AGE, pET-28b, [e]OxC	* **Cytotoxicity activity.**	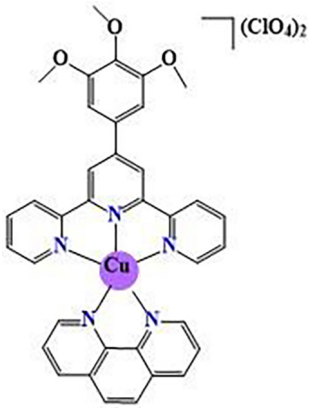	[66]
49-Ru$_4$	pCMUT, AGE, PC	***Photocytotoxicity activity:** MTT assay. Cellular ROS generation.	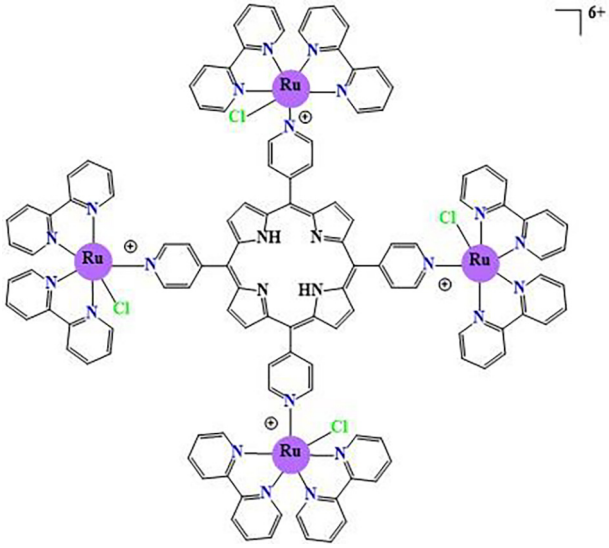	[215]

[a]AGE = Agarose gel electrophoresis,
[b]PC = Photocleavage,
[c]HC = Hydrolytic cleavage,
[d]PAGE = Polyacrylamide gel electrophoresis,
[e]OxC = Oxidative cleavage.

In another study, they prepared Cu(II)–dipeptide complexes, [Cu(Gly-gly)(HPBM)(H_2O)]ClO_4 (**57-Cu**) and [Cu(Gly-L-leu)(HPBM)(H_2O)]ClO_4 (**58-Cu**), where HPBM is 5-methyl-2-(2′-pyridyl) benzimidazole, Fig. 18 (B). Their results displayed that the complexes efficiently cleave pBR322 DNA through oxidative pathway *via* the generation of hydroxyl radicals. The results of antimicrobial activity against G^+ (*B. subtilis* and *S. aureus*) and G^- (*E. coli* and *P. aeruginosa*) bacteria indicated that the complexes are more sensitive toward G^+ bacteria. Both complexes displayed cytotoxicity against A549, HeLa, and PC-3 cells than LO_2 (human normal liver cells). Moreover, the complexes induced apoptotic death in HeLa cells through the rise of ROS levels, decline of mitochondrial membrane potential, and Caspase-3 activation as well as increasing the expression of Bcl-2 family proteins. Interestingly, their findings indicated that the antibacterial and antitumor activity of **58-Cu** was significantly higher than **57-Cu,** consistent with its higher DNA cleavage characteristics [220].

In 2015, the synergistic effect between redox-active complexes and tetrapeptides ligands in oxidative DNA cleavage was studied by Brabec and co-workers [221]. They prepared Zn(II) and Cu(II) complexes containing the tetradentate Ligands (^{Me2}PyTACN and BPBP) conjugated to the cationic tetrapeptides sequence (LKKL), [Zn(OTf)$_2$(^{Me2}PyTACN)-LKKL-NH_2] (**59-Zn**), [Cu(OTf)$_2$(^{Me2}PyTACN)-LKKL-NH_2] (**60-Cu**), [Zn(OTf)$_2$(BPBP)-LKKL-NH_2] (**61-Zn**), and [Cu(OTf)$_2$(BPBP)-LKKL-NH_2] (**62-Cu**), where ^{Me2}PyTACN is 1,4-dimethyl-7-(2-pyridylmethyl)-1,4,7-triazacyclononane and (*S,S′*)-BPBP is (*2S,2S′*)-1,1′-bis(pyrid-2-ylmethyl)-2,2′-bipyrrolidine), Fig. 19. Only the metallopeptides **60-Cu** and **62-Cu** effectively cleaved pUC18 plasmid DNA *via* an oxidative pathway by the generation of ROS. Additionally, these metallopeptides gave ~4-fold and ~23-fold rate accelerations, respectively in the DNA cleavage process in comparison with their parent complexes, $[Cu(PyTACN)]^{2+}$ and $[Cu(BPBP)]^{2+}$. The results of PAGE indicated that these metallopeptides did not show sequence-specific DNA cleavage. Therefore, they deduced that these high nuclease activity is for the presence of the cationic tetrapeptide that have efficiently high binding affinity toward DNA, consequently the metal ion brings in close proximity to minor groove of DNA to easily promote the cleavage process. Their *in vitro* cytotoxicity results showed all of metallopeptides have low cytotoxic effect against MCF-7 and

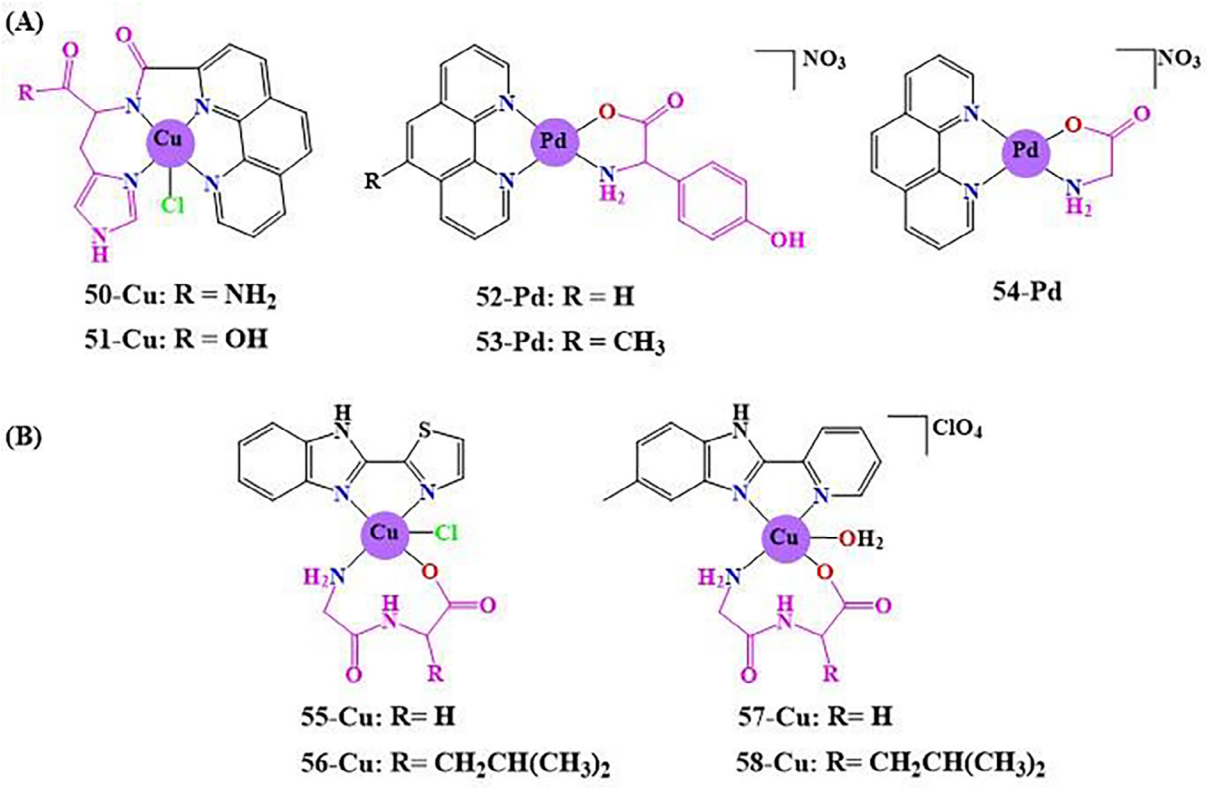

Fig. 18. The molecular structures of (A) amino acids-based complexes: **50-Cu**, **51-Cu**, **52- Pd**, **53- Pd,** and **54- Pd** [217–218] and (B) dipeptide-based complexes: **55-Cu**, **56-Cu**, **57-Cu,** and **58-Cu** [219–220].

CAPAN-1 cancer cells. Accordingly, they suggested maybe these metallopeptides did not have effective cellular delivery.

In 2018, Keyes and co-workers [222] reported a Ru(II)-peptide conjugate, $[Ru(tap)_2(bpyArCONH\text{-}ahx\text{-}VQRKRQKLMP\text{-}CONH_2]^{6+}$ (**63-Ru**), where tap is 1,4,5,8-tetraazaphenanthrene, Fig. 20. They prepared this conjugate from $Ru(tap)_2$, bpyArCOOH (a conjugatable bpy derivative), and NLS sequence of the NF-κB transcription factor peptide, H_2N-ahx-VQRKRQKLMP-$CONH_2$ (ahx is aminohexyl linker). Their cytotoxicity results indicated that **63-Ru** has low dark toxicity on HeLa cells with IC_{50} value of 83.4 μM. But when this metallopeptide was irradiated under weak blue light (440 nm) for 15 min, the IC_{50} value decreased to 51.8 μM. Results of DNA photocleavage exhibited that **63-Ru** is able to cleave pUC19 DNA by singlet oxygen independent photocleavage mechanism. They concluded that this photocleavage mechanism involves direct oxidative cleavage of the guanine base or Type I pathway that facilitated by electron transfer. This was taken to indicate that the mechanism of photoinduced cell death by **63-Ru** may occur by a similar mechanism.

5.2.2. ATCUN peptide motif

The ATCUN (amino terminal Cu^{2+}- and Ni^{2+}-binding) peptide motif consists a tripeptide sequence where typically a His amino acid sits at the 3rd position forming a NH_2-Xxx-Xxx-His triad and Xxx can be any amino acid, Fig. 21 (A). The Cu^{2+} and Ni^{2+} ions bind to the ATCUN motif with high affinity ($K_D \sim 1.18 \times 10^{-16}$ M and $\sim 1 \times 10^{-16}$ M, respectively) with four nitrogen atoms including the imidazole side chain of His, two nitrogen atoms existing in the deprotonated amide backbone from the residue Xxx, and a free N-terminal amine in a square planar geometry and two surfaces accessible for binding to a targeted biomolecule [223–225]. The ATCUN motif is found naturally at the N-terminus of peptides and proteins, *viz.* Cu–DAH in human serum albumin, Cu–DSH in histatin 5, Cu–DTH in bovine serum albumin, and Cu–GNH in Neuromedin C [226].

In 2015, the role of charge and stereochemistry of ATCUN motif on antimicrobial activity was investigated by Angeles-Boza et al. [227]. For this purpose, they conjugated *sh*-Buforin as antibacterial peptide (RAGLQFPVGRVHRLLRK-NH_2) with the Cu-RTH as ATCUN motif (**64-Cu**) and compared it to a derivative containing a Cu-VIH motif (**65-Cu**), Fig. 21 (B). Also, they used L- and D- enantiomers of amino acids in ACTUN and *sh*-Buforin moiety. Their results exhibited that the Cu-VIH-*sh*-Buforin conjugate cleave pUC19 DNA faster than the Cu-RTH-*sh*-Buforin. Interestingly, DNA cleavage activity depends on the stereochemistry of the *sh*-Buforin and not to the stereochemistry of the ATCUN motif. Their results from antimicrobial assays indicated that the D-peptides are more active than their L counterparts. Also, in the conjugates that have the same RTH or VIH motif, stereochemical changes of the ATCUN motif did not affect the antimicrobial activity. Finally, they found the following interesting findings: i) there is an intense correlation between the DNA cleavage activity and the MIC values. ii) An ATCUN motif with positive charge has the high DNA binding affinity but always antimicrobial activity does not increase in comparison to a neutral ATCUN motif. iii) Stereochemistry changes of the peptide in ATCUN-*sh*-Buforin conjugate leads to stronger antimicrobial activity, due to the more nuclease activity and stability of the peptides.

From 2015 to 2019, Cowan's group investigated biological activity of ATCUN motif-based complexes [37,47,228]. First, they studied cleavage of G-quadruplex telomeric DNA by a Cu-GGHK-acridine derivative (**66-Cu**), Fig. 22. Acridine is a G4 ligand and

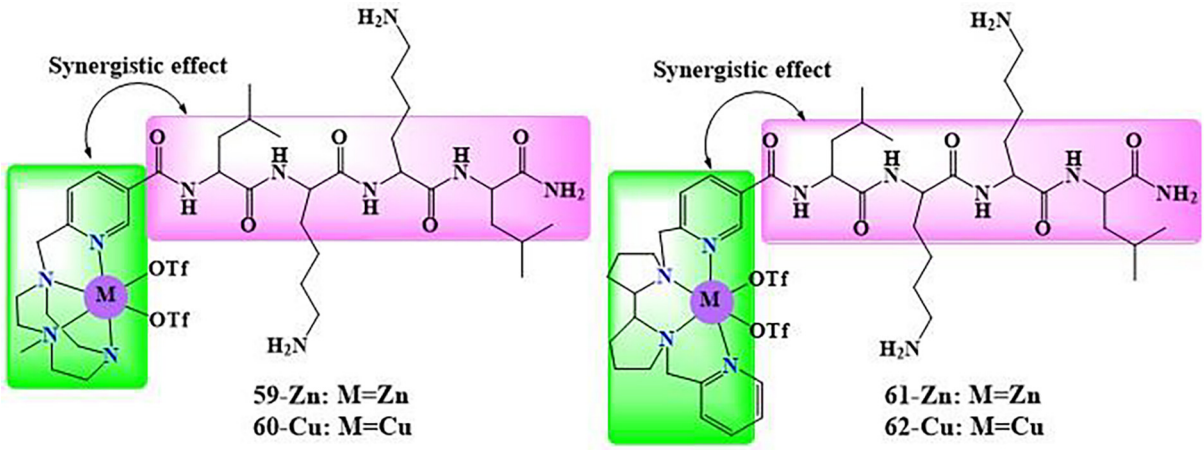

Fig. 19. The molecular structures of tetrapeptide-coordinated complexes (**59-Zn**, **60-Cu**, **61-Zn**, and **62-Cu**) [221].

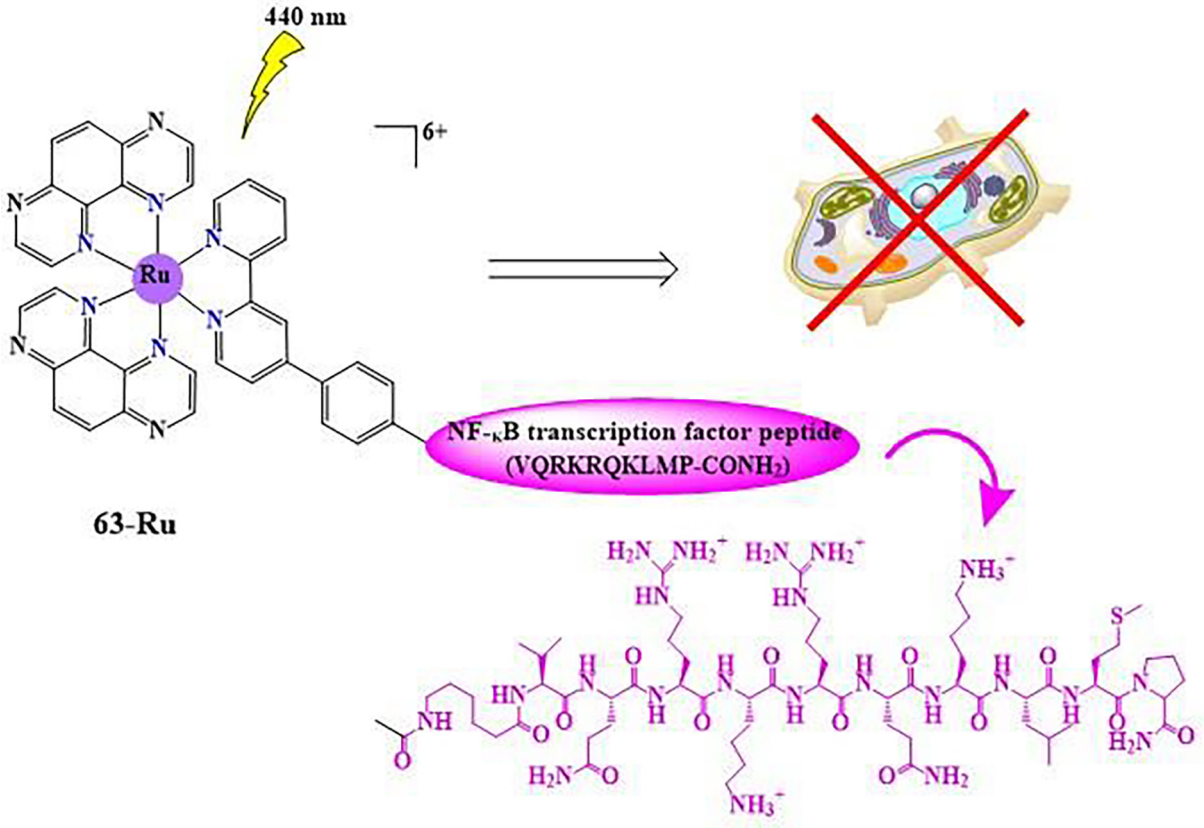

Fig. 20. The molecular structure of **63-Ru** [222].

result in able to bring the Cu-GGH moiety in close vicinity to the telomeric G4 sequence. The results of PAGE exhibited the Cu-GGHK-acridine selectively bounds to G4 telomere sequence and efficiently promotes cleavage of G4 DNA. The studies of cleavage by MALDI-TOF MS indicated that **66-Cu** is able to cleave G4 DNA *via* both hydrolytic and oxidative cleavage pathways. Moreover, **66-Cu** showed more significant cytotoxicity against MCF-7 than the metal-free ligand, GGHK-acridine. This conjugate could shorten the length of telomeric DNA in MCF-7 cells that was determined by real-time PCR and induce efficient both cellular senescence and apoptosis in this cells [37].

In 2015, another study with metallopeptides as catalytic metallodrugs was published by Cowan's group [47]. They prepared new ATCUN metallodrugs based on the LaR2C peptide, Cu-GGHKY KETDLLILFKDDYFAKKNEERK-NH_2 (**67-Cu**) and Cu-GGHKYKETDL-NH_2 (**68-Cu**), Fig. 22. The human La protein is an RNA-binding polypeptide which belongs to the RNA recognition motifs (RRMs) family and can bind with a variety of RNAs such as viral RNA. LaR2C (KYKETDLLILFKDDYFAKKNEERK) is a dominant negative synthetic peptide which derived from the La RRM2 and is able to selectively bind to the stem-loop IV (SLIV) of HCV IRES RNA. Both complexes were able to catalytically degrade RNA with pseudo-Michaelis–Menten behavior. The antiviral activity of the com-

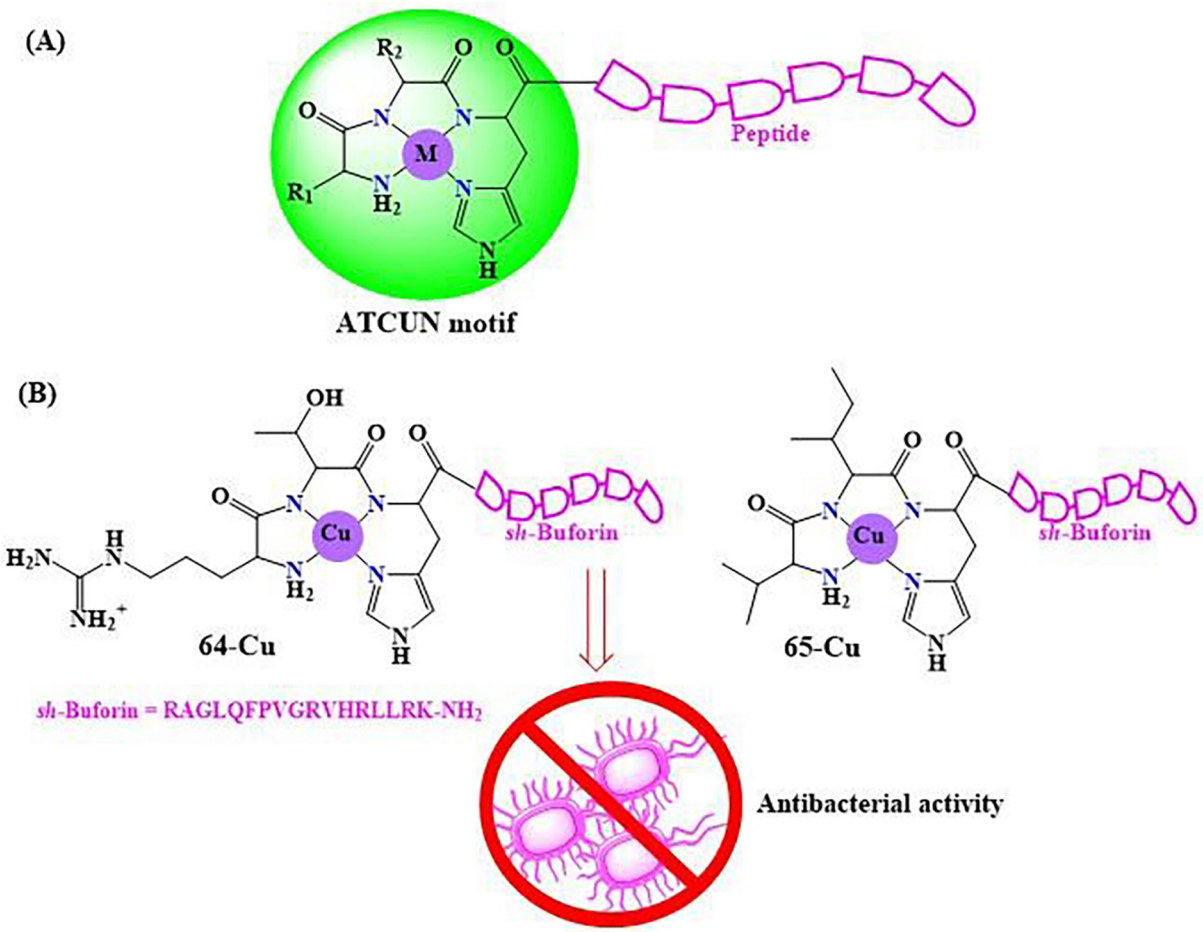

Fig. 21. The molecular structures of (A) an ATCUN motif [226] and (B) **64-Cu** and **65-Cu** [227].

plexes was evaluated by an FDA accepted cellular replicon assay. Both complexes indicated anti-HCV activity with the antiviral IC_{50} values of 0.75 and 2.17 μM for **67-Cu** and **68-Cu**, respectively. Moreover, neither of the complexes displayed significant toxicity to cells, TC_{50} > 50 μM.

In 2019, biological activity of Cu-ATCUN motif based on Sub5 peptide was investigated. Sub5 peptide is a linear synthetic derivative of bactenecin with the sequence of RRWKIVVIRWRR-NH_2 [228]. They prepared two Cu-ATCUN complexes, Cu-GGHRRW KIVVIRWRR-NH_2 (**69-Cu**) and Cu-GGHGRRWKIVVIRWRR-NH_2 (**70-Cu**), Fig. 22, with a glycine linking the metal-ATCUN and Sub5 targeting domain in the latter. Their results indicated that Sub5 peptide has high antimicrobial activity against all of G^- and G^+ microbes with MIC values in the range of 0.5–4.0 μM. While **69-Cu** and **70-Cu** derivatives indicated more selective antimicrobial activity with a two to three-fold improved activity against some microbes relative to Sub5. The cytotoxicity results of metallopeptides did not show cytotoxicity at concentrations below 50 μM against human dermal fibroblasts. Their results using pUC19 plasmid DNA and 16S A-site rRNA indicated that both Sub5 and the metallopeptides can interact with either DNA or RNA, but no nuclease activity is observed in solution. Moreover, they investigated the extent of cellular DNA damage. Sub5 and metallopeptiides induced DNA damage to the same extent and their cellular DNA damage in *S. epidermidis* was 3-fold greater extent than in *E. coli*. Such difference could be a result of cell-wall differences between the two bacteria, thus enabling enhanced cell permeability. Finally, their findings supported that these metallopeptides for their selective and effective antimicrobial activity and no cytotoxicity on human cells, could be suitable candidates for future as antimicrobial drug.

In the same year, a series of Cu(II) complexes with different sequences of the ATCUN motif as selective artificial nucleases toward G-quadruplex or duplex telomeric DNA were investigated [138]. They prepared Cu(II) complexes with GGH, GDH, and DGH, different sequences of the ATCUN motif, which conjugated to the naphthalene diimide core. Additionally, xylyl linker were also designed as two isomers of *m*-xylyl and *p*-xylyl (structures **71-Cu** to **76-Cu**), Fig. 23. The obtained products from cleavage of G4 and duplex telomeric DNA by the Cu(II)-ATCUN complexes analyzed using denaturing-PAGE and relative cleavage rates at different nucleotides were measured. The results exhibited that two factors of ATCUN motif sequence and the xylyl linker substitution significantly influence on the cleavage rates at different sites of DNA. All Cu(II)-ATCUN complexes indicated that significantly stronger cleave G-quadruplex telomeric DNA than duplex telomeric DNA. This selective cleavage activity is due to the higher binding affinity of Cu complexes to G-quadruplex DNA than to the duplex DNA. Their results indicated that the omplexes with a GDH sequence underwent higher cellular uptake relative to their GGH and DGH equivalents. Intracellular nuclease activity findings also indicated that all complexes at 0.5 μM are able to reduce telomere length (20–50%) after 3 day. All Cu(II)-ATCUN complexes can significantly inhibit proliferation of cancer cells with IC_{50} values in the range of 1.1–47.7 μM and exhibited higher cytotoxic effect on cancer cells than normal cells, due to the reduction of telomere length is mainly restricted to the S phase.

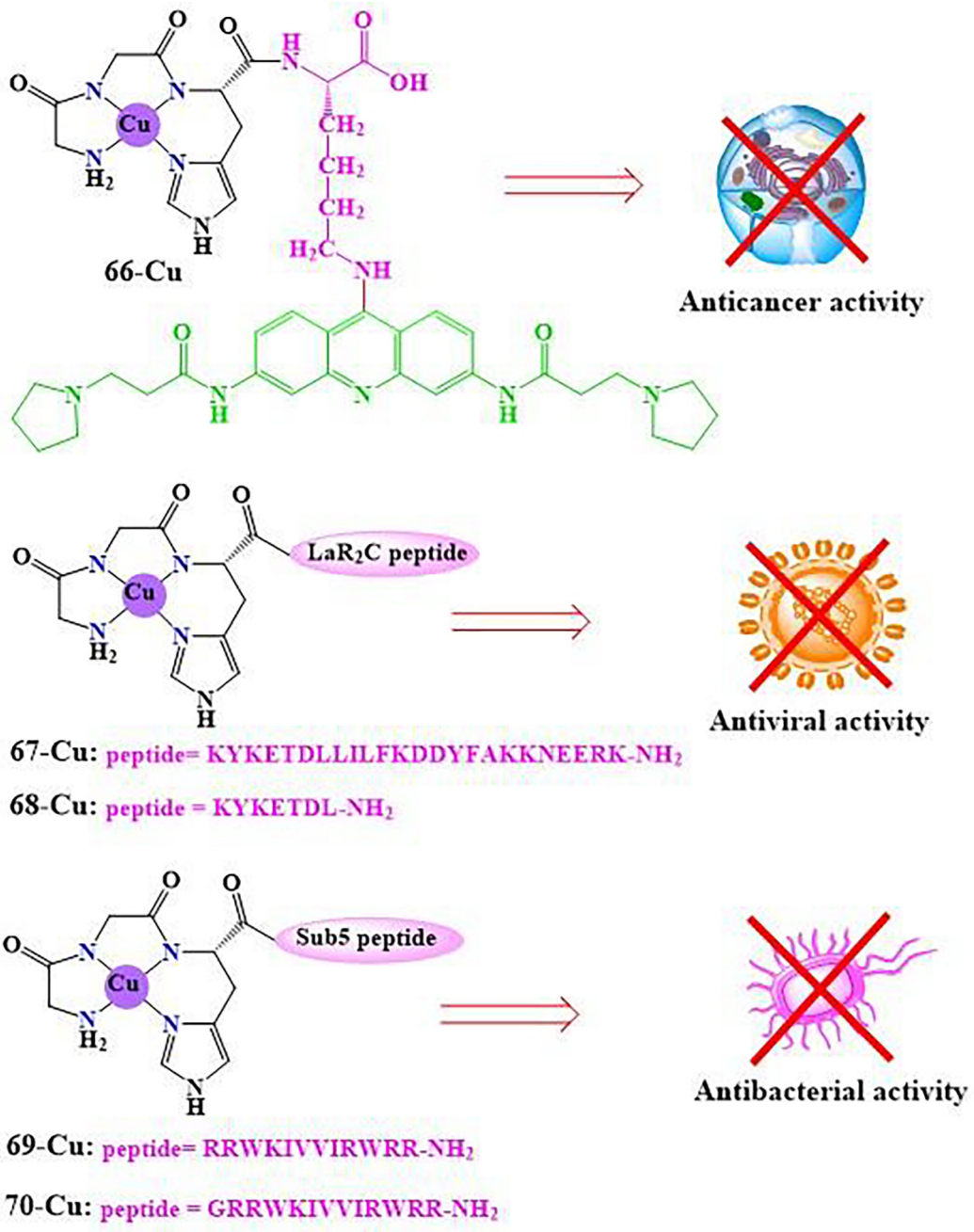

Fig. 22. The molecular structures of **66-Cu**, **67-Cu**, **68-Cu**, **69-Cu**, and **70-Cu** [37,47,228].

Nonetheless, one can find an array of more AMSs comprising of peptide ligands in the literature. A few further instances of such complexes are summarized in the Table 2.

5.3. Antibacterial and anti-inflammatory drugs

It is accepted that pharmacological and toxicological properties of many known drugs are modified when administered in the form of metallic complexes due to possible synergistic activity of metal ions [233]. Besides, metal-drug complexes may pose different biological activities from parent drugs, the fact that has gained considerable attention [233–236]. In this section, metal complexes containing known drugs with metallonuclease activities are highlighted.

5.3.1. Antimicrobial quinolones

In 2014, Patel and co-workers [237] reported a series of Ru(II)– and Ru(III)–fluoroquinolone complexes: [Ru(pefloxacin)$(PPh_3)_2Cl_2$] (**89-Ru**), [Ru(ofloxacin)$(PPh_3)_2Cl_2$] (**90-Ru**), [Ru(sparfloxacin)$(PPh_3)_2Cl_2$] (**91-Ru**), [Ru(pefloxacin)$(PPh_3)_3Cl$] (**92-Ru**), [Ru(ofloxacin)$(PPh_3)_3Cl$] (**93-Ru**), and [Ru(sparfloxacin)$(PPh_3)_3Cl$] (**94-Ru**), Fig. 24. Their experimental results showed that all of the complexes cleave DNA more efficient than the metal salt and free fluoroquinolones (pefloxacin, ofloxacin, and sparfloxacin). Antibacterial experiments demonstrated that the complexes have considerably higher activities compared to free fluoroquinolones against G^+ and G^- bacteria under identical experimental conditions. The *in vivo* cytotoxic effects of the complexes were investigated by the Brine shrimp lethality bioassay. The LC_{50} values of the fluoroquinolone complexes ranged from 6.27 to 16.05 $\mu g\ mL^{-1}$. Interest-

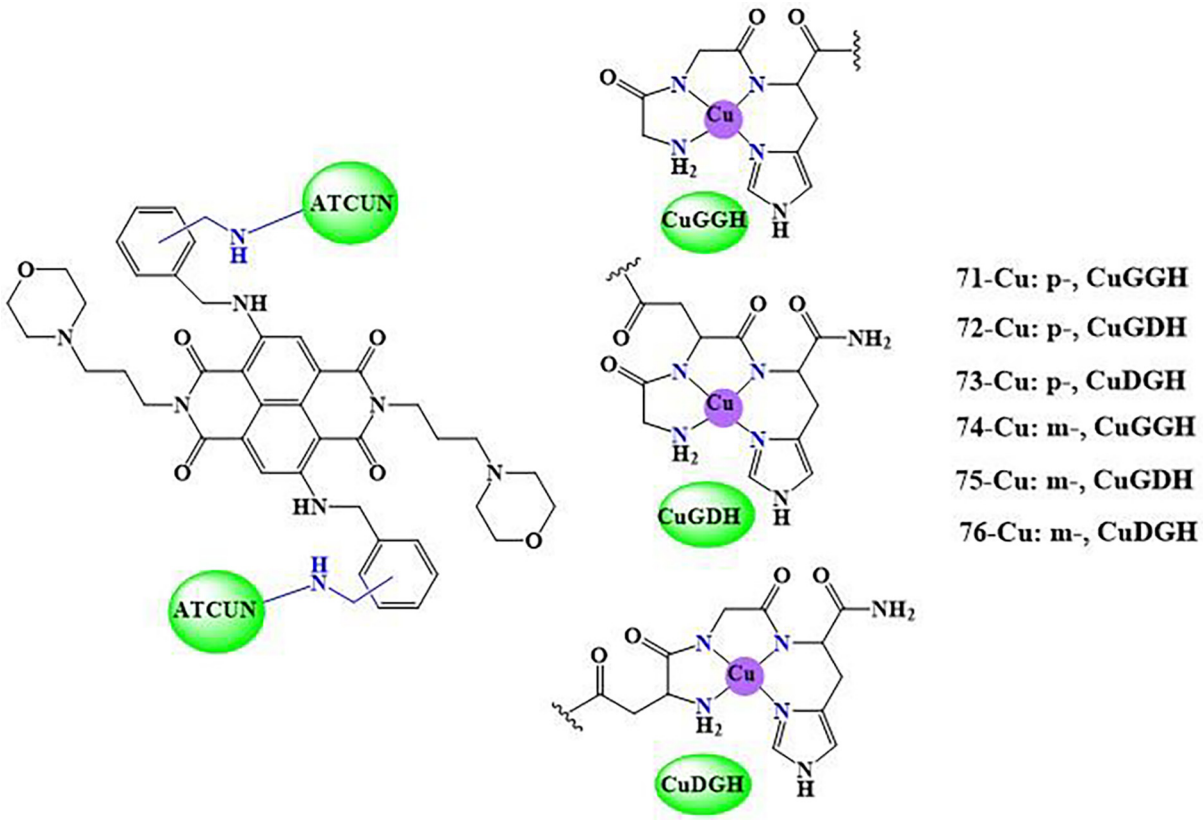

Fig. 23. The molecular structures of **71-Cu** to **76-Cu** [138].

ingly, the Ru(III)–fluoroquinolone complexes indicated superior biological activities to the complexes bearing Ru(II). The authors attributed this to the difference in DNA-binding affinity between Ru(II) and Ru(III) complexes.

In 2014, Arjmand's group [238] evaluated cleavage and antiproliferative properties of Cu(II) complexes coordinated to the antibacterial drug nalidixic acid (NAL), $[Cu(NAL)_2(diaminocyclohexane)_2]$ (**95-Cu**), Fig. 25. Mechanistic studies demonstrated that **95-Cu** is able to cleave pBR322 DNA *via* an oxidative pathway where $^1O_2$ is probably responsible for the nuclease activity. Also, the preferential major groove binding affinity of the complex towards pBR322 was approved in the presence of known minor and major groove binders. Moreover, yeast tRNA cleavage by **95-Cu** was both time and concentration dependent. A clonogenic assay against human osteoblastoma (U2OS) cell line indicated that the complex inhibits the colony-forming of cells. Moreover, flow cytometry analysis revealed a cell cycle arrest at S phase.

In 2017, Palaniandavar et al. [239] reported bioactivity of a series of water soluble mixed ligand Cu(II) complexes with nalidixic acid and polypyridyl as co-ligands, $[Cu(NAL)(bpy)(H_2O)](ClO_4)$ (**96-Cu**), $[Cu(NAL)(phen)(H_2O)](ClO_4)$ (**97-Cu**), $[Cu(NAL)(dimethylphen)(H_2O)](ClO_4)$ (**98-Cu**), and $[Cu(NAL)(tetramethylphen)(H_2O)](ClO_4)$ (**99-Cu**), Fig. 25. The ability of this series of complexes for pUC19 DNA cleavage decreases in the order of **99-Cu** > **98-Cu** > **97-Cu** > **96-Cu**. The complexes **98-Cu** and **99-Cu** showed more selective and efficient double-strand DNA cleavage possibly owing to their strong hydrophobic methyl substituents that cause strong distortion on DNA. Similarly, the complexes **98-Cu** and **99-Cu** imposed excellent cytotoxicity against MCF-7 cells mainly through apoptotic mode in comparison with their phen and bpy analogues, **96-Cu** and **97-Cu**. Their findings strongly indicated that the existence of substitutions of methyl on polypyridyl ligands is a strong factor in the bioactivity of Cu(II) complexes.

In 2020, another report was published by Islama and Palaniandavar's group [240] in continuation of their studies on NAL. They evaluated pUC19 DNA cleavage and cytotoxicity of Cu(II) complex, $[Cu(ethylenediamine)_2(NAL)_2]$ **(100-Cu)**, Fig. 25. They observed that **100-Cu** oxidatively cleaved the plasmid DNA *via* $^{\bullet}OH$ radical generation. Also, the complex was a more efficient cleaver than its precursor complex, $[Cu(ethylenediamine)_2]^{2+}$. However, **100-Cu** exhibited low *in vitro* cytotoxicity against A549 cells (IC_{50} value > 200 μM).

In 2019, Kellett and co-workers [241] aimed at production of a multi-modal therapeutic agent and investigated biological properties of a ciprofloxacin derivative (CipA) possessing well-known anti-proliferative and anti-bacterial characteristics [242]. For this, they synthesized Cu(II) complexes with general formula [Cu(CipA)(NN)Cl], where NN is phen (**101-Cu**), dpq (**102-Cu**), and dppz (**103-Cu**), Fig. 26. All the three complexes exhibited excellent nuclease activity; **102-Cu** was the most efficient catalyst in the series. All three complexes cleaved pUC19 DNA through generation of superoxide that is the predominant ROS in catalyzed DNA scission. The complexes displayed excellent *in vitro* cytotoxicity effects compared to free CipA against MCF-7 and prostate (DU145) carcinoma cells. These complexes acted more selective and indicated higher antibacterial activity against G^+ bacteria over G^- bacteria, a property different from native cipro. Another encouraging feature was that the complex **103-Cu** played more potent against Methicillin-resistant *S. aureus* (MRSA) as compared to the CipA ligand itself. Base on their observations in *in vivo* toxicity assay using *Galleria mellonella* model, they deduced that these complexes, particularly **103-Cu** as an antibiotic candidate, possessing remarkable potential to be introduced as a novel prophylactic metallo-antibiotic.

Table 2
Further instances of AMSs containing peptide ligands.

AMS	Substrate, Method, Mechanism	Toxicity studies	Molecular structure	Ref.
77-Cu	HCV IRES RNA, Fluorescence and MALDI-TOF MS.	* **Cellular HCV replicon assay.**	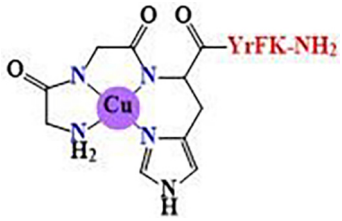	[46]
78-Cu	pUC19, [a]AGE, [b]OxC	* **Antimicrobial activity:** Intracellular ROS generation.	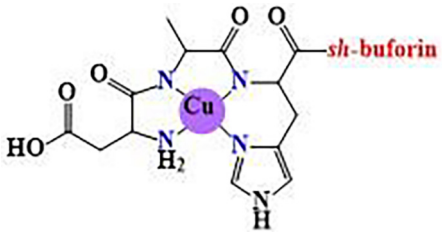	[226]
79-Cu	pUC19, AGE, OxC	* **Antimicrobial activity:** Intracellular ROS generation.	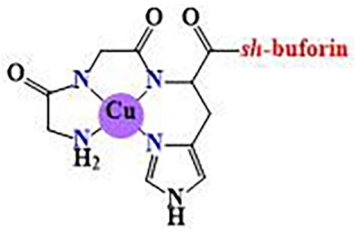	[226]
80-Cu	pUC19/ 16 s RNA, AGE	***Antimicrobial activity.**		[229]
81-Cu		HCV IRES RNA, AEG, Fluorescence spectroscopy and MALDI-TOF MS	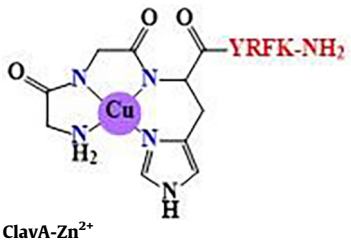	[48]
82-Zn	pUC19, AGE	***Antimicrobial activity.**	**ClavA-Zn^{2+}**	[42]
83-Cu	pUC19 = AGE $22G_4$ = [c]PAGE OxC	***Cytotoxicity activity:** MTT assay.	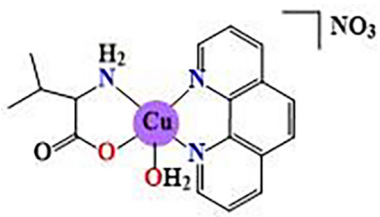	[137]
84-Cu	pUC19, AGE, [d]HC	***Cytotoxicity activity:** MTT assay. ***Antibacterial activity.**	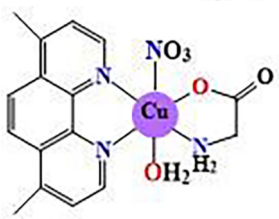	[230]

Table 2 (*continued*)

AMS	Substrate, Method, Mechanism	Toxicity studies	Molecular structure	Ref.
85-Cu$_2$	pUC19, AGE, HC	*Cytotoxicity activity: MTT assay. *Antibacterial activity.	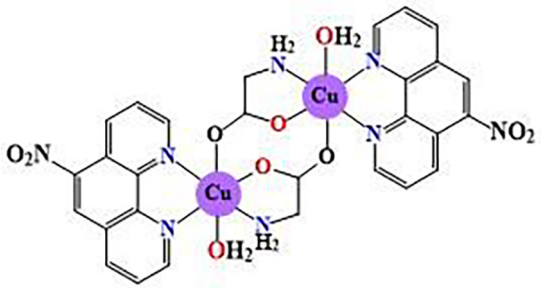	[230]
86-Cu	pBR322, AGE, OxC	*Cytotoxicity activity: MTT assay. *Antibacterial activity.	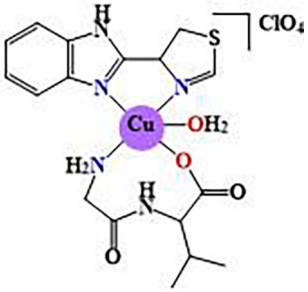	[231]
87-Cu	pBR322, AGE, OxC	*Cytotoxicity activity: MTT assay. *Antibacterial activity.	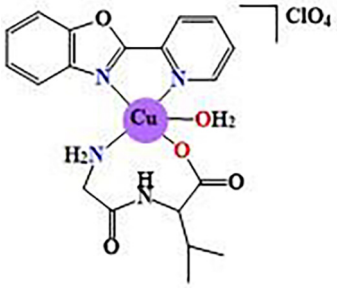	[231]
88-Cu	pBR322, AGE, OxC	*Cytotoxicity activity: MTT assay. Cell cycle analysis. Caspase activity assays. Cellular ROS generation.	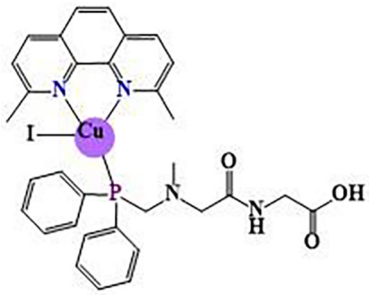	[232]

[a] AGE = Agarose gel electrophoresis,
[b] OxC = Oxidative cleavage,
[c] PAGE = Polyacrylamide gel electrophoresis.
[d] HC = Hydrolytic cleavage.

5.3.2. Non-steroidal anti-inflammatory drugs (NSAIDs)

In 2017, anticancer activity of the Cu(II) complexes on breast cancer stem cells (HMLER-shEcad) and bulk breast cancer cells (HMLER) was published by Suntharalingam's group [243] who evaluated four complexes that contain region-isomeric vanillin Schiff base derivatives ((E)-5/4/3/2-methoxy-2-(((2-(methylthio)ethyl)imino)methyl)phenol) and the NSAID naproxen, (**104-Cu**, **105-Cu**, **106-Cu**, and **107-Cu**), Fig. 27 (A). DNA cleavage studies indicated that **105-Cu** and **107-Cu** were the most effective cleavers. The complex **107-Cu** interacted with DNA *via* groove binding and catalyzed oxidative DNA cleavage (at 10 μM). The **107-Cu** indicated highest cytotoxicity against HMLER-shEcad and HMLER and lower potency (2-fold) towards the normal fibroblast cells. Moreover, **107-Cu** effectively inhibited mammosphere formation at IC_{20} value after 5 days incubation (38% decreases) which was similar to the efficacy of the novel anticancer drug salinomycin. Cellular mechanistic studies indicated that **107-Cu** increases intracellular ROS levels, damages DNA, and triggers caspase dependent apoptosis.

In 2018, another study involving naproxen was carried out by Patra et al. [244] who investigated biological activity of two square-planar platinum(II) complexes with formula

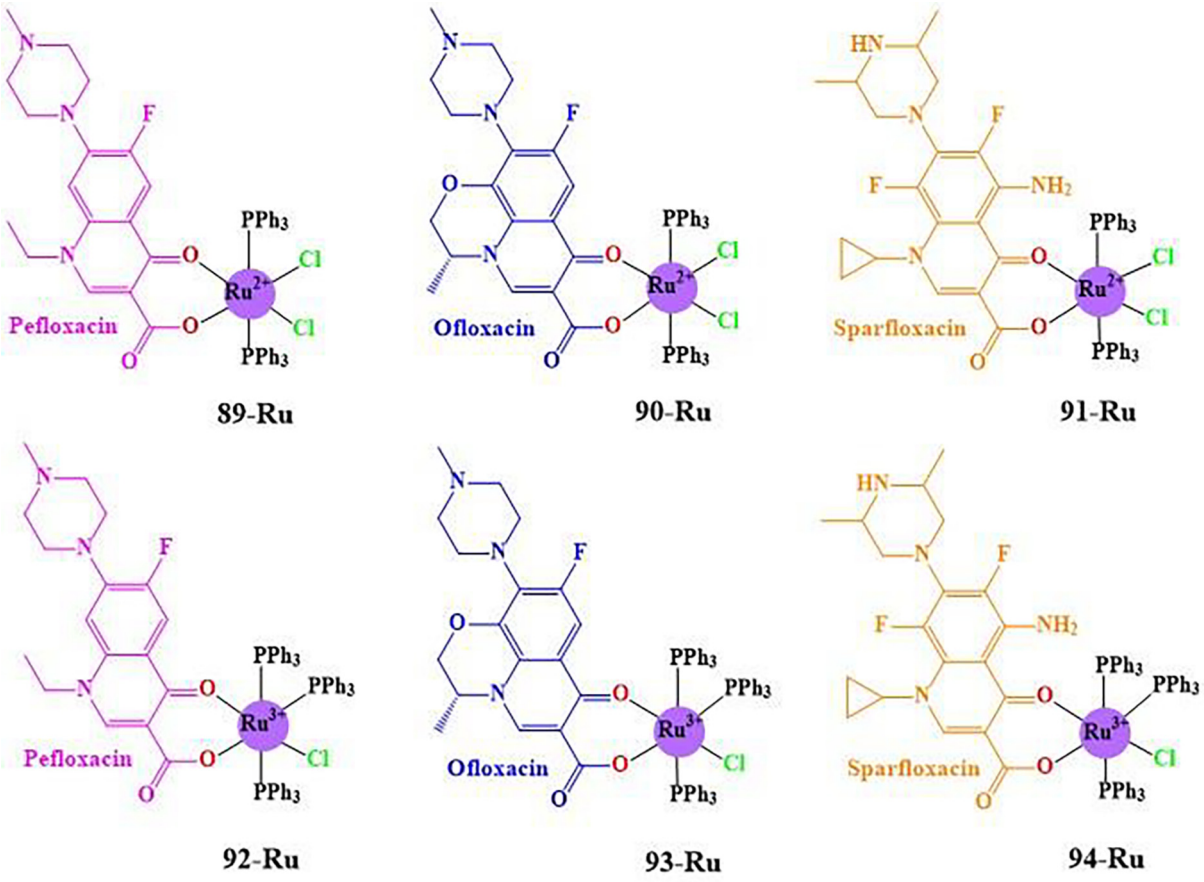

Fig. 24. The molecular structures of Ru(II)– and Ru(III)–fluoroquinolone complexes (**89-Ru** to **94-Ru**) [237].

[Pt(dach(naproxen)Cl] (**108-Pt**) and [Pt(dach)(naproxen)$_2$] (**109-Pt**), where dach is (1*R*,2*R*)-dichloro(cyclohexane-1,2-diamine), Fig. 27 (B). The complexes exhibited efficient photocleavage activity upon photo-exposure at 365 nm while free naproxen was inactive under similar conditions displaying the key role of Pt(II) ion in ROS generation. Interestingly, the complexes were cytotoxic in dark but exhibited an enhanced photocytotoxicity (~2-fold increase) in HeLa cells. The comet assay results showed both complexes are able to break the cellular DNA when exposure to light. Nonetheless, these complexes demonstrated no evident effects on HepG2 cells and very low toxicity towards noncancerous cells, projecting a type of tumor selectivity potentiating their introduction as tumor-specific phototherapeutic PDT agents.

In 2019, Valko and co-workers [245] investigated novel Cu(II) complexes containing mixed ligands of phen as an intercalation ligand and some NSAID drugs including flufenamic, mefenamic, tolfenamic acid as redox-cycling functional moieties, [Cu(tolfenamic)$_2$(phen)] (**110-Cu**), [Cu(mefenamic)$_2$(phen)] (**111-Cu**), and [Cu(flufenamic)$_2$(phen)] (**112-Cu**). The most important difference among the NSAID drugs used here is the nature of their substituents, see Fig. 28 (A). Their complexes indicated hydrolytic pBSK DNA cleavage in the order of **112-Cu** > **111-Cu** > **110-Cu**. In the presence of H_2O_2, all the complexes efficiently cleaved DNA by oxidative mechanism. They also exhibited significant selectivity in their cytotoxicity against HT-29, HeLa, and breast cancer cells (T-47D) in comparison to the mesenchymal stromal cell line (MSC). Most interestingly, **112-Cu** was the most promising case from the viewpoint of biological activity due to the presence of fluorine substituents that participate in the formation of weak hydrogen-bonds with DNA.

In 2020, a binuclear Zn(II) complex comprising the NSAID diclofenac and nicotinamide neutral linker (Nic), [Zn$_2$(diclofenac)$_4$(Nic)$_2$] (**113-Zn$_2$**) (Fig. 28 (B)), was investigated by Moura et al. [246]. The complex had low cleavage activity on pBSK II plasmid DNA with no significant difference in the dark or under UV light. Cytotoxicity assay against brine shrimp, *Artemia salina*, showed that the complex was not able to produce >10% lethality up to a maximum concentration of 1200 $\mu g.mL^{-1}$ after 24 h. Finally, they deduced that the complex with low DNA cleavage activity and toxicity against *Artemia salina* can be introduced as an anti-inflammatory agent with improved properties in comparison to the parent drug.

Nonetheless, one can find an array of more AMSs bearing known medicines in the literature. A few further instances of such complexes are summarized in Table 3.

6. Conclusions and future perspectives

In this review, we systematically highlighted the studies conducted on nuclease-like metalloscissors especially in the past five years. A deep comprehension of the structure–activity relationship of AMSs and the factors that affect their therapeutic potential is critically essential for the rational design of ideal therapeutic agents in the future. We hope that this review with novel strategies and ideas motivates scientists to improve new research opportunities. To note, the scope of nuclease-like metalloscissors mentioned

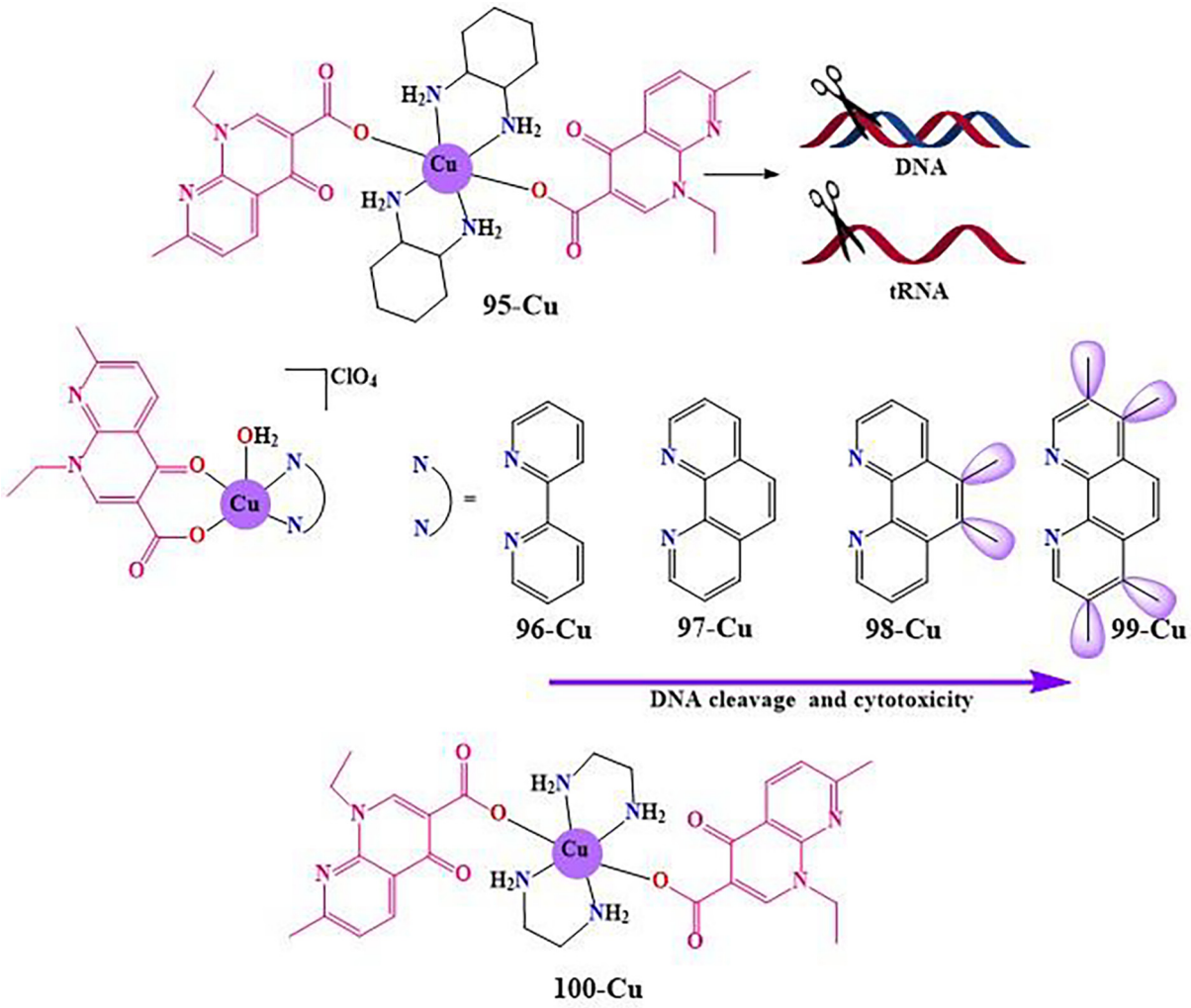

Fig. 25. The molecular structures of **95-Cu** to **100-Cu** [238–240].

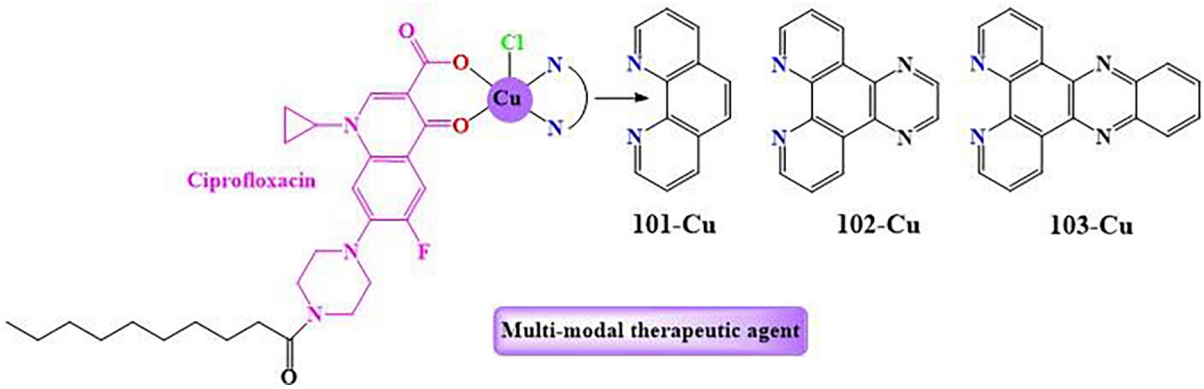

Fig. 26. The molecular structures of **101-Cu**, **102-Cu**, and **103-Cu** [241].

here contains metal complexes with DNA/RNA cleaving properties as therapeutic candidates, in which other enzyme-like activities are not included. This review summarizes the mechanism of nucleic acid cleavage (hydrolytic, oxidative, and/or photo-induced cleavage), model substrates and instrumentations employed in cleavage studies, and therapeutic applications of metalloscissors. Finally, review elaborates *in vitro* and *in vivo* pharma studies of different types of metal complexes which coordinated to different ligands (polypyridyl ligands, peptide ligands, quinolones antibacterial and non-steroidal anti-inflammatory drugs) as novel therapeutic candidates in cancer and bacterial and viral infections therapy as well as cancer and microbial infections photodynamic therapy. The novelty of this review relies on the comprehensive discussion of the recent progress conducted on

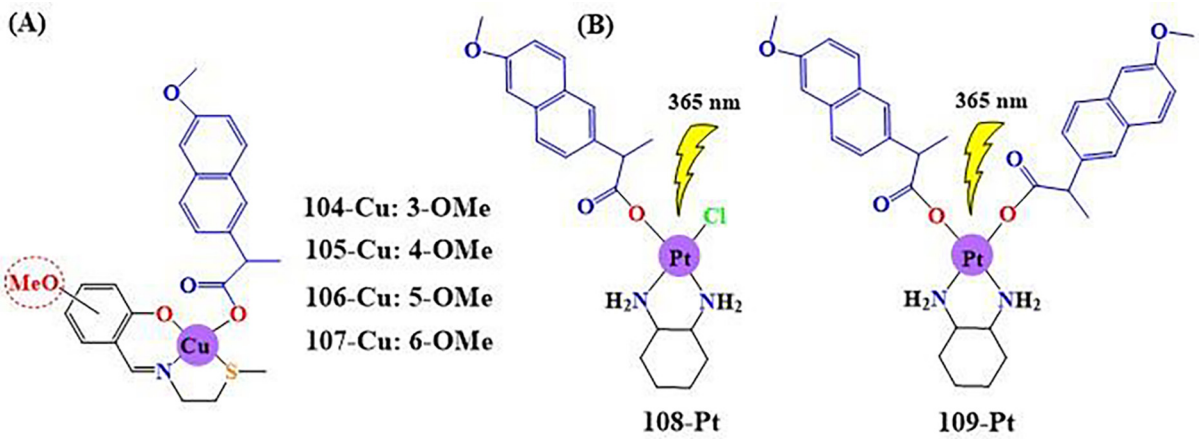

Fig. 27. The molecular structures of metal complexes with naproxen: (A) **104-Cu** to **107-Cu** [243] and (B) **108-Pt** and **109-Pt** [244].

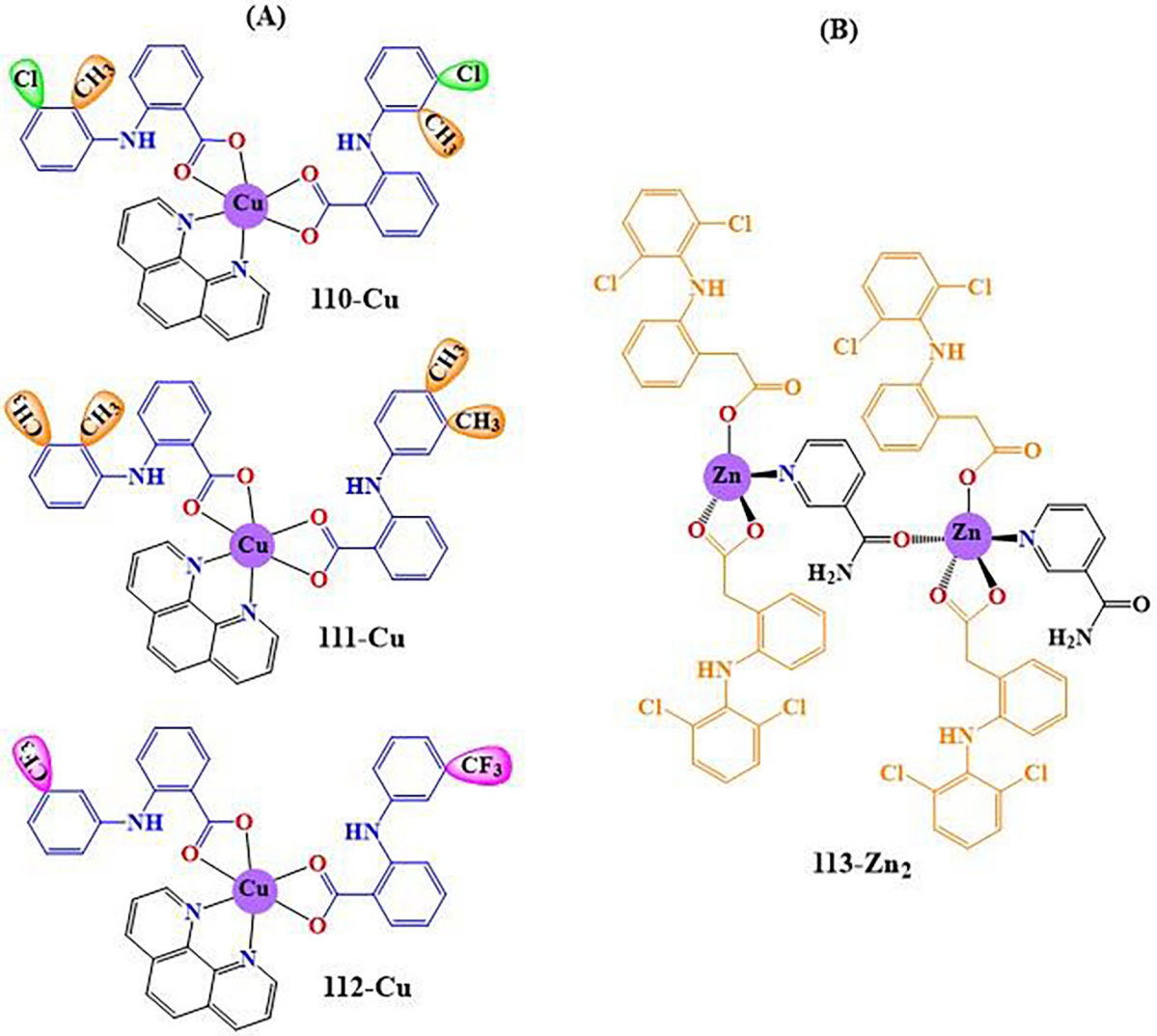

Fig. 28. The molecular structures of (A) [Cu(tolfenamic)$_2$(phen)] (**110-Cu**), [Cu(mefenamic)$_2$(phen)] (**111-Cu**), and [Cu(flufenamic)$_2$(phen)] (**112-Cu**) [245] and (B) [Zn_2(-diclofenac)$_4$(Nic)$_2$] (**113-Zn_2**) [246].

the metal complexes with nuclease-like activity and their therapeutic applications.

Diseases like cancer and microbial infections are considered as the greatest concerns to global public health. One of the most serious challenges in the treatment of these diseases is no sufficient efficacy of current drugs due to resistance and mutations. The unexpected emergence and the global spread of the concurrent COVID-19 pandemic have put the health systems in a difficult sit-

Table 3
Further instances of AMSs containing known drugs.

AMS	Substrate, Method, Mechanism	Toxicity studies	Molecular structure	Ref.
114-Co	pUC19, [a]AGE, [b]OxC	***Cytotoxicity activity against cancer stem cells.** MTT assay. Mammosphere growth assay. Cellular uptake. Immunoblotting analysis. Apoptosis induction studies.	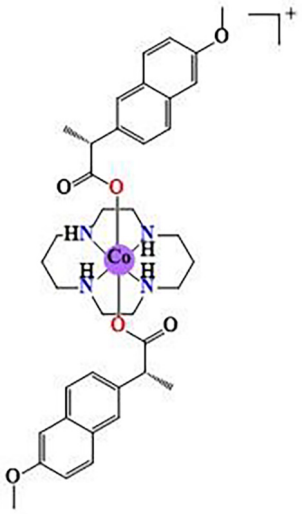	[247]
115-Co	pUC19, AGE, OxC	***Cytotoxicity activity against cancer stem cells.** MTT assay. Mammosphere growth assay. Cellular uptake. Immunoblotting analysis. Apoptosis induction studies.	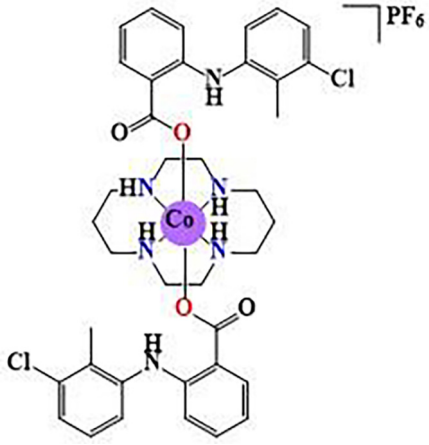	[248]
116-Zn	pBluescript KS II, AGE, [c]PC	***Antioxidant activity**	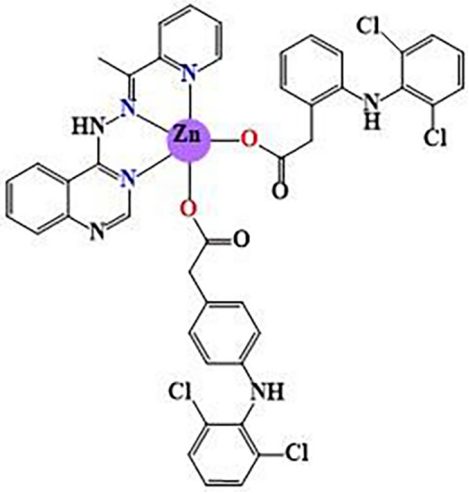	[249]

(*continued on next page*)

Table 3 (*continued*)

AMS	Substrate, Method, Mechanism	Toxicity studies	Molecular structure	Ref.
117-Cu	pBR322, AGE, OxC	*Cytotoxicity activity: MTT assay.	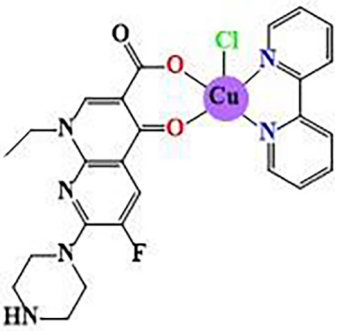	[250]
118-Zn	pUC18, AGE	*Cytotoxicity activity: MTT assay. *Antibacterial activity.	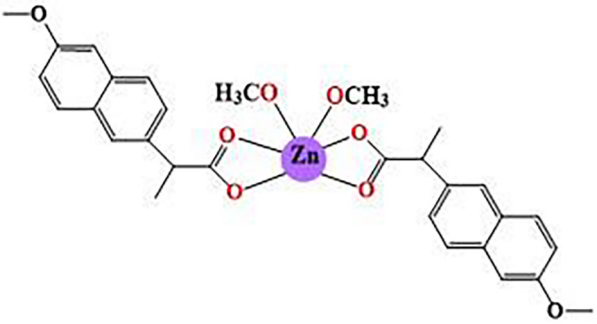	[251]
119-Ni	pUC18, AGE	*Cytotoxicity activity: MTT assay. Apoptosis induction studies. Gene expression.	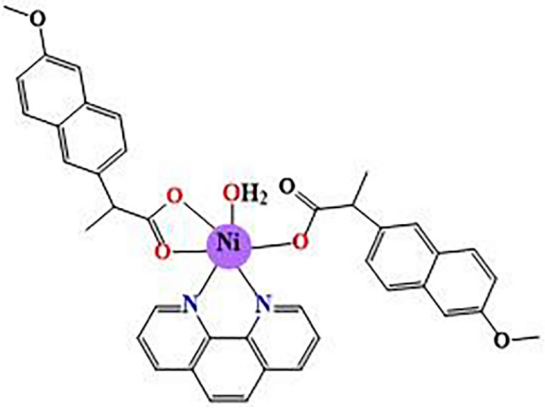	[252]

[a] AGE = Agarose gel electrophoresis,
[b] OxC = Oxidative cleavage,
[c] PC = Photocleavage.

uation. Consequently, it is remarkably clear that there is an urgent need for the design of new compounds and introduction of new generations of drugs with novel therapeutic properties. Catalytic metallodrugs possessing nucleases-like activity can be used as an effective therapeutic strategy. Introduction of artificial metalloscissors that target disease-associated DNA/RNA can improve drug efficacy and provide a mode of action distinct from traditional drugs. This therapeutic strategy has been inspired from natural metallonucleases as well as metallopeptide antibiotics. The metallobleomycins are among the best DNA cleaving metallopeptide antibiotics with potential therapeutic applications and can be considered front runner metalloscissors. Although AMSs possess unique characteristics, their practical applications have been limited by some challenges. In order to overcome these limitations, the new research opportunities are summarized as follows:

(1) Structure–activity relationship: Current understanding of structure–activity relationships of the AMSs does not seem to be enough to allow provision of generalized rules. More experimental and theoretical studies should actively aid in the process of AMSs design with high nuclease efficiency and consequently better therapeutic potential.

(2) Substrate selectivity: Much attention needs to be paid to novel AMSs with high substrate selectivity and specificity. Conjugation of metal complexes with bioactive molecules such as peptides and proteins, nucleotides, and vitamins can facilitate recognition of specific substrates and result in efficient site-specific nucleic acid cleavage.

(3) Mechanism of action: Further studies are needed to more precisely illustrate the DNA/RNA cleavage and also intracellular mechanism when AMSs are applied. The action mechanism will have to be comprehensively studied to allow better adjustment of AMSs' nuclease and biological activities.

(4) Multienzyme-like catalysts: According to the physiochemical properties of metal complexes, construction of AMSs possessing multienzyme-like activity should come under focus of research and development in the future.

(5) Photo-based therapeutic approaches: this successful alternative treatment should be developed for cancer therapy. Moreover, with the growing number of pathogens and viruses resistant towards commonly used drugs, PDT seems to be a very promising substitute to conventional antibiotics and antiviral drugs. We expect to see more growth on the presence of AMSs as PDT agents on the market in near future. Ideal metal complexes as PS agents should be designed with high solubility in aqueous media, high photochemical stability, being nontoxic in the dark, and strong light absorption capacity coupled with high molar extinction coefficient in the phototherapeutic window (600–900 nm).

(6) Targeted therapy: For many therapeutic applications, an important challenge is lack of targeted drug delivery. Therefore, it is now well-recognized that new approaches are needed to introduce novel agents or formulations to improve targeted therapy. One of the attractive approaches is formulation of AMSs in drug delivery systems *viz*., liposomes, niosomes, and polymers. Another promising approach is antibody-AMS, protein-AMS, vitamin-AMS, and polysaccharide-AMS conjugations. We expect to see more growth on these fronts in the future.

(7) Nanozymology field: Enormous progress has been made in designing and preparation of nanomaterials with enzyme-like activity, namely nanozymes. We have addressed the combination of AMSs with nanoparticles for improvement of their nuclease-like activity in the "Introduction". However, there is still a lot of room for expansion of this field.

(8) Practical therapeutic applications: Researchers need to focus on the preparation of new AMSs with low toxicity and high efficiency. Successful application of AMSs to clinical use strongly depends on their biocompatibility, biodegradability, and therapeutic biosafety. Further studies are necessary to explore *in vivo* practical therapeutic applications.

Declaration of Competing Interest

The authors declare that they have no known competing financial interests or personal relationships that could have appeared to influence the work reported in this paper.

Acknowledgements

Authors would like to thank the Vice-Chancellorship for Research, Kerman University of Medical Sciences, Kerman, Iran, for their effective support.

Appendix A. Supplementary data

Supplementary data to this article can be found online at https://doi.org/10.1016/j.ccr.2022.214417.

References:

[1] S. Mhatre, S. Naik, V. Patravale, A molecular docking study of EGCG and theaflavin digallate with the druggable targets of SARS-CoV-2, Comput. Biol. Med. 129 (2021) 104137, https://doi.org/10.1016/j.compbiomed.2020.104137.

[2] World Health Organization, Coronavirus disease (COVID-2019) situation, Retrieved from https://www.who.int/emergencies/diseases/novel-coronavirus-2019/situation-reports. (27 July 2021).

[3] K. Rosner, DNase1: a new personalized therapy for cancer?, Expert Rev Anticancer Ther. 11 (7) (2011) 983–986, https://doi.org/10.1586/era.11.90.

[4] L.A. Alexeeva, O.A. Patutina, A.V. Sen'kova, M.A. Zenkova, N.L. Mironova, Inhibition of invasive properties of murine melanoma by bovine pancreatic DNase I *in vitro* and *in vivo*, Mol. Biol. 51 (4) (2017) 562–570, https://doi.org/10.1134/S0026893317040021.

[5] I. Lee, Ranpirnase (Onconase®), a cytotoxic amphibian ribonuclease, manipulates tumour physiological parameters as a selective killer and a potential enhancer for chemotherapy and radiation in cancer therapy, Expert Opin. Biol. Ther. 8 (6) (2008) 813–827, https://doi.org/10.1517/14712598.8.6.813.

[6] W. Ardelt, B. Ardelt, Z. Darzynkiewicz, Ribonucleases as potential modalities in anticancer therapy, Eur. J. Pharmacol. 625 (1-3) (2009) 181–189, https://doi.org/10.1016/j.ejphar.2009.06.067.

[7] X. Dan, W. Liu, J.H. Wong, T.B. Ng, A ribonuclease isolated from wild ganoderma lucidum suppressed autophagy and triggered apoptosis in colorectal cancer cells, Front. Pharmacol. 7 (2016), https://doi.org/10.3389/fphar.2016.00217 e217.

[8] X. Si, S. Ma, Y. Xu, D. Zhang, N. Shen, H. Yu, Y. Zhang, W. Song, Z. Tang, X. Chen, Hypoxia-sensitive supramolecular nanogels for the cytosolic delivery of ribonuclease A as a breast cancer therapeutic, J. Control. Release 320 (2020) 83–95, https://doi.org/10.1016/j.jconrel.2020.01.021.

[9] Y. Liu, H. Nie, R. Mao, B. Mitra, D. Cai, R. Yan, J.-T. Guo, T.M. Block, N. Mechti, H. Guo, A. Siddiqui, Interferon-inducible ribonuclease ISG20 inhibits hepatitis B virus replication through directly binding to the epsilon stem-loop structure of viral RNA, PLOS Pathog. 13 (4) (2017) e1006296, https://doi.org/10.1371/journal.ppat.1006296.

[10] R.S. Mahmud, C. Müller, Y. Romanova, A. Mostafa, V. Ulyanova, S. Pleschka, O. Ilinskaya, Ribonuclease from *bacillus* acts as an antiviral agent against negative- and positive-Sense single stranded human respiratory RNA viruses, BioMed Res. Int. 2017 (2017) 1–11, https://doi.org/10.1155/2017/5279065.

[11] C. Xia, Y.-C. Chen, H. Gong, W. Zeng, G.-P. Vu, P. Trang, S. Lu, J. Wu, F. Liu, Inhibition of hepatitis B virus gene expression and replication by ribonuclease P, Mol. Ther. 21 (5) (2013) 995–1003, https://doi.org/10.1038/mt.2013.37.

[12] B. Becknell, J.D. Spencer, A review of ribonuclease 7's structure, regulation, and contributions to host defense, Int. J. Mol. Sci. 17 (2016) 423, https://doi.org/10.3390/ijms17030423.

[13] Z. Yu, J.A. Cowan, Metal complexes promoting catalytic cleavage of nucleic acids– biochemical tools and therapeutics, Curr. Opin. Chem. Biol. 43 (2018) 37–42, https://doi.org/10.1016/j.cbpa.2017.10.029.

[14] Z. Yu, J.A. Cowan, Catalytic metallodrugs: Substrate-selective metal catalysts as therapeutics, Chem. Eur. J. 23 (57) (2017) 14113–14127, https://doi.org/10.1002/chem.201701714.

[15] P. Gonzalez, K. Bossak, E. Stefaniak, C. Hureau, L. Raibaut, W. Bal, P. Faller, N-terminal Cu-binding motifs (Xxx-Zzz-His, Xxx-His) and their derivatives: Chemistry, biology and medicinal applications, Chem. Eur. J. 24 (32) (2018) 8029–8041, https://doi.org/10.1002/chem.v24.3210.1002/chem.201705398.

[16] D.S. Sigman, D.R. Graham, V. D'Aurora, A.M. Stern, Oxygen-dependent cleavage of DNA by the 1,10-phenanthroline. cuprous complex. Inhibition of *Escherichia coli* DNA polymerase I, J. Biol. Chem. 254 (24) (1979) 12269–12272, https://doi.org/10.1016/S0021-9258(19)86305-6.

[17] Z. Thompson, J.A. Cowan, Artificial metalloenzymes: Recent developments and innovations in bioinorganic catalysis, Small 16 (27) (2020) 2000392, https://doi.org/10.1002/smll.v16.2710.1002/smll.202000392.

[18] A. Erxleben, Interactions of copper complexes with nucleic acids, Coord. Chem. Rev. 360 (2018) 92–121, https://doi.org/10.1016/j.ccr.2018.01.008.

[19] A. Erxleben, Mechanistic studies of homo- and heterodinuclear zinc phosphoesterase mimics: What has been learned?, Front Chem. 7 (2019), https://doi.org/10.3389/fchem.2019.00082.

[20] T. McGivern, S. Afsharpour, C.J. Marmion, Copper complexes as artificial DNA metallonucleases: From sigman's reagent to next generation anti-cancer agent?, Inorg Chim. Acta 472 (2018) 12–39, https://doi.org/10.1016/j.ica.2017.08.043.

[21] T. Joshi, B. Graham, L. Spiccia, Macrocyclic metal complexes for metalloenzyme mimicry and sensor development, Acc. Chem. Res. 48 (8) (2015) 2366–2379, https://doi.org/10.1021/acs.accounts.5b00142.

[22] C. Wende, C. Lüdtke, N. Kulak, Copper complexes of N-donor ligands as artificial nucleases, Eur. J. Inorg. Chem. 2014 (16) (2014) 2597–2612, https://doi.org/10.1002/ejic.v2014.1610.1002/ejic.201400032.

[23] D. Desbouis, I.P. Troitsky, M.J. Belousoff, L. Spiccia, B. Graham, Copper(II), zinc (II) and nickel(II) complexes as nuclease mimetics, Coord. Chem. Rev. 256 (11-12) (2012) 897–937, https://doi.org/10.1016/j.ccr.2011.12.005.

[24] L. Yu, F. Li, J. Wu, J. Xie, S. Li, Development of the aza-crown ether metal complexes as artificial hydrolase, J. Inorg. Biochem. 154 (2016) 89–102, https://doi.org/10.1016/j.jinorgbio.2015.09.011.

[25] C.M. Agbale, M.H. Cardoso, I.K. Galyuon, O.L. Franco, Designing metallodrugs with nuclease and protease activity, Metallomics 8 (11) (2016) 1159–1169, https://doi.org/10.1039/C6MT00133E.

[26] F. Mancin, P. Scrimin, P. Tecilla, Paolo Tecilla, Progress in artificial metallonucleases, Chem. Commun. 48 (45) (2012) 5545, https://doi.org/10.1039/c2cc30952a.
[27] F. Li, J. Xie, F. Feng, Copper and zinc complexes of diaza-crown ether as artificial nucleases for efficient hydrolytic cleavage of DNA, New J. Chem. 39 (2015) 5654–5660, https://doi.org/10.1039/c4nj02193b.
[28] S. Zehra, S. Tabassum, H.A. Al-Lohedan, F. Arjmand, A zwitterionic Zn(II) benzothiazole nanohybrid conjugate as hydrolytic DNA cleavage agent, Inorg. Chem. Commun. 93 (2018) 69–72, https://doi.org/10.1016/j.inoche.2018.05.008.
[29] Z. Molphy, D. Montagner, S.S. Bhat, C. Slator, C. Long, A. Erxleben, A. Kellett, A phosphate-targeted dinuclear Cu(II) complex combining major groove binding and oxidative DNA cleavage, Nucleic Acids Res. 46 (2018) 9918–9931, https://doi.org/10.1093/nar/gky806.
[30] Y. Kadoya, K. Fukui, M. Hata, R. Miyano, Y. Hitomi, S. Yanagisawa, M. Kubo, M. Kodera, Oxidative DNA cleavage, formation of μ-1,1-hydroperoxo species, and cytotoxicity of dicopper(II) complex supported by a *p*-cresol-derived amide-tether ligand, Inorg. Chem. 58 (21) (2019) 14294–14298, https://doi.org/10.1021/acs.inorgchem.9b02093.
[31] J. Weynand, A. Moreno-Betancourt, F. Loiseau, N. Berthet, E. Defrancq, B. Elias, Redox-active bis-cyclometalated iridium(III) complex as a DNA photo-cleaving agent, Inorg. Chem. 59 (4) (2020) 2426–2433, https://doi.org/10.1021/acs.inorgchem.9b03312.
[32] M.H. Kaulage, B. Maji, S. Pasadi, S. Bhattacharya, K. Muniyappa, Novel ruthenium azo-quinoline complexes with enhanced photonuclease activity in human cancer cells, Eur. J. Med. Chem. 139 (2017) 1016–1029, https://doi.org/10.1016/j.ejmech.2017.08.059.
[33] V. Singh, K. Sharma, B. Shankar, S.K. Awasthi, R.D. Gupta, Heteroleptic Cu(II)–polypyridyl complexes as photonucleases, New J. Chem. 40 (2016) 5906–5913, https://doi.org/10.1039/c6nj00409a.
[34] L. Gao, Y. Zhang, L. Zhao, W. Niu, Y. Tang, F. Gao, P. Cai, Q. Yuan, X. Wang, H. Jiang, X. Gao, An artificial metalloenzyme for catalytic cancer-specific DNA cleavage and operando imaging, Sci. Adv. 6 (2020) eabb1421, https://doi.org/10.1126/sciadv.abb1421.
[35] Y. Guo, Y. He, S. Wu, S. Zhang, D. Song, Z. Zhu, Z. Guo, X. Wang, Enhancing cytotoxicity of a monofunctional platinum complex via a dual-DNA-damage approach, Inorg. Chem. 58 (19) (2019) 13150–13160, https://doi.org/10.1021/acs.inorgchem.9b02033.
[36] S. Parveen, J.A. Cowan, Z. Yu, F. Arjmand, Enantiomeric copper based anticancer agents promoting sequence-selective cleavage of G-quadruplex telomeric DNA and non-random cleavage of plasmid DNA, Metallomics 12 (2020) 988–999, https://doi.org/10.1039/d0mt00084a.
[37] Z. Yu, M. Han, J.A. Cowan, Toward the design of a catalytic metallodrug: Selective cleavage of G-quadruplex telomeric DNA by an anticancer copper–acridine–ATCUN complex, Angew. Chem. Int. Ed. 127 (6) (2015) 1921–1925, https://doi.org/10.1002/ange.201410434.
[38] Q. Cao, Y.i. Li, E. Freisinger, P.Z. Qin, R.K.O. Sigel, Z.-W. Mao, G-quadruplex DNA targeted metal complexes acting as potential anticancer drugs, Inorg. Chem. Front. 4 (1) (2017) 10–32, https://doi.org/10.1039/C6QI00300A.
[39] D.H. Nakahata, R.E.F. de Paiva, W.R. Lustri, C.M. Ribeiro, F.R. Pavan, G.G. da Silva, A.L.T.G. Ruiz, J.E. de Carvalho, P.P. Corbi, Sulfonamide-containing copper (II) metallonucleases: Correlations with in vitro antimycobacterial and antiproliferative activities, J. Inorg. Biochem. 187 (2018) 85–96, https://doi.org/10.1016/j.jinorgbio.2018.07.011.
[40] J.C. Joyner, W.F. Hodnick, A.S. Cowan, D. Tamuly, R. Boyd, J.A. Cowan, Antimicrobial metallopeptides with broad nuclease and ribonuclease activity, Chem. Commun. 49 (2013) 2118–2120, https://doi.org/10.1039/c3cc38977d.
[41] Z. Chen, H. Ji, C. Liu, W. Bing, Z. Wang, X. Qu, A Multinuclear metal complex based DNase-mimetic artificial enzyme: Matrix cleavage for combating bacterial biofilms, Angew. Chem. Int. Ed. 55 (36) (2016) 10732–10736, https://doi.org/10.1002/anie.201605296.
[42] S.A. Juliano, S. Pierce, J.A. deMayo, M.J. Balunas, A.M. Angeles-Boza, Exploration of the innate immune system of *styela clava*: Zn^{2+} binding enhances the antimicrobial activity of the tunicate peptide clavanin A, Biochem. 56 (10) (2017) 1403–1414, https://doi.org/10.1021/acs.biochem.6b01046.
[43] M.D.J. Libardo, A.A. Bahar, B. Ma, R. Fu, L.E. McCormick, J. Zhao, S.A. McCallum, R. Nussinov, D. Ren, A.M. Angeles-Boza, M.L. Cotten, Nuclease activity gives an edge to host-defense peptide piscidin 3 over piscidin 1, rendering it more effective against persisters and biofilms, FEBS J. 284 (21) (2017) 3662–3683, https://doi.org/10.1111/febs.2017.284.issue-2110.1111/febs.14263.
[44] G. Kumaravel, N. Raman, A treatise on benzimidazole based Schiff base metal (II) complexes accentuating their biological efficacy: Spectroscopic evaluation of DNA interactions, DNA cleavage and antimicrobial screening, Mater. Sci. Eng. C 70 (2017) 184–194, https://doi.org/10.1016/j.msec.2016.08.069.
[45] M. Manjunath, A.D. Kulkarni, G.B. Bagihalli, S. Malladi, S.A. Patil, Bio-important antipyrine derived Schiff bases and their transition metal complexes: Synthesis, spectroscopic characterization, antimicrobial, anthelmintic and DNA cleavage investigation, J. Mol. Struct. 1127 (2017) 314–321, https://doi.org/10.1016/j.molstruc.2016.07.123.
[46] S.S. Bradford, M.J. Ross, I. Fidai, J.A. Cowan, Insight into the recognition, binding, and reactivity of catalytic metallodrugs targeting stem loop IIb of hepatitis C IRES RNA, ChemMedChem. 9 (2014) 1275–1285, https://doi.org/10.1002/cmdc.201400070.
[47] M.J. Ross, S.S. Bradford, J.A. Cowan, Catalytic metallodrugs based on the LaR2C peptide target HCV SLIV IRES RNA, Dalton Trans. 44 (48) (2015) 20972–20982, https://doi.org/10.1039/C5DT02837J.
[48] M.J. Ross, I. Fidai, J.A. Cowan, Analysis of structure-activity relationships based on the HCV SLIIb IRES RNA-targeting GGHYRFK-Cu complex, ChemBioChem. 18 (2017) 1743–1754, https://doi.org/10.1002/cbic.201700228.
[49] J.C. Joyner, K.D. Keuper, J.A. Cowan, Kinetics and mechanisms of oxidative cleavage of HIV RRE RNA by Rev-coupled transition metal–chelates, Chem. Sci. 4 (2013) 1707–1718, https://doi.org/10.1039/c3sc22135k.
[50] B. Gyurcsik, A. Czene, Towards artificial metallonucleases for gene therapy: recent advances and new perspectives, Future Med. Chem. 3 (15) (2011) 1935–1966, https://doi.org/10.4155/fmc.11.139.
[51] N. Fantoni, T. Lauria, A. Kellett, Genome engineering with synthetic copper nucleases, Synlett 26 (19) (2015) 2623–2626, https://doi.org/10.1055/s-0000008310.1055/s-005-3045510.1055/s-0035-1560709.
[52] C. Mari, V. Pierroz, R. Rubbiani, M. Patra, J. Hess, B. Spingler, L. Oehninger, J. Schur, I. Ott, L. Salassa, S. Ferrari, G. Gasser, DNA intercalating Ru^{II} polypyridyl complexes as effective photosensitizers in photodynamic therapy, Chem. Eur. J. 20 (44) (2014) 14421–14436, https://doi.org/10.1002/chem.v20.4410.1002/chem.201402796.
[53] V.A. Oliveira, H. Terenzi, L.B. Menezes, O.A. Chaves, B.A. Iglesias, Evaluation of DNA-binding and DNA-photocleavage ability of tetra-cationic porphyrins containing peripheral $[Ru(bpy)_2Cl]^+$ complexes: Insights for photodynamic therapy agents, J. Photochem. Photobiol. B: Biol. 211 (2020) 111991, https://doi.org/10.1016/j.jphotobiol.2020.111991.
[54] K. Mitra, A. Shettar, P. Kondaiah, A.R. Chakravarty, Biotinylated platinum(II) ferrocenylterpyridine complexes for targeted photoinduced cytotoxicity, Inorg. Chem. 55 (11) (2016) 5612–5622, https://doi.org/10.1021/acs.inorgchem.6b0068010.1021/acs.inorgchem.6b00680.s001.
[55] F.D. Abreu, T.d.F. Paulo, M.H. Gehlen, R.A. Ando, L.G.F. Lopes, A.C.S. Gondim, M.A. Vasconcelos, E.H. Teixeira, E.H.S. Sousa, I.M.M. de Carvalho, Aryl-substituted ruthenium(II) complexes: A strategy for enhanced photocleavage and efficient DNA binding, Inorg. Chem. 56 (15) (2017) 9084–9096, https://doi.org/10.1021/acs.inorgchem.7b0110810.1021/acs.inorgchem.7b01108.s001.
[56] A.M. Homrich, G. Farias, S.M. Amorim, F.R. Xavier, R.A. Gariani, A. Neves, H. Terenzi, R.A. Peralta, Effect of chelate ring size of binuclear copper(II) complexes on catecholase activity and DNA cleavage, Eur. J. Inorg. Chem. 2021 (18) (2021) 1710–1721, https://doi.org/10.1002/ejic.v2021.1810.1002/ejic.202001170.
[57] T.P. Camargo, A. Neves, R.A. Peralta, C. Chaves, E.C.P. Maia, E.H. Lizarazo-Jaimes, D.A. Gomes, T. Bortolotto, D.R. Norberto, H. Terenzi, D.L. Tierney, G. Schenk, Second-sphere effects in dinuclear $Fe^{III}Zn^{II}$ hydrolase biomimetics: Tuning binding and reactivity properties, Inorg. Chem. 57 (1) (2018) 187–203, https://doi.org/10.1021/acs.inorgchem.7b0238410.1021/acs.inorgchem.7b02384.s001.
[58] A. Shanmugapriya, R. Jain, D. Sabarinathan, G. Kalaiarasi, F. Dallemer, R. Prabhakaran, Structurally different mono, bi and trinuclear Pd(II) complexes and their DNA/Protein interaction, DNA cleavage, anti-oxidant, anti-microbial and cytotoxicity studies, New J. Chem. 41 (2017) 10324–10338, https://doi.org/10.1039/c7nj01556a.
[59] N. Dutta, S. Haldar, G. Vijaykumar, S. Paul, A.P. Chattopadhyay, L. Carrella, M. Bera, Phosphatase-like activity of tetranuclear iron(III) and zinc(II) complexes, Inorg. Chem. 57 (17) (2018) 10802–10820, https://doi.org/10.1021/acs.inorgchem.8b0144110.1021/acs.inorgchem.8b01441.s001.
[60] P. Sureshbabu, Q.M. Junaid, C. Upadhyay, W. Victoria, V. Pitchavel, S. Natarajan, S. Sabiah, Di and tetranuclear Cu(II) complexes with simple 2-aminoethylpyridine: Magnetic properties, phosphodiester hydrolysis, DNA binding/cleavage, cytotoxicity and catecholase activity, Polyhedron 164 (2019) 202–218, https://doi.org/10.1016/j.poly.2019.02.015.
[61] M. Afzal, M. Usman, H.A. Al-Lohedan, S. Tabassum, Synthesis and characterization of heterobimetallic Sn^{IV}-Cu^{II}/Zn^{II} complexes: DFT studies, cleavage potential and cytotoxic activity, J. Biomol. Struct. Dyn. 38 (4) (2020) 1130–1142, https://doi.org/10.1080/07391102.2019.1596837.
[62] Y. Kadoya, M. Hata, Y. Tanaka, A. Hirohata, Y. Hitomi, M. Kodera, Dicopper(II) complexes of *p*-cresol-2,6-bis(dpa) amide-tether ligands: Large enhancement of oxidative DNA cleavage, cytotoxicity, and mechanistic insight by intracellular visualization, Inorg. Chem. 60 (8) (2021) 5474–5482, https://doi.org/10.1021/acs.inorgchem.0c02954.
[63] P. Joshi, N. Hussain, S.R. Ali, R. Dhiman, V.K. Bhardwaj, Enhanced activity of trinuclear Zn(II) complex towards phosphate ester bond cleavage by introducing three metal cooperativity, New J. Chem. 42 (2017) 2204–2215, https://doi.org/10.1039/c7nj03759g.
[64] S. Swavey, M. DeBeer, K. Li, Photoinduced interactions of supramolecular ruthenium(II) complexes with plasmid DNA: Synthesis and spectroscopic, electrochemical, and DNA photocleavage studies, Inorg. Chem. 54 (7) (2015) 3139–3147, https://doi.org/10.1021/ic502340p.
[65] S. Swavey, K. Li, A dimetallic osmium(II) complex as a potential phototherapeutic agent: Binding and photocleavage studies with plasmid DNA, Eur. J. Inorg. Chem. 2015 (33) (2015) 5551–5555, https://doi.org/10.1002/ejic.201500995.
[66] S. Jain, K. Bhar, S. Kumar, S. Bandyopadhyaya, S. Tapryal, C.C. Mandal, A.K. Sharma, Homo- and heteroleptic trimethoxy terpyridine-Cu(II) complexes: Synthesis, characterization, DNA/BSA binding, DNA cleavage and cytotoxicity

studies, Dalton Trans. 49 (2020) 4100–4113, https://doi.org/10.1039/d0dt00209g.
[67] K. Ghosh, S. Chattopadhyay, Synthetic stratagem and structures of two heteroleptic cobalt(III) complexes acting as biomimetic catalysts: Role of co-ligands in catalytic activities, Polyhedron 170 (2019) 495–507, https://doi.org/10.1016/j.poly.2019.05.062.
[68] J. Hormann, M. van der Meer, B. Sarkar, N. Kulak, From cyclen to 12-crown-4 copper(II) complexes: Exchange of donor atoms improves DNA cleavage activity, Eur. J. Inorg. Chem. 2015 (28) (2015) 4722–4730, https://doi.org/10.1002/ejic.v2015.2810.1002/ejic.201500596.
[69] E.Y. Tirel, N.H. Williams, Enhancing phosphate diester cleavage by a zinc complex through controlling nucleophile coordination, Chem. Eur. J. 21 (19) (2015) 7053–7056, https://doi.org/10.1002/chem.201500619.
[70] D. Bím, E. Svobodová, V. Eigner, L. Rulíšek, J. Hodačová, Copper(II) and zinc(II) complexes of conformationally constrained polyazamacrocycles as efficient catalysts for RNA model substrate cleavage in aqueous solution at physiological pH, Chem. Eur. J. 22 (30) (2016) 10426–10437, https://doi.org/10.1002/chem.201601175.
[71] S.D. Kettenmann, Y. Nossol, F.R. Louka, J.R. Legrande, E. Marine, R.C. Fischer, F. A. Mautner, V. Hergl, N. Kulak, S.S. Massoud, Copper(II) complexes with tetradentate piperazine-based ligands: DNA cleavage and cytotoxicity, Inorganics 9 (2021) 12, https://doi.org/10.3390/inorganics9020012.
[72] J. Heinrich, N.F. König, S. Sobottka, B. Sarkar, N. Kulak, Flexible *vs.* rigid bis(2-benzimidazolyl) ligands in Cu(II) complexes: Impact on redox chemistry and oxidative DNA cleavage activity, J. Inorg. Biochem. 194 (2019) 223–232, https://doi.org/10.1016/j.jinorgbio.2019.01.016.
[73] M. Zhao, H.B. Wang, L.N. Ji, Z.W. Mao, Insights into metalloenzyme microenvironments: biomimetic metal complexes with a functional second coordination sphere, Chem. Soc. Rev. 42 (2013) 8360–8375, https://doi.org/10.1039/c3cs60162e.
[74] L. Tjioe, T. Joshi, B. Graham, L. Spiccia, Synthesis and phosphate ester cleavage properties of copper(II) complexes of guanidinium-bridged bis(1,4,7-triazacyclononane) ligands, Polyhedron 120 (2016) 11–17, https://doi.org/10.1016/j.poly.2016.04.040.
[75] C. Pereira, G. Farias, F.G. Maranha, N. Castilho, G. Schenk, B. de Souza, H. Terenzi, A. Neves, R.A. Peralta, Guanidine- and purine-functionalized ligands of $Fe^{III}Zn^{II}$ complexes: effects on the hydrolysis of DNA, J. Biol. Inorg. Chem. 24 (5) (2019) 675–691, https://doi.org/10.1007/s00775-019-01680-3.
[76] C.C.V. Chaves, G. Farias, M.D. Formagio, A. Neves, R.M. Peralta, J.M.G. Mikcha, B. de Souza, R.A. Peralta, Three new dinuclear nickel(II) complexes with amine pendant-armed ligands: Characterization, DFT study, antibacterial and hydrolase-like activity, Inorg. Chim. Acta 507 (2020) 119559, https://doi.org/10.1016/j.ica.2020.119559.
[77] R. Salvio, The guanidinium unit in the catalysis of phosphoryl transfer reactions: From molecular spacers to nanostructured supports, Chem. Eur. J. 21 (31) (2015) 10960–10971, https://doi.org/10.1002/chem.v21.3110.1002/chem.201500789.
[78] G.A.D.S. Silva, A.L. Amorim, B.D. Souza, P. Gabriel, H. Terenzi, E. Nordlander, A. Neves, R.A. Peralta, Synthesis and characterization of $Fe^{III}(\mu\text{-}OH)Zn^{II}$ complexes: Effects of second coordination sphere and increase in the chelate ring size on the hydrolysis of a phosphate diester and DNA, Dalton Trans. 46 (2017) 11380–11394, https://doi.org/10.1039/c7dt02035j.
[79] M. Zhao, S.S. Xue, X.Q. Jiang, L. Zheng, L.N. Ji, Z.W. Mao, Phosphate ester hydrolysis catalyzed by a dinuclear cobalt(II) complex equipped with intramolecular β-cyclodextrins, J. Mol. Catal. A Chem. 396 (2015) 346–352, https://doi.org/10.1016/j.molcata.2014.10.020.
[80] Y.H. Zhou, L.Q. Chen, J. Tao, J.L. Shen, D.Y. Gong, R.R. Yun, Y. Cheng, Effective cleavage of phosphodiester promoted by the zinc(II) and copper(II) inclusion complexes of β-cyclodextrin, J. Inorg. Biochem. 163 (2016) 176–184, https://doi.org/10.1016/j.jinorgbio.2016.07.011.
[81] R. Salvio, S. Volpi, R. Cacciapaglia, F. Sansone, L. Mandolini, A. Casnati, Upper rim bifunctional cone-calix[4]arenes based on a ligated metal ion and a guanidinium unit as DNAase and RNAase mimics, J. Org. Chem. 81 (11) (2016) 4728–4735, https://doi.org/10.1021/acs.joc.6b0064410.1021/acs.joc.6b00644.s001.
[82] R. Salvio, S. Volpi, R. Cacciapaglia, A. Casnati, L. Mandolini, F. Sansone, Ribonuclease activity of an artificial catalyst that combines a ligated Cu^{II} ion and a guanidinium group at the upper rim of a cone calix[4]arene platform, J. Org. Chem. 80 (11) (2015) 5887–5893, https://doi.org/10.1021/acs.joc.5b00965.
[83] B. de Souza, R. Heying, A.J. Bortoluzzi, J.B. Domingos, A. Neves, The effect of chain size on the modeling of second sphere effects in biomimetic complexes, J. Mol. Catal. A Chem. 397 (2015) 76–84, https://doi.org/10.1016/j.molcata.2014.11.006.
[84] A.B. Rahman, H. Imafuku, Y. Miyazawa, A. Kafle, H. Sakai, Y. Saga, S. Aoki, Catalytic hydrolysis of phosphate monoester by supramolecular phosphatases formed from a monoalkylated dizinc(II) complex, cyclic diimide units, and copper(II) in two-phase solvent system, Inorg. Chem. 58 (9) (2019) 5603–5616, https://doi.org/10.1021/acs.inorgchem.8b03586.
[85] S. Aoki, A. Bin Rahman, Y. Hisamatsu, Y. Miyazawa, M. Zulkefeli, Y. Saga, T. Tanaka, Development of metallosupramolecular phosphatases based on the combinatorial self-assembly of metal complexes and organic building blocks for the catalytic hydrolysis of phosphate monoesters, Results Chem. 3 (2021) 100133, https://doi.org/10.1016/j.rechem.2021.100133.
[86] A.B. Rahman, H. Okamoto, Y. Miyazawa, S. Aoki, Design and synthesis of supramolecular phosphatases formed from a bis(Zn^{2+}-cyclen) complex, barbital-crown-K^+ conjugate and Cu^{2+} for the catalytic hydrolysis of phosphate monoester, Eur. J. Inorg. Chem. 2021 (2021) 1213–1223, https://doi.org/10.1002/ejic.202100161.
[87] Y. Miyazawa, A.B. Rahman, Y. Saga, H. Imafuku, Y. Hisamatsu, S. Aoki, Catalytic hydrolysis of phosphate monoester by supramolecular complexes formed by the self-assembly of a hydrophobic bis(Zn^{2+}-cyclen) complex, copper, and barbital units that are functionalized with amino acids in a two-phase solvent system, Micromachines 10 (2019) 452, https://doi.org/10.3390/mi10070452.
[88] Y. Hisamatsu, Y. Miyazawa, K. Yoneda, M. Miyauchi, M. Zulkefeli, S. Aoki, Supramolecular complexes formed by the self-assembly of hydrophobic bis(Zn^{2+}-cyclen) complexes, copper, and di- or triimide units for the hydrolysis of phosphate mono- and diesters in two-phase solvent systems (Cyclen=1,4,7,10-Tetraazacyclododecane), Chem. Pharm. Bull. 64 (2016) 451–464, https://doi.org/10.1248/cpb.c15-01014.
[89] C. Schattschneider, S.D. Kettenmann, S. Hinojosa, J. Heinrich, N. Kulak, Biological activity of amphiphilic metal complexes, Coord. Chem. Rev. 385 (2019) 191–207, https://doi.org/10.1016/j.ccr.2018.12.007.
[90] F. Mancin, L.J. Prins, P. Pengo, L. Pasquato, P. Tecilla, P. Scrimin, Hydrolytic metallo-nanozymes: From micelles and vesicles to gold nanoparticles, Molecules 21 (2016) 1014, https://doi.org/10.3390/molecules21081014.
[91] P. Solís Muñana, G. Ragazzon, J. Dupont, C.-J. Ren, L.J. Prins, J.-Y. Chen, Substrate-induced self-assembly of cooperative catalysts, Angew. Chem. Int. Ed. 130 (50) (2018) 16707–16712, https://doi.org/10.1002/ange.201810891.
[92] A. Nomura, M. Kodera, Y. Hitomi, Enhanced oxidative DNA cleavage activity of iron complex of pentadentate mono-carboxamide ligand having spermine as DNA binding domain, Chem. Lett. 49 (11) (2020) 1353–1355, https://doi.org/10.1246/cl.200493.
[93] H.-G. Fu, Y. Chen, Q. Yu, Y. Liu, A tumor-targeting Ru/polysaccharide/protein supramolecular assembly with high photodynamic therapy ability, Chem. Commun. 55 (21) (2019) 3148–3151, https://doi.org/10.1039/C8CC09964B.
[94] N. Castilho, P. Gabriel, T.P. Camargo, A. Neves, H. Terenzi, Targeting an artificial metal nuclease to DNA by a simple chemical modification and its drastic effect on catalysis, ACS Med. Chem. Lett. 11 (3) (2020) 286–291, https://doi.org/10.1021/acsmedchemlett.9b0028910.1021/acsmedchemlett.9b00289.s001.
[95] A. Panattoni, A.H. El-Sagheer, T. Brown, A. Kellett, M. Hocek, Oxidative DNA cleavage with clip-phenanthroline triplex forming oligonucleotide hybrids, ChemBioChem 21 (7) (2020) 991–1000, https://doi.org/10.1002/cbic.v21.710.1002/cbic.201900670.
[96] N. Zuin Fantoni, B. McGorman, Z. Molphy, D. Singleton, S. Walsh, A.H. El-Sagheer, V. McKee, T. Brown, A. Kellett, Development of gene-targeted polypyridyl triplex forming oligonucleotide hybrids, ChemBioChem 21 (24) (2020) 3563–3574, https://doi.org/10.1002/cbic.v21.2410.1002/cbic.202000408.
[97] T. Lauria, C. Slator, V. McKee, M. Müller, S. Stazzoni, A.L. Crisp, T. Carell, A. Kellett, A click chemistry approach to developing molecularly targeted DNA scissors, Chem. Eur. J. 26 (70) (2020) 16782–16792, https://doi.org/10.1002/chem.v26.7010.1002/chem.202002860.
[98] M. Tosolini, T. Gianferrara, G. Mion, L. Dovigo, F. Mancin, C. Sissi, P. Tecilla, Interaction with plasmid DNA of Hoechst-TACN conjugates, Supramol. Chem. 32 (2) (2020) 91–105, https://doi.org/10.1080/10610278.2019.1699657.
[99] C. Sissi, L. Dovigo, M.L. Greco, A. Ciancetta, S. Moro, J.W. Trzciński, F. Mancin, P. Rossi, G. Spalluto, P. Tecilla, P, Tecilla, Conjugates between minor groove binders and Zn(II)-tach complexes: Synthesis, characterization, and interaction with plasmid DNA, Tetrahedron 73 (21) (2017) 3014–3024, https://doi.org/10.1016/j.tet.2017.04.013.
[100] M. Diez-Castellnou, F. Mancin, P. Scrimin, Efficient phosphodiester cleaving nanozymes resulting from multivalency and local medium polarity control, J. Am. Chem. Soc. 136 (4) (2014) 1158–1161, https://doi.org/10.1021/ja411969e.
[101] J. Czescik, S. Zamolo, T. Darbre, F. Mancin, P. Scrimin, Factors influencing the activity of nanozymes in the cleavage of an RNA model substrate, Molecules 24 (2019) 2814, https://doi.org/10.3390/molecules24152814.
[102] J. Hernández-Gil, S. Ferrer, A. Castiñeiras, M. Liu-González, F. Lloret, Á. Ribes, L. Čoga, A. Bernecker, J.C. Mareque-Rivas, Two novel ternary dicopper(II) μ-guanazole complexes with aromatic amines strongly activated by quantum dots for DNA cleavage, Inorg. Chem. 53 (1) (2014) 578–593, https://doi.org/10.1021/ic4027249.
[103] S.A. Trammell, R. Nita, B. Martin, M.H. Moore, J. Fontana, S. Talebzadeh, D.A. Knight, Photo-enhanced hydrolysis of bis(4-nitrophenyl) phosphate using Cu (II) bipyridine-capped plasmonic nanoparticles, RSC Adv. 6 (2016) 41618–41621, https://doi.org/10.1039/c6ra07119h.
[104] J. Czescik, S. Zamolo, T. Darbre, R. Rigo., C. Sissi, A. Pecina, L. Riccardi, M. De Vivo, F. Mancin, P. Scrimin, A gold nanoparticle nanonuclease relying on a Zn (II) mononuclear complex, Angew. Chem. Int. Ed. 60 (3) (2021) 1423–1432, https://doi.org/10.1002/anie.v60.310.1002/anie.202012513.
[105] J. Czescik, F. Mancin, R. Strömberg, P. Scrimin, The mechanism of cleavage of RNA phosphodiesters by a gold nanoparticle nanozyme, Chem. Eur. J. 27 (31) (2021) 8143–8148, https://doi.org/10.1002/chem.202100299.
[106] A. Pecina, D. Rosa-Gastaldo, L. Riccardi, S. Franco-Ulloa, E. Milan, P. Scrimin, F. Mancin, M. De Vivo, On the metal-aided catalytic mechanism for phosphodiester bond cleavage performed by nanozymes, ACS Catal. 11 (14) (2021) 8736–8748, https://doi.org/10.1021/acscatal.1c01215.

[107] Y. Sun, C. Zhao, T. Cui, H. Qin, J. Niu, J. Ren, X. Qu, Near-infrared-traceable DNA nano-hydrolase: specific eradication of telomeric G-overhang in vivo, Nucleic Acids Res. 48 (2020) 9986–9994, https://doi.org/10.1093/nar/gkaa693.
[108] T.H. Sanatkar, H. Hadadzadeh, Z. Jannesari, T. Khayamian, M. Ebrahimi, H.A. Rudbari, M. Torkzadeh-Mahani, M. Anjomshoa, Characterization, photocleavage, molecular modeling, and DNA- and BSA-binding studies of Cu(II) and Ni(II) complexes with the non-steroidal anti-inflammatory drug meloxicam, Inorg. Chim. Acta 423 (2014) 256–272, https://doi.org/10.1016/j.ica.2014.08.060.
[109] M. Anjomshoa, H. Hadadzadeh, M. Torkzadeh-Mahani, S.J. Fatemi, M. Adeli-Sardou, H.A. Rudbari, V.M. Nardo, A mononuclear Cu(II) complex with 5,6-diphenyl-3-(2-pyridyl)-1,2,4-triazine: Synthesis, crystal structure, DNA- and BSA-binding, molecular modeling, and anticancer activity against MCF-7, A-549, and HT-29 cell lines, Eur. J. Med. Chem. 96 (2015) 66–82, https://doi.org/10.1016/j.ejmech.2015.04.020.
[110] M. Anjomshoa, S.J. Fatemi, M. Torkzadeh-Mahani, H. Hadadzadeh, DNA- and BSA-binding studies and anticancer activity against human breast cancer cells (MCF-7) of the zinc(II) complex coordinated by 5,6-diphenyl-3-(2-pyridyl)-1,2,4-triazine, Spectrochim, Acta Part A: Mol. Biomol. Spectrosc. 127 (2014) 511–520, https://doi.org/10.1016/j.saa.2014.02.048.
[111] M. Anjomshoa, M. Torkzadeh-Mahani, E. Dashtrazmi, M. Adeli-Sardou, Sonochemical synthesis and characterization of the copper(II) nanocomplex: DNA- and BSA-binding, cell imaging, and cytotoxicity against the human carcinoma cell lines, J. Fluoresc. 26 (2016) 545–558, https://doi.org/10.1007/s10895-015-1739-2.
[112] M. Anjomshoa, M. Torkzadeh-Mahani, M. Shakeri, M. Adeli-Sardou, The Zn(II) nanocomplex: Sonochemical synthesis, characterization, DNA- and BSA-binding, cell imaging, and cytotoxicity against the human carcinoma cell lines, J. Fluoresc. 26 (3) (2016) 1007–1020, https://doi.org/10.1007/s10895-016-1788-1.
[113] M. Anjomshoa, M. Torkzadeh-Mahani, *In vitro* DNA and BSA-binding, cell imaging and anticancer activity against human carcinoma cell lines of mixed ligand copper(II) complexes, Spectrochim, Acta Part A: Mol. Biomol. Spectrosc. 150 (2015) 390–402, https://doi.org/10.1016/j.saa.2015.05.076.
[114] M. Anjomshoa, H. Hadadzadeh, S.J. Fatemi, M. Torkzadeh-Mahani, A mononuclear Ni(II) complex with 5,6-diphenyl-3-(2-pyridyl)-1,2,4-triazine: DNA- and BSA-binding and anticancer activity against human breast carcinoma cells, Spectrochim, Acta Part A: Mol. Biomol. Spectrosc. 136 (2015) 205–215, https://doi.org/10.1016/j.saa.2014.09.016.
[115] M. Anjomshoa, M. Torkzadeh-Mahani, M. Sahihi, C. Rizzoli, M. Ansari, J. Janczak, S. Sherafat Esfahani, F. Ataei, M. Dehkhodaei, B. Amirheidari, Tris-chelated complexes of nickel(II) with bipyridine derivatives: DNA binding and cleavage, BSA binding, molecular docking, and cytotoxicity, J. Biomol. Struc. Dyn. 37 (15) (2019) 3887–3904, https://doi.org/10.1080/07391102.2018.1534700.
[116] M. Anjomshoa, M. Torkzadeh-Mahani, J. Janczak, C. Rizzoli, M. Sahihi, F. Ataei, M. Dehkhodaei, Synthesis, crystal structure and Hirshfeld surface analysis of copper(II) complexes: DNA- and BSA- binding, molecular modeling, cell imaging and cytotoxicity, Polyhedron 119 (2016) 23–38, https://doi.org/10.1016/j.poly.2016.08.018.
[117] A. Mandegary, M. Torshabi, M. Seyedabadi, B. Amirheidari, E. Sharif, M.H. Ghahremani, Indomethacin-enhanced anticancer effect of arsenic trioxide in A549 cell line: Involvement of apoptosis and phospho-ERK and p38 MAPK pathways, BioMed Res. Int. 2013 (2013) 1–9, https://doi.org/10.1155/2013/237543.
[118] H. Forootanfar, M. Adeli-Sardou, M. Nikkhoo, M. Mehrabani, B. Amir-Heidari, A.R. Shahverdi, M. Shakibaie, Antioxidant and cytotoxic effect of biologically synthesized selenium nanoparticles in comparison to selenium dioxide, J. Trace Elem. Med. Biol. 28 (1) (2014) 75–79, https://doi.org/10.1016/j.jtemb.2013.07.005.
[119] S. Alonso-de Castro, A. Terenzi, J. Gurruchaga-Pereda, L. Salassa, Catalysis concepts in medicinal inorganic chemistry, Chem. Eur. J. 25 (27) (2019) 6651–6660, https://doi.org/10.1002/chem.201806341.
[120] R. Jastrzab, M. Nowak, M. Skrobańska, A. Tolińska, M. Zabiszak, M. Gabryel, Ł. Marciniak, M.T. Kaczmarek, DNA as a target for lanthanide(III) complexes influence, Coord. Chem. Rev. 382 (2019) 145–159, https://doi.org/10.1016/j.ccr.2018.12.018.
[121] R.F. Brissos, A. Caubet, P. Gamez, Possible DNA-interacting pathways for metal-based compounds exemplified with copper coordination compounds, Eur. J. Inorg. Chem. 2015 (16) (2015) 2633–2645, https://doi.org/10.1002/ejic.v2015.1610.1002/ejic.201500175.
[122] S. Mikkola, T. Lönnberg, H. Lönnberg, Phosphodiester models for cleavage of nucleic acids, Beilstein J. Org. Chem. 14 (2018) 803–837, https://doi.org/10.3762/bjoc.14.68.
[123] S.S. Massoud, R.S. Perkins, F.R. Louka, W. Xu, A.L. Roux, Q. Dutercq, R.C. Fischer, F.A. Mautner, M. Handa, Y. Hiraoka, G.L. Kreft, T. Bortolotto, H. Terenzi, Efficient hydrolytic cleavage of plasmid DNA by chloro-cobalt(II) complexes based on sterically hindered pyridyl tripod tetraamine ligands: synthesis, crystal structure and DNA cleavage, Dalton Trans. 43 (2014) 10086–10103, https://doi.org/10.1039/c4dt00615a.
[124] J. Hormann, S. Streller, N. Kulak, Synthesis and evaluation of artificial DNA scissors: An interdisciplinary undergraduate experiment, J. Chem. Educ. 95 (10) (2018) 1848–1855, https://doi.org/10.1021/acs.jchemed.7b00662.
[125] J. Heinrich, J. Stubbe, N. Kulak, Cu(II) complexes with hydrazone-functionalized phenanthrolines as self-activating metallonucleases, Inorg. Chim. Acta 481 (2018) 79–86, https://doi.org/10.1016/j.ica.2017.11.015.
[126] K. Kumar, A. Kumar Dhara, V. Kumar Chaudhary, N. Sandip, P. Roy, P. Verma, K. Ghosh, The influence of the tertiary butyl group in the ligand frame on the catalytic activities, DNA cleavage ability and cytotoxicity of dinuclear nickel (II) complexes, Inorg. Chim. Acta 495 (2019) 118993, https://doi.org/10.1016/j.ica.2019.118993.
[127] Q. Jiang, N. Xiao, P. Shi, Y. Zhu, Z. Guo, Design of artificial metallonucleases with oxidative mechanism, Coord. Chem. Rev. 251 (15-16) (2007) 1951–1972, https://doi.org/10.1016/j.ccr.2007.02.013.
[128] C.J. Burrows, J.G. Muller, Oxidative nucleobase modifications leading to strand scission, Chem. Rev. 98 (3) (1998) 1109–1152, https://doi.org/10.1021/cr960421s.
[129] F. Heinemann, J. Karges, G. Gasser, Critical overview of the use of Ru(II) polypyridyl complexes as photosensitizers in one-photon and two-photon photodynamic therapy, Acc. Chem. Res. 50 (11) (2017) 2727–2736, https://doi.org/10.1021/acs.accounts.7b00180.
[130] S. Monro, K.L. Colón, H. Yin, J. Roque, P. Konda, S. Gujar, R.P. Thummel, L. Lilge, C.G. Cameron, S.A. McFarland, Transition metal complexes and photodynamic therapy from a tumor-centered approach: Challenges, opportunities, and highlights from the development of TLD1433, Chem. Rev. 119 (2) (2019) 797–828, https://doi.org/10.1021/acs.chemrev.8b00211.
[131] M. Dichiara, O. Prezzavento, A. Marrazzo, V. Pittala, L. Salerno, A. Rescifina, E. Amata, Recent advances in drug discovery of phototherapeutic non-porphyrinic anticancer agents, Eur. J. Med. Chem. 142 (2017) 459–485, https://doi.org/10.1016/j.ejmech.2017.08.070.
[132] M.R. Hamblin, Upconversion in photodynamic therapy: plumbing the depths, Dalton Trans. 47 (26) (2018) 8571–8580, https://doi.org/10.1039/C8DT00087E.
[133] P. Murat, S. Balasubramanian, Existence and consequences of G-quadruplex structures in DNA, Curr. Opin. Genet. Dev. 25 (2014) 22–29, https://doi.org/10.1016/j.gde.2013.10.012.
[134] G.N. Parkinson, M.P.H. Lee, S. Neidle, Crystal structure of parallel quadruplexes from human telomeric DNA, Nature 417 (6891) (2002) 876–880, https://doi.org/10.1038/nature755.
[135] Z. Yu, A.L. Hendricks, J.A. Cowan, G-quadruplex targeting chemical nucleases as a nonperturbative tool for analysis of cellular G-quadruplex DNA, iScience 24 (2021) 102661. 10.1016/j.isci.2021.102661.
[136] M. Nadai, F. Doria, M. Scalabrin, V. Pirota, V. Grande, G. Bergamaschi, V. Amendola, F.R. Winnerdy, A.Tuân. Phan, S.N. Richter, M. Freccero, A catalytic and selective scissoring molecular tool for quadruplex nucleic acids, J. Am. Chem. Soc. 140 (44) (2018) 14528–14532, https://doi.org/10.1021/jacs.8b0533710.1021/jacs.8b05337.s001.
[137] F. Arjmand, S. Sharma, S. Parveen, L. Toupet, Z. Yu, J.A. Cowan, Copper(II) L/D-valine-(1,10-phen) complexes target human telomeric G-quadruplex motifs and promote site-specific DNA cleavage and cellular cytotoxicity, Dalton Trans. 49 (2020) 9888–9899, https://doi.org/10.1039/d0dt01527j.
[138] Z. Yu, K.D. Fenk, D. Huang, S. Sen, J.A. Cowan, Rapid telomere reduction in cancer cells induced by G-Quadruplex-targeting copper complexes, J. Med. Chem. 62 (10) (2019) 5040–5048, https://doi.org/10.1021/acs.jmedchem.9b00215.
[139] J.W. Rausch, S.F.J. Le Grice, HIV Rev assembly on the Rev response element (RRE): A structural perspective, Viruses 7 (2015) 3053–3075, https://doi.org/10.3390/v7062760.
[140] J.E. Wynn, W.L. Santos, HIV-1 drug discovery: Targeting folded RNA structures with branched peptides, Org. Biomol. Chem. 13 (21) (2015) 5848–5858, https://doi.org/10.1039/C5OB00589B.
[141] J. Fernandes, B. Jayaraman, A. Frankel, The HIV-1 Rev response element, RNA Bio. 9 (1) (2012) 6–11, https://doi.org/10.4161/rna.9.1.18178.
[142] S. Prado, M. Beltrán, M. Coiras, L.M. Bedoya, J. Alcamí, J. Gallego, Bioavailable inhibitors of HIV-1 RNA biogenesis identified through a Rev-based screen, Biochem. Pharmacol. 107 (2016) 14–28, https://doi.org/10.1016/j.bcp.2016.02.007.
[143] K.E. Berry, S. Waghray, S.A. Mortimer, Y. Bai, J.A. Doudna, Crystal structure of the HCV IRES central domain reveals strategy for start-codon positioning, Structure 19 (10) (2011) 1456–1466, https://doi.org/10.1016/j.str.2011.08.002.
[144] J. Chakraborty, A. Kanungo, T. Mahata, K. Kumar, G. Sharma, R. Pal, K.S. Ahammed, D. Patra, B. Majhi, S. Chakrabarti, S. Das, S. Dutta, Quinoxaline derivatives disrupt the base stacking of hepatitis C virus-internal ribosome entry site RNA: reduce translation and replication, Chem. Commun. 55 (93) (2019) 14027–14030, https://doi.org/10.1039/C9CC06531H.
[145] C. Romero-López, A. Berzal-Herranz, The 5BSL3.2 functional RNA domain connects distant regions in the hepatitis C virus genome, Front. Microbiol. 8 (2017) 2093, https://doi.org/10.3389/fmicb.2017.02093.
[146] B. Kandasamy, S. Vanhaecht, F.M. Nkala, T. Beelen, B.S. Bassil, T.N. Parac-Vogt, U. Kortz, Gallium(III)-containing, sandwich-type heteropolytungstates: Synthesis, solution characterization, and hydrolytic studies toward phosphoester and phosphoanhydride bond cleavage, Inorg. Chem. 55 (18) (2016) 9204–9211, https://doi.org/10.1021/acs.inorgchem.6b01030.
[147] T.K.N. Luong, P. Shestakova , T.T. Mihaylov, G. Absillis, K. Pierloot, T.N. Parac-Vogt, Multinuclear diffusion NMR spectroscopy and DFT modeling: A powerful combination for unraveling the mechanism of phosphoester bond hydrolysis catalyzed by metal-substituted polyoxometalates, Chem. Eur. J. 21 (2015) 4428–4439. https://doi.org/10.1002/chem.201405810.
[148] V.K. Bhardwaj, A. Singh, Comparative DNA binding abilities and phosphatase-like activities of mono–, di–, and trinuclear Ni(II) complexes: The influence of ligand denticity, metal–metal distance, and coordinating solvent/ anion on

kinetics studies, Inorg. Chem. 53 (19) (2014) 10731–10742, https://doi.org/10.1021/ic501961d.
[149] N. Cheng, Y. Chen, J. Yu, J.-jing. Li, Y. Liu, Enhanced DNA binding and photocleavage abilities of β-cyclodextrin appended Ru(II) complex through supramolecular strategy, Bioconjugate Chem. 29 (6) (2018) 1829–1833, https://doi.org/10.1021/acs.bioconjchem.8b0019110.1021/acs.bioconjchem.8b00191.s001.
[150] Y. Zhang, Q. Zhou, Y. Zheng, K. Li, G. Jiang, Y. Hou, B. Zhang, X. Wang, DNA photocleavage by non-innocent ligand-based Ru(II) complexes, Inorg. Chem. 55 (9) (2016) 4296–4300, https://doi.org/10.1021/acs.inorgchem.6b00028.s001.
[151] A.I.B. Romo, V.S. Dibo, D.S. Abreu, M.S.P. Carepo, A.C. Neira, I. Castillo, L. Lemus, O.R. Nascimento, P.V. Bernhardt, E.H.S. Sousa, I.C.N. Diógenes, Ascorbyl and hydroxyl radical generation mediated by a copper complex adsorbed on gold, Dalton Trans. 48 (37) (2019) 14128–14137, https://doi.org/10.1039/C9DT01726G.
[152] P. Bilski, K. Reszka, M. Bilska, C.F. Chignell, Oxidation of the spin trap 5,5-dimethyl-1-pyrroline *N*-oxide by singlet oxygen in aqueous solution, J. Am. Chem. Soc. 118 (6) (1996) 1330–1338, https://doi.org/10.1021/ja952140s.
[153] J.-L. Clément, N. Ferré, D. Siri, H. Karoui, A. Rockenbauer, P. Tordo, Assignment of the EPR spectrum of 5,5-dimethyl-1-pyrroline *N*-oxide (DMPO) superoxide spin adduct, J. Org. Chem. 70 (4) (2005) 1198–1203, https://doi.org/10.1021/jo048518z.
[154] J.W. Yang, Y.L. Lin, C. Dong, C.Q. Zhou, J.X. Chen, B. Wang, Z.Z. Zhou, B. Sun, W. H. Chen, Synthesis, hydrolytic DNA-cleaving activities and cytotoxicities of EDTA analogue-tethered pyrrole-polyamide dimer-based Ce(IV) complexes, Eur. J. Med. Chem. 87 (2014) 168–174, https://doi.org/10.1016/j.ejmech.2014.09.057.
[155] J.C. Joyner, K.D. Keuper, J.A. Cowan, Analysis of RNA cleavage by MALDI-TOF mass spectrometry, Nucleic Acids Res. 41 (2013) e2. https://doi.org/10.1093/nar/gks811.
[156] C. Griffith, A.S. Dayoub, T. Jaranatne, N. Alatrash, A. Mohamedi, K. Abayan, Z.S. Breitbach, D.W. Armstrong, F.M. MacDonnell, Cellular and cell-free studies of catalytic DNA cleavage by ruthenium polypyridyl complexes containing redox-active intercalating ligands, Chem. Sci. 8 (5) (2017) 3726–3740, https://doi.org/10.1039/C6SC04094B.
[157] S. Leichnitz, J. Heinrich, N. Kulak, A fluorescence assay for the detection of hydrogen peroxide and hydroxyl radicals generated by metallonucleases, Chem. Commun. 54 (95) (2018) 13411–13414, https://doi.org/10.1039/C8CC06996D.
[158] C. Wende, N. Kulak, Fluorophore ATCUN complexes: Combining agent and probe for oxidative DNA cleavage, Chem. Commun. 51 (62) (2015) 12395–12398, https://doi.org/10.1039/C5CC04508H.
[159] M.Ángeles. Martínez, M.P. Carranza, A. Massaguer, L. Santos, J.A. Organero, C. Aliende, R. de Llorens, I. Ng-Choi, L. Feliu, M. Planas, A.M. Rodríguez, B.R. Manzano, G. Espino, Félix.A. Jalón, Synthesis and biological evaluation of Ru (II) and Pt(II) complexes bearing carboxyl groups as potential anticancer targeted drugs, Inorg. Chem. 56 (22) (2017) 13679–13696, https://doi.org/10.1021/acs.inorgchem.7b0117810.1021/acs.inorgchem.7b01178.s001.
[160] I. Correia, S. Roy, C.P. Matos, S. Borovic, N. Butenko, I. Cavaco, F. Marques, J. Lorenzo, A. Rodríguez, V. Moreno, J.C. Pessoa, Vanadium(IV) and copper(II) complexes of salicylaldimines and aromatic heterocycles: Cytotoxicity, DNA binding and DNA cleavage properties, J. Inorg. Biochem. 147 (2015) 134–146, https://doi.org/10.1016/j.jinorgbio.2015.02.021.
[161] J.P. Rada, B.S.M. Bastos, L. Anselmino, C.H.J. Franco, M. Lanznaster, R. Diniz, C. O. Fernández, M. Menacho-Márquez, A.M. Percebom, N.A. Rey, Binucleating hydrazonic ligands and their μ-hydroxodicopper(II) complexes as promising structural motifs for enhanced antitumor activity, Inorg. Chem. 58 (13) (2019) 8800–8819, https://doi.org/10.1021/acs.inorgchem.9b0119510.1021/acs.inorgchem.9b01195.s001.
[162] A.R. Won, R. Kim, M.J. Jung, S.K. Kim, Y.A. Lee, Dependence of the base sequence on the [Cu(2,2'-bipyridine)$_2$(NO$_3$)](NO$_3$)-induced oxidative DNA cleavage probed by linear dichroism, Inorg. Chim. Acta 471 (2018) 34–39, https://doi.org/10.1016/j.ica.2017.10.009.
[163] A. Banasiak, J. Cassidy, J. Colleran, A novel quantitative electrochemical method to monitor DNA double-strand breaks caused by a DNA cleavage agent at a DNA sensor, Biosens. Bioelectron. 117 (2018) 217–223, https://doi.org/10.1016/j.bios.2018.05.058.
[164] X. Zhang, X. Liu, D.L. Phillips, C. Zhao, Hydrolysis mechanisms of BNPP mediated by facial copper(II) complexes bearing single alkyl guanidine pendants: cooperation between the metal centers and the guanidine pendants, Dalton Trans. 45 (2016) 1593–1603.
[165] L.F. Esteves, N.A. Rey, H.F. Dos Santos, L.A.S. Costa, Theoretical proposal for the whole phosphate diester hydrolysis mechanism promoted by a catalytic promiscuous dinuclear copper(II) complex, Inorg. Chem. 55 (6) (2016) 2806–2818, https://doi.org/10.1021/acs.inorgchem.5b02604.
[166] X. Zhang, X. Liu, D.L. Phillips, C. Zhao, Mechanistic insights into the factors that influence the DNA nuclease activity of mononuclear facial copper complexes containing hetero-substituted cyclens, ACS Catal. 6 (1) (2016) 248–257, https://doi.org/10.1021/acscatal.5b01735.
[167] T. Miao, Q. Deng, H. Gao, X. Fu, S. Li, Theoretical studies on DNA-cleavage mechanism of copper(II) complexes: Probing generation of reactive oxygen species, J. Chem. Inf. Model. 58 (4) (2018) 859–866, https://doi.org/10.1021/acs.jcim.8b00055.
[168] X. Zhang, Y. Zhu, X. Zheng, D.L. Phillips, C. Zhao, Mechanismic investigation on the cleavage of phosphate monoester catalyzed by unsymmetrical macrocyclic dinuclear complexes: The selection of metal centers and the intrinsic flexibility of the ligand, Inorg. Chem. 53 (7) (2014) 3354–3361, https://doi.org/10.1021/ic402717x.
[169] X. Zhang, X. Zheng, D.L. Phillips, C. Zhao, Mechanistic investigation of the cleavage of phosphodiester catalyzed by a symmetrical oxyimine-based macrocyclic dinuclear zinc complex: a DFT study, Dalton Trans. 43 (43) (2014) 16289–16299, https://doi.org/10.1039/C4DT01491J.
[170] H. Daver, B. Das, E. Nordlander, F. Himo, Theoretical study of phosphodiester hydrolysis and transesterification catalyzed by an unsymmetric biomimetic dizinc complex, Inorg. Chem. 55 (4) (2016) 1872–1882, https://doi.org/10.1021/acs.inorgchem.5b0273310.1021/acs.inorgchem.5b02733.s001.
[171] X. Zhang, Y. Zhu, H. Gao, C. Zhao, Solvolysis mechanisms of RNA phosphodiester analogues promoted by mononuclear zinc(II) complexes: Mechanisic determination upon solvent medium and ligand effects, Inorg. Chem. 53 (22) (2014) 11903–11912, https://doi.org/10.1021/ic501084a.
[172] X. Zhang, X. Xu, H. Xu, X. Zhang, D.L. Phillips, C. Zhao, Mechanistic investigation into the cleavage of a phosphomonoester mediated by a symmetrical oxyimine-based macrocyclic zinc(II) complex, ChemPhysChem 15 (9) (2014) 1887–1898, https://doi.org/10.1002/cphc.v15.910.1002/cphc.201301216.
[173] X. Zhou, X.-P. Zhang, W. Li, D.L. Phillips, Z. Ke, C. Zhao, Electronic effect on bimetallic catalysts: cleavage of phosphodiester mediated by Fe(III)−Zn(II) purple acid phosphatase mimics, Inorg. Chem. 59 (17) (2020) 12065–12074, https://doi.org/10.1021/acs.inorgchem.0c0101110.1021/acs.inorgchem.0c01011.s001.
[174] H. Yue, Y. Zhu, Y. Wang, G. Chen, Investigation and improvement of DNA cleavage models of polyamide + Cu(II) nuclease + OOH$^-$ ligands bound to DNA, BMC Struct. Biol. 10 (2010) 35, https://doi.org/10.1186/1472-6807-10-35.
[175] M.E. Alberto, J. Pirillo, N. Russo, C. Adamo, Theoretical exploration of type I/type II dual photoreactivity of promising Ru(II) dyads for PDT approach, Inorg. Chem. 55 (21) (2016) 11185–11192, https://doi.org/10.1021/acs.inorgchem.6b01782.
[176] J. Chen, J. Stubbe, Bleomycins: Towards better therapeutics, Nat. Rev. Cancer 5 (2) (2005) 102–112, https://doi.org/10.1038/nrc1547.
[177] C.A. Claussen, E.C. Long, Nucleic acid recognition by metal complexes of bleomycin, Chem. Rev. 99 (9) (1999) 2797–2816, https://doi.org/10.1021/cr980449z.
[178] V.D. Latta, A. Cecchettini, S.D. Ry, M.A. Morales, Bleomycin in the setting of lung fibrosis induction: From biological mechanisms to counteractions, Pharmacol. Res. 97 (2015) 122–130, https://doi.org/10.1016/j.phrs.2015.04.012.
[179] C. Pérez-Arnaiz, M.I. Acuña, N. Busto, I. Echevarría, M. Martínez-Alonso, G. Espino, B. García, F. Domínguez, Thiabendazole-based Rh(III) and Ir(III) biscyclometallated complexes with mitochondria-targeted anticancer activity and metal-sensitive photodynamic activity, Eur. J. Med. Chem. 157 (2018) 279–293, https://doi.org/10.1016/j.ejmech.2018.07.065.
[180] A. Coates, Y. Hu, R. Bax, C. Page, The future challenges facing the development of new antimicrobial drugs, Nat. Rev. Drug Discov. 1 (11) (2002) 895–910, https://doi.org/10.1038/nrd940.
[181] M. Zaiou, Multifunctional antimicrobial peptides: therapeutic targets in several human diseases, J. Mol. Med. 85 (4) (2007) 317–329, https://doi.org/10.1007/s00109-006-0143-4.
[182] J.L. Alexander, Z. Thompson, J.A. Cowan, Antimicrobial metallopeptides, ACS Chem. Biol. 13 (4) (2018) 844–853, https://doi.org/10.1021/acschembio.7b00989.
[183] M. Mital, Z. Ziora, Biological applications of Ru(II) polypyridyl complexes, Coord. Chem. Rev. 375 (2018) 434–458, https://doi.org/10.1016/j.ccr.2018.02.013.
[184] C.D. Natale, I.D. Benedictis, A.D. Benedictis, D. Marasco, Metal–peptide complexes as promising antibiotics to fight emerging drug resistance: new perspectives in tuberculosis, Antibiotics 9 (2020) 337, https://doi.org/10.3390/antibiotics9060337.
[185] M. Jezowska-Bojczuk, K. Stokowa-Sołtys, Peptides having antimicrobial activity and their complexes with transition metal ions, Eur. J. Med. Chem. 143 (2018) 997–1009, https://doi.org/10.1016/j.ejmech.2017.11.086.
[186] Q. Jia, Q. Song, P. Li, W. Huang, Rejuvenated photodynamic therapy for bacterial infections, Adv. Healthcare Mater. 8 (14) (2019) 1900608, https://doi.org/10.1002/adhm.v8.1410.1002/adhm.201900608.
[187] F. Cieplik, D. Deng, W. Crielaard, W. Buchalla, E. Hellwig, A. Al-Ahmad, T. Maisch, Antimicrobial photodynamic therapy–what we know and what we don't, Crit. Rev. Microbiol. 44 (5) (2018) 571–589, https://doi.org/10.1080/1040841X.2018.1467876.
[188] A. Almeida, Photodynamic therapy in the inactivation of microorganisms, Antibiotics 9 (2020) 138, https://doi.org/10.3390/antibiotics9040138.
[189] M.R. Hamblin, H. Abrahamse, Can light-based approaches overcome antimicrobial resistance?, Drug Dev Res. 80 (1) (2019) 48–67, https://doi.org/10.1002/ddr.21453.
[190] A. Wiehe, J.M. O'Brien, M.O. Senge, Trends and targets in antiviral phototherapy, Photochem. Photobiol. Sci. 18 (11) (2019) 2565–2612, https://doi.org/10.1039/C9PP00211A.
[191] N. Mukherjee, S. Podder, S. Banerjee, S. Majumdar, D. Nandi, A.R. Chakravarty, Targeted photocytotoxicity by copper(II) complexes having vitamin B6 and photoactive acridine moieties, Eur. J. Med. Chem. 122 (2016) 497–509, https://doi.org/10.1016/j.ejmech.2016.07.003.

[192] F. Darabi, H. Hadadzadeh, J. Simpson, A. Shahpiri, A water-soluble Pd(II) complex with a terpyridine ligand: experimental and molecular modeling studies of the interaction with DNA and BSA; and *in vitro* cytotoxicity investigations against five human cancer cell lines, New J. Chem. 40 (2016) 9081–9097, https://doi.org/10.1039/c6nj01880g.
[193] Y. Zhang, Q. Zhou, N. Tian, C. Li, X. Wang, Ru(II)-complex-based DNA photocleaver having intense absorption in the phototherapeutic window, Inorg. Chem. 56 (4) (2017) 1865–1873, https://doi.org/10.1021/acs.inorgchem.6b02459.
[194] V.M. Manikandamathavan, M. Thangaraj, T. Weyhermuller, R.P. Parameswari, V. Punitha, N.N. Murthy, B.U. Nair, Novel mononuclear Cu (II) terpyridine complexes: Impact of fused ring thiophene and thiazole head groups towards DNA/BSA interaction, cleavage and antiproliferative activity on HepG2 and triple negative CAL-51 cell line, Eur. J. Med. Chem. 135 (2017) 434–446, https://doi.org/10.1016/j.ejmech.2017.04.030.
[195] S.-Q. Zhang, T.-T. Meng, J. Li, F. Hong, J. Liu, Y. Wang, L.-H. Gao, H. Zhao, K.-Z. Wang, Near-IR/visible-emitting thiophenyl-based Ru(II) complexes: Efficient photodynamic therapy, cellular uptake, and DNA binding, Inorg. Chem. 58 (20) (2019) 14244–14259, https://doi.org/10.1021/acs.inorgchem.9b02420.
[196] S. Paul, P. Kundu, U. Bhattacharyya, A. Garai, R.C. Maji, P. Kondaiah, A.R. Chakravarty, Ruthenium(II) conjugates of boron-dipyrromethene and biotin for targeted photodynamic therapy in red light, Inorg. Chem. 59 (1) (2020) 913–924, https://doi.org/10.1021/acs.inorgchem.9b03178.
[197] S. Li, J. Zhao, X. Wang, G. Xu, S. Gou, Q. Zhao, Design of a tris-heteroleptic Ru (II) complex with red-light excitation and remarkably improved photobiological activity, Inorg. Chem. 59 (15) (2020) 11193–11204, https://doi.org/10.1021/acs.inorgchem.0c01860.
[198] W. Hua, G. Xu, J. Zhao, J. Lu, W. Sun, S. Gou, DNA Targeting Ru(II)-polypyridyl complex with long-lived intraligand excited state as potential photodynamic therapy agent, Chem. Eur. J. 26 (2020) 17495–17503, https://doi.org/10.1002/chem.202003031.
[199] P. Liu, B.-Y. Wu, J. Liu, Y.-C. Dai, Y.-J. Wang, K.-Z. Wang, DNA binding and photocleavage properties, cellular uptake and localization, and *in-vitro* cytotoxicity of dinuclear ruthenium(II) complexes with varying lengths in bridging alkyl linkers, Inorg. Chem. 55 (4) (2016) 1412–1422, https://doi.org/10.1021/acs.inorgchem.5b0193410.1021/acs.inorgchem.5b01934.s001.
[200] M.G. Walker, P.J. Jarman, M.R. Gill, X. Tian, H. Ahmad, P.A.N. Reddy, L. McKenzie, J.A. Weinstein, A.J.H.M. Meijer, G. Battaglia, C.G.W. Smythe, J.A. Thomas, A self-assembled metallomacrocycle singlet oxygen sensitizer for photodynamic therapy, Chem. Eur. J. 22 (17) (2016) 5996–6000, https://doi.org/10.1002/chem.201600852.
[201] O.A. Lenis-Rojas, C. Roma-Rodrigues, A.R. Fernandes, F. Marques, D. Pérez-Fernández, J. Guerra-Varela, L. Sánchez, D. Vázquez-García, M. López-Torres, A. Fernández, J.J. Fernández, Dinuclear $Ru^{II}(bipy)_2$ derivatives: Structural, biological, and in vivo zebrafish toxicity evaluation, Inorg. Chem. 56 (12) (2017) 7127–7144, https://doi.org/10.1021/acs.inorgchem.7b00790.
[202] G.A. Bhat, R. Maqbool, A.A. Dar, M. Ul Hussain, R. Murugavel, Selective formation of discrete versus polymeric copper organophosphates: DNA cleavage and cytotoxic activity, Dalton Trans. 46 (39) (2017) 13409–13420, https://doi.org/10.1039/C7DT02763J.
[203] L. Conti, A. Bencini, C. Ferrante, C. Gellini, P. Paoli, M. Parri, G. Pietraperzia, B. Valtancoli, C. Giorgi, Highly charged ruthenium(II) polypyridyl complexes as effective photosensitizer in photodynamic therapy, Chem. Eur. J. 25 (45) (2019) 10606–10615, https://doi.org/10.1002/chem.201901570.
[204] L. Conti, A. Mengoni, G.E. Giacomazzo, L. Mari, M. Perfetti, C. Fagorzi, L. Sorace, B. Valtancoli, C. Giorgi, Exploring the potential of highly charged Ru (II)- and heteronuclear Ru(II)/Cu(II)-polypyridyl complexes as antimicrobial agents, J. Inorg. Biochem. 220 (2021) 111467, https://doi.org/10.1016/j.jinorgbio.2021.111467.
[205] X.L. Zhao, Z.S. Li, A.G. Zhang, P. Liu, X.M. Song, K.Z. Wang, pH and DNA luminescence switching, DNA photocleavage and cytotoxic properties of two thiophene-containing ruthenium(II) complexes, Eur. J. Med. Chem. 87 (2014) 10–22, https://doi.org/10.1016/j.ejmech.2014.09.041.
[206] B. Annaraj, M.A. Neelakantan, Synthesis, crystal structure, spectral characterization and biological exploration of water soluble Cu(II) complexes of vitamin B6 derivative, Eur. J. Med. Chem. 102 (2015) 1–8, https://doi.org/10.1016/j.ejmech.2015.07.041.
[207] B.Đ. Glišić, J. Nikodinovic-Runic, T. Ilic-Tomic, H. Wadepohl, A. Veselinović, I. M. Opsenica, M.I. Djuran, Synthesis, cytotoxic activity and DNA-binding properties of copper(II) complexes with terpyridine, Polyhedron 139 (2018) 313–322, https://doi.org/10.1016/j.poly.2017.11.008.
[208] W. Villarreal, L. Colina-Vegas, G. Visbal, O. Corona, R.S. Corrêa, J. Ellena, M.R. Cominetti, A.A. Batista, M. Navarro, Copper(I)–phosphine polypyridyl complexes: Synthesis, characterization, DNA/HSA binding study, and antiproliferative activity, Inorg. Chem. 56 (7) (2017) 3781–3793, https://doi.org/10.1021/acs.inorgchem.6b02419.
[209] U. Yıldız, A. Şengül, I. Kandemir, F. Cömert, S. Akkoç, B. Coban, The comparative study of the DNA binding and biological activities of the quaternized dicnq as a dicationic form and its platinum(II) heteroleptic cationic complex, Bioorg. Chem. 87 (2019) 70–77, https://doi.org/10.1016/j.bioorg.2019.03.009.
[210] H.Y. Khan, M.O. Ansari, G.G.H.A. Shadab, S. Tabassum, F. Arjmand, Evaluation of cytotoxic activity and genotoxicity of structurally well characterized potent cobalt(II) phen–based antitumor drug entities: An *in vitro* and *in vivo* approach, Bioorg. Chem. 88 (2019) 102963, https://doi.org/10.1016/j.bioorg.2019.102963.
[211] C.P. Matos, Z. Adiguzel, Y. Yildizhan, B. Cevatemre, T.B. Onder, O. Cevik, P. Nunes, L.P. Ferreira, M.D. Carvalho, D.L. Campos, F.R. Pavan, J.C. Pessoa, M.H. Garcia, A.I. Tomaz, I. Correia, C. Acilan, May iron(III) complexes containing phenanthroline derivatives as ligands be prospective anticancer agents?, Eur J. Med. Chem. 176 (2019) 492–512, https://doi.org/10.1016/j.ejmech.2019.04.070.
[212] K. Malarz, D. Zych, M. Kuczak, R. Musioł, A. Mrozek-Wilczkiewicz, Anticancer activity of 4'-phenyl-2,2':6',2''-terpyridines-behind the metal complexation, Eur. J. Med. Chem. 189 (2020) 112039, https://doi.org/10.1016/j.ejmech.2020.112039.
[213] C.T. Pich, P.R. dos Santos, T.V.O. Fortunato, M. Chiarello, I.M. de Oliveira, B.Q. Soares, N.E. Ghermani, M. Machado, M. Roesch-Ely, F. Dumas, H. Terenzi, J.A. P. Henriques, S. Moura, Mixed ternary mononuclear copper(II) complexes based on valproic acid with 1,10-phenanthroline and 2,2'-bipyridine ligands: DNA interaction and cytotoxicity in V79 cells, J. Braz. Chem. Soc. 30 (2019) 597–613, https://doi.org/10.21577/0103-5053.20180229.
[214] A.P. de Sousa, A.C.S. Gondim, E.H. S. Sousa, L.G. de França Lopes, E.H. Teixeira, M.A. Vasconcelos, P.H.R. Martins, E.J.T. Medeiros, A.A. Batista, A.K.M. Holanda, Biphosphinic ruthenium complexes as the promising antimicrobial agents, New J. Chem. 44 (48) (2020) 21318–21325, https://doi.org/10.1039/D0NJ03122D.
[215] B.S. Vizzotto, R.S. Dias, B.A. Iglesias, L.F. Krause, A.R. Viana, A.P. Schuch, DNA photocleavage and melanoma cells cytotoxicity induced by a *meso*-tetra-ruthenated porphyrin under visible light irradiation, J. Photochem. Photobiol. B Biol. 209 (2020) 111922, https://doi.org/10.1016/j.jphotobiol.2020.111922.
[216] S. Parveen, F. Arjmand, D.K. Mohapatra, Zinc(II) complexes of Pro-Gly and Pro-Leu dipeptides: Synthesis, characterization, *in vitro* DNA binding and cleavage studies, J. Photochem. Photobiol. B 126 (2013) 78–86, https://doi.org/10.1016/j.jphotobiol.2013.07.009.
[217] S.M.G. Leite, L.M.P. Lima, S. Gama, F. Mendes, M. Orio, I. Bento, A. Paulo, R. Delgado, O. Iranzo, Copper(II) complexes of phenanthroline and histidine containing ligands: Synthesis, characterization and evaluation of their DNA cleavage and cytotoxic activity, Inorg. Chem. 55 (22) (2016) 11801–11814, https://doi.org/10.1021/acs.inorgchem.6b01884.
[218] D. İnci, R. Aydın, Ö. Vatan, O. Şahinc, N. Çinkılıç, Water soluble binary and ternary palladium(II) complexes containing amino acids and intercalating ligands: Synthesis, characterization, biomolecular interactions and cytotoxicities, New J. Chem. 43 (2019) 4681–4697, https://doi.org/10.1039/c8nj05934a.
[219] X.B. Fu, J.J. Zhang, D.D. Liu, Q. Gan, H.W. Gao, Z.W. Mao, X.Y. Le, Cu(II)–dipeptide complexes of 2-(4'-thiazolyl)benzimidazole: Synthesis, DNA oxidative damage, antioxidant and *in vitro* antitumor activity, J. Inorg. Biochem. 143 (2015) 77–87, https://doi.org/10.1016/j.jinorgbio.2014.12.006.
[220] Y.Y. Qi, Q. Gan, Y.X. Liu, Y.H. Xiong, Z.W. Mao, X.Y. Le, Two new Cu(II) dipeptide complexes based on 5-methyl-2-(2'-pyridyl) benzimidazole as potential antimicrobial and anticancer drugs: Special exploration of their possible anticancer mechanism, Eur. J. Med. Chem. 154 (2018) 220–232, https://doi.org/10.1016/j.ejmech.2018.05.023.
[221] M. Soler, E. Figueras, J. Serrano-Plana, M. González-Bártulos, A. Massaguer, A. Company, M.Á. Martínez, J. Malina, V. Brabec, L. Feliu, M. Planas, X. Ribas, M. Costas, Design, preparation, and characterization of Zn and Cu metallopeptides based on tetradentate aminopyridine ligands showing enhanced DNA cleavage activity, Inorg. Chem. 54 (22) (2015) 10542–10558, https://doi.org/10.1021/acs.inorgchem.5b01680.
[222] C.S. Burke, A. Byrne, T.E. Keyes, Targeting Photo-induced DNA destruction by Ru(II) tetraazaphenathrene in live cells by signal peptide, J. Am. Chem. Soc. 140 (2018) 6945–6955, https://doi.org/10.1021/jacs.8b02711.
[223] B.K. Maiti, N. Govil, T. Kundu, J.J.G. Moura, Designed metal-ATCUN derivatives: redox- and non-redox-based applications relevant for chemistry, biology, and medicine, iScience 23 (2020) 101792. https://doi.org/10.1016/j.isci.2020.101792.
[224] S. Bradford, J.A. Cowan, Catalytic metallodrugs targeting HCV IRES RNA, Chem. Commun. 48 (2012) 3118–3120, https://doi.org/10.1039/c2cc17377h.
[225] Y. Jin, J.A. Cowan, DNA cleavage by copper-ATCUN complexes. Factors influencing cleavage mechanism and linearization of dsDNA, J. Am. Chem. Soc. 127 (23) (2005) 8408–8415, https://doi.org/10.1021/ja050398510.1021/ja0503985.s001.
[226] M.D. Libardo, J.L. Cervantes, J.C. Salazar, A.M. Angeles-Boza, Improved bioactivity of antimicrobial peptides by addition of amino-terminal copper and nickel (ATCUN) binding motifs, ChemMedChem 9 (2014) 1892–1901, https://doi.org/10.1002/cmdc.201402033.
[227] M.D.J. Libardo, T.J. Paul, R. Prabhakar, A.M. Angeles-Boza, Hybrid peptide ATCUN-*sh*-Buforin: Influence of the ATCUN charge and stereochemistry on antimicrobial activity, Biochimie 113 (2015) 143–155, https://doi.org/10.1016/j.biochi.2015.04.008.
[228] J.L. Alexander, Z. Thompson, Z. Yu, J.A. Cowan, Cu-ATCUN derivatives of Sub5 exhibit enhanced antimicrobial activity via multiple modes of action, ACS Chem. Biol. 14 (3) (2019) 449–458, https://doi.org/10.1021/acschembio.8b01087.
[229] J.L. Alexander, Z. Yu, J.A. Cowan, Amino terminal copper and nickel binding motif derivatives of Ovispirin-3 display increased antimicrobial activity via lipid oxidation, J. Med. Chem. 60 (24) (2017) 10047–10055, https://doi.org/10.1021/acs.jmedchem.7b0111710.1021/acs.jmedchem.7b01117.s001.

[230] D. İnci, R. Aydın, Ö. Vatan, T. Sevgi, D. Yılmaz, Y. Zorlu, Y. Yerli, B. Çoşut, E. Demirkan, N. Çinkılıç, Synthesis and crystal structures of novel copper(II) complexes with glycine and substituted phenanthrolines: reactivity towards DNA/BSA and in vitro cytotoxic and antimicrobial evaluation, J. Biol. Inorg. Chem. 22 (1) (2017) 61–85, https://doi.org/10.1007/s00775-016-1408-1.
[231] Y.Y. Qi, Y.X. Liu, Q. Gan, Y.H. Xiong, Z.W. Mao, X.Y. Le, Three new mixed-ligand copper(II) complexes containing glycyl-L-valine and N, N-aromatic heterocyclic compounds: Synthesis, characterization, DNA interaction, cytotoxicity and antimicrobial activity, Appl. Organometal. Chem. 32 (2018), https://doi.org/10.1002/aoc.4126 e4126.
[232] U.K. Komarnickaa, S. Kozieł, R. Starosta, A. Kyzioł, Selective Cu(I) complex with phosphine-peptide (SarGly) conjugate contra breast cancer: Synthesis, spectroscopic characterization and insight into cytotoxic action, J. Inorg. Biochem. 186 (2018) 162–175, https://doi.org/10.1016/j.jinorgbio.2018.06.009.
[233] G. Psomas, D.P. Kessissoglou, Quinolones and non-steroidal anti-inflammatory drugs interacting with copper(II), nickel(II), cobalt(II) and zinc(II): structural features, biological evaluation and perspectives, Dalton Trans. 42 (2013) 6252–6276, https://doi.org/10.1039/c3dt50268f.
[234] C.N. Banti, S.K. Hadjikakou, Non-steroidal anti-inflammatory drugs (NSAIDs) in metal complexes and their effect at the cellular level, Eur. J. Inorg. Chem. 2016 (19) (2016) 3048–3071, https://doi.org/10.1002/ejic.v2016.1910.1002/ejic.201501480.
[235] A. Cuprys, R. Pulicharla, S.K. Brar, P. Drogui, M. Verma, R.Y. Surampalli, Fluoroquinolones metal complexation and its environmental impacts, Coord. Chem. Rev. 376 (2018) 46–61, https://doi.org/10.1016/j.ccr.2018.05.019.
[236] T.D.M. Pham, Z.M. Ziora, M.A.T. Blaskovich, Quinolone antibiotics, Med. Chem. Commun. 10 (10) (2019) 1719–1739, https://doi.org/10.1039/C9MD00120D.
[237] M.N. Patel, H.N. Joshi, C.R. Patel, Cytotoxic, DNA binding, DNA cleavage and antibacterial studies of ruthenium–fluoroquinolone complexes, J. Chem. Sci. 126 (3) (2014) 739–749, https://doi.org/10.1007/s12039-014-0597-9.
[238] F. Arjmand, I. Yousuf, T. Hadda, L. Toupet, Synthesis, crystal structure and antiproliferative activity of Cu(II) nalidixic acide-DACH conjugate: Comparative *in vitro* DNA/RNA binding profile, cleavage activity and molecular docking studies, Eur. J. Med. Chem. 81 (2014) 76–88, https://doi.org/10.1016/j.ejmech.2014.04.080.
[239] R. Loganathan, M. Ganeshpandian, N.S.P. Bhuvanesh, M. Palaniandavar, A. Murugananthan, S.K. Ghosh, A. Riyasdeen, M.A. Akbarsha, DNA and protein binding, double-strand DNA cleavage and cytotoxicity of mixed ligand copper (II) complexes of the antibacterial drug nalidixic acid, J. Inorg. Biochem. 174 (2017) 1–13, https://doi.org/10.1016/j.jinorgbio.2017.05.001.
[240] M. Sharma, M. Ganeshpandian, A. Sanjeev, A. Tamilarasan, V.S.K. Mattaparthi, N.S. Islam, M. Palaniandavar, Bis- and mixed-ligand copper(II) complexes of nalidixic acid the antibacterial drug: mode of nalidixate coordination determines DNA binding and cleavage and cytotoxicity, Inorg. Chim. Acta 504 (2020) 119450, https://doi.org/10.1016/j.ica.2020.119450.
[241] Z. Ude, K. Kavanagh, B. Twamley, M. Pour, N. Gathergood, A. Kellett, C.J. Marmion, A new class of prophylactic metallo-antibiotic possessing potent anti-cancer and anti-microbial properties, Dalton Trans. 48 (24) (2019) 8578–8593, https://doi.org/10.1039/C9DT00250B.
[242] J. Azéma, B. Guidetti, A. Korolyov, R. Kiss, C. Roques, P. Constant, M. Daffé, M. Malet-Martino, Synthesis of lipophilic dimeric C-7/C-7-linked ciprofloxacin and C-6/C-6-linked levofloxacin derivatives. Versatile in vitro biological evaluations of monomeric and dimeric fluoroquinolone derivatives as potential antitumor, antibacterial or antimycobacterial agents, Eur. J. Med. Chem. 46 (2011) 6025–6038, https://doi.org/10.1016/j.ejmech.2011.10.014.
[243] C. Lu, A. Eskandari, P.B. Cressey, K. Suntharalingam, Cancer stem cell and bulk cancer cell active copper(II) complexes with vanillin Schiff base derivatives and naproxen, Chem. Eur. J. 23 (47) (2017) 11366–11374, https://doi.org/10.1002/chem.201701939.
[244] P. Srivastava, K. Singh, M. Verma, S. Sivakumar, A.K. Patra, Photoactive platinum(II) complexes of nonsteroidal anti-inflammatory drug naproxen: Interaction with biological targets, antioxidant activity and cytotoxicity, Eur. J. Med. Chem. 144 (2018) 243–254, https://doi.org/10.1016/j.ejmech.2017.12.025.
[245] M. Simunkova, P. Lauro, K. Jomova, L. Hudecova, M. Danko, S. Alwasel, I.M. Alhazza, S. Rajcaniova, Z. Kozovska, L. Kucerova, J. Moncol, L. Svorc, M. Valko, Redox-cycling and intercalating properties of novel mixed copper(II) complexes with non-steroidal anti-inflammatory drugs tolfenamic, mefenamic and flufenamic acids and phenanthroline functionality: Structure, SOD-mimetic activity, interaction with albumin, DNA damage study and anticancer activity, J. Inorg. Biochem. 194 (2019) 97–113, https://doi.org/10.1016/j.jinorgbio.2019.02.010.
[246] P.R. dos Santos, C.T. Pich, D. Back, F. Smiderle, F. Dumas, S. Moura, Synthesis, chemical characterization and DNA interaction study of new diclofenac and ibuprofen zinc(II)-nicotinamide ternary complexes as cyclooxygenase inhibitor prototypes, J. Inorg. Biochem. 206 (2020) 111046, https://doi.org/10.1016/j.jinorgbio.2020.111046.
[247] P.B. Cressey, A. Eskandari, P.M. Bruno, C. Lu, M.T. Hemann, K. Suntharalingam, The potent inhibitory effect of a naproxen-appended cobalt(III)-cyclam complex on cancer stem cells, ChemBioChem 17 (18) (2016) 1713–1718, https://doi.org/10.1002/cbic.v17.1810.1002/cbic.201600368.
[248] P.B. Cressey, A. Eskandari, K. Suntharalingam, A cancer stem cell potent cobalt (III)–cyclam complex bearing two tolfenamic acid moieties, Inorganics 5 (2017) 12, https://doi.org/10.3390/inorganics5010012.
[249] C. Kakoulidou, P.S. Gritzapis, A.G. Hatzidimitriou, K.C. Fylaktakidou, G. Psomas, Zn(II) complexes of (*E*)-4-(2-(pyridin-2-ylmethylene)hydrazinyl) quinazoline in combination with non-steroidal anti-inflammatory drug sodium diclofenac: Structure, DNA binding and photo-cleavage studies, antioxidant activity and interaction with albumin, J. Inorg. Biochem. 211 (2020) 111194, https://doi.org/10.1016/j.jinorgbio.2020.111194.
[250] M. Kumar, G. Kumar, D.T. Masram, Copper(II) complexes containing Enoxacin and heterocyclic ligands: Synthesis, crystal structures and their biological Perspectives, New J. Chem. 44 (2020) 8595–8613, https://doi.org/10.1039/d0nj01192d.
[251] A.A. Khandar, Z. Mirzaei-Kalar, N. Shahabadi, S. Hadidi, H. Abolhasani, S.A. Hosseini-Yazdi, A. Jouyban, Antimicrobial, cytotoxicity, molecular modeling and DNA cleavage/binding studies of zinc-naproxen complex: switching DNA binding mode of naproxen by coordination to zinc ion, J. Biomol. Struct. Dyn. (2020), https://doi.org/10.1080/07391102.2020.1854858.
[252] Z. Mirzaei-Kalar, A.A. Khandar, J.M. White, H. Abolhasani, T. Komeili Movahhed, S.P. Best, A. Jouyban, Investigation of biological activity of nickel (II) complex with naproxen and 1,10-phenanthroline ligands, J. Biomol. Struct. Dyn. 39 (18) (2021) 6939–6954, https://doi.org/10.1080/07391102.2020.1804454.